

**Biosynthesis and Regulation of Production of the Antibiotic
Myxovirescin A in *Myxococcus xanthus* DK1622**

Dissertation zur Erlangung des Grades des Doktors der Naturwissenschaften
der Naturwissenschaftlich-Technischen Fakultät III
(Chemie, Pharmazie, Bio- und Werkstoffwissenschaften)
der Universität des Saarlandes

von

Vesna Simunovic

Saarbrücken, Germany, Mai 2007

© 2007

Vesna Simunovic

All Rights Reserved

Tag des Kolloquiums: den 27 June 2007

Dekan: Uni Müller

Berichterstatter: Prof. Dr. Rolf Müller

Prof. Dr. Manfred Schmitt

List of publications featured in this dissertation:

Simunovic V., Zapp J., Rashid S., Krug D., Meiser, P., Müller R.

Myxovirescin A Biosynthesis is Directed by Hybrid Polyketide Synthases/Nonribosomal Peptide Synthetase, 3-Hydroxy-3-Methylglutaryl-CoA Synthases, and *trans*-Acting Acyltransferases.

ChemBioChem. 2006 Aug; 7(8):1206-20. DOI: 10.1002/cbic.200600075

Simunovic V., Müller R.

3-Hydroxy-3-Methylglutaryl-CoA-Like Synthases Direct the Formation of Methyl and Ethyl Side Groups in the Biosynthesis of the Antibiotic Myxovirescin A.

ChemBioChem. 2007 Mar; 8(5):497-500. DOI: 10.1002/cbic.200700017

Simunovic V., Müller R.

Mutational Analysis of the Myxovirescin Biosynthetic Gene Cluster Reveals Novel Insights into the Functional Elaboration of Polyketide Backbones.

ChemBioChem. 2007 July, 8, DOI: 10.1002/cbic.200700153

Meetings

The 32nd International Conference on the Biology of the Myxobacteria

Harrison Hot Springs, British Columbia, Canada, July 10-13, 2005. Oral presentation.

Myxovirescin Biosynthesis: An intriguing megasynthetase consisting of polyketide synthases, nonribosomal peptide synthetase, 3-hydroxy-3-methylglutaryl-CoA synthases and *trans*-acting acyltransferases. Page 42.

Abstract

Myxobacteria produce a variety of secondary metabolites displaying important biological activities. Recent sequencing of the *Myxococcus xanthus* DK1622 genome revealed its high potential for the production of secondary metabolites and led to the identification of the myxovirescin biosynthetic gene cluster. In silico analysis of myxovirescin megasynthetase resulted in the proposal that a number of discrete enzymes work together with the multimodular PKS to build myxovirescin scaffold, unique for the presence of two different β -alkyl groups. To test the myxovirescin biosynthetic model, fourteen in-frame deletion mutants in the myxovirescin biosynthetic gene cluster were created, and their effects on the production of myxovirescin antibiotics evaluated by HPLC-MS analysis of the resulting mutant extracts. Novel myxovirescin analogues arising from certain mutant backgrounds were structurally elucidated to identify the specific positions of these modifications. In silico analysis of an additional 11 kb region encoded upstream from the myxovirescin gene clusters were proposed to be involved in the regulation of its production. Genetic disruption of a gene encoding for a serine/threonine kinase, and two additional genes encoding for proteins of unknown functions, were shown to positively regulate myxovirescin production.

Zusammenfassung

Myxobakterien haben sich in den letzten drei Jahrzehnten als vielseitige Produzenten unterschiedlichster Sekundärmetaboliten (SM) mit zum Teil starker biologischer Wirkung erwiesen. Unter diesen Bakterien sind diverse Multiproduzenten bekannt, zu denen auch das Bakterium *Myxococcus xanthus* DK1622 zählt. Die erst vor kurzem abgeschlossene Sequenzierung des Gesamtgenoms von *Myxococcus xanthus* DK1622 zeigt das enorme Potential für die Produktion verschiedenster SMs. Auf diesem Weg konnte ebenfalls das Myxoverescin-Biosynthese-gencluster identifiziert werden. Die annotierte Genomsequenz lieferte erste Möglichkeiten für eine in silico Analyse der Myxovirescin Megasyntase und führte zum Postulat eines möglichen Biosynthesewegs. In diesem bildet eine multimodulare PKS das Myxovirescin-Grundgerüst, welches nachträglich durch verschiedene separate Enzyme modifiziert wird. Diese Enzyme katalysieren den Einbau zweier ungewöhnlicher β -Alkylgruppen. Um die Beteiligung des identifizierten Genclusters an der Myxovirescin-Biosynthese zu beweisen, wurden vierzehn "in-frame" Deletionsmutanten erzeugt. Die Auswirkung der jeweiligen Mutation auf die Produktion des Antibiotikums wurde mittels HPLC/MS Analyse der erhaltenen Kulturextrakte untersucht. Um in den neuen Myxovirescin-Derivaten die spezifische Veränderung innerhalb des Moleküls zu identifizieren, wurde deren Struktur aufgeklärt. Stromaufwärts des Biosynthese-genclusters konnte eine ca. 11 kb große genomische Region identifiziert werden, in der Gene kodiert sind, die möglicherweise regulatorische Auswirkungen auf die Myxovirescin-Produktion haben. Durch Geninaktivierungen, sowohl eines Serin/Threonin Kinase kodierenden Gens, als auch zweier Gene mit unbekannter Funktion, konnte eindeutig gezeigt werden, dass die jeweiligen Enzyme an der Produktionsregulation beteiligt sind.

Acknowledgments

I would like to thank my mentor, Prof. Dr. Rolf Müller, for his guidance during my PhD work, as well as numerous comments and critical readings in preparation of my manuscripts and this dissertation. I would further like to thank Prof. Dr. Manfred Schmitt for reading this work and being in my doctoral Committee. I would also like to acknowledge Dr. Axel Sandman for translation of the introductory and concluding parts of this work. Drs. Helge Bode and Silke Wenzel are thanked for the critical reading of my papers. Special thanks to Dr. Kira Weissman for significant help in the preparation of the third paper and for editing parts of my dissertation. A big "thank you" goes to Dr. Josef Zapp for teaching me all the secrets of nuclear magnetic resonance (NMR) spectroscopy and natural product structure elucidation. I would also like to acknowledge Prof. Dr. Giffhorn for allowing me the use of fermentors and Drs. Gert-Wieland Kohring and Christian Zimmer for their outstanding assistance with the fermentors. Daniel Krug is thanked for performing the high resolution mass spectrometry (HRMS) measurements and help with the quantitative MS measurements. Michael Ring is thanked for the fabulous help in the domain of computers. It has also been an exceptional pleasure to work with Nora Luniak, Dr. Shwan Rachid, Irene Kochems and Brigitte Lelarge- thank you for your kindness and expertise. I would also acknowledge the past and present members of Prof. Müller's laboratory. Great thanks go to my close friends and family for their emotional support in the past years. Finally, this work would not have been possible without the financial support provided by the Deutsche Forschungsgemeinschaft (DFG) and the Bundesministerium für Bildung und Forschung (BMBF).

Table of Contents

	Page
List of Publications and meetings	<i>iv</i>
Abstract (English version)	<i>v</i>
Abstract (German version)	<i>vi</i>
Acknowledgements	<i>vii</i>
Table of Contents	<i>viii</i>
Chapter	
1 Introduction	1
2 Myxovirescin A Biosynthesis is Directed by Hybrid Polyketide Synthases/Nonribosomal Peptide Synthetase, 3-Hydroxy-3-Methylglutaryl–CoA Synthases and <i>trans</i> -Acting Acyltransferases	28
3 3-Hydroxy-3-Methylglutaryl-CoA-like Synthases Direct the Formation of Methyl and Ethyl Side Groups in the Biosynthesis of the Antibiotic Myxovirescin A	70
4 Mutational Analysis of the Myxovirescin Biosynthetic Gene Cluster Reveals Novel Insights into the Functional Elaboration of Polyketide Backbones	85
5 Regulation of myxovirescin production in <i>M. xanthus</i> DK1622	109
6 Discussion	118
Summary (English version)	138
Summary (German version)	140
References	142
<i>Curriculum vitae</i>	148

Chapter 1

Introduction

Natural products-importance, applications, and impacts

The serendipitous discovery of penicillin-producing fungus *Penicillium notatum* by Alexander Fleming, coupled to the later success of Florey and Chain in the development of the large scale fermentative process for the production of penicillin, has marked the beginnings of the modern era in natural product research.^[1] This discovery has triggered the golden fever in the discovery of new antibiotics (1940-1960) that were largely based on screenings of soil samples for the presence of microorganisms capable to produce biologically active compounds. Attempts to cultivate these microorganisms, optimize the production of these agents, elucidate their structures, and discover ways of their biosyntheses has made the field of natural product research evolve into an interdisciplinary science which combines multiple aspects of microbiology, molecular genetics, chemistry, biochemistry and recently genomics.

In addition to the development of numerous classes of antibiotics in human clinical use, such as penicillins (β -lactams), streptomycin (aminoglycosides), erythromycin (polyketide macrolactones) and vancomycin (glycopeptides), the major impact of natural product research on the history of medicine have had discoveries of immunosuppressive drugs cyclosporine and FK-506 (**Figure 1**). The discovery, followed by the later success in the proper administration of these drugs has overcome the major limitation in the field of organ transplantation-rejection of the newly acquired organs by the host immune system.^[2]

Effects of the available antibiotic therapies are evident in the greatly decreased death rates caused by infectious diseases ranging from 797 cases per 100 000 in 1900 to 36 cases per 100 000 in 1980, as reported in the United States.^[3] However, increased longevity of humans has caused an inevitable increase in the incidence of cancers. Consequently, development of new and effective agents for cancer chemotherapy remains high on the priority lists of both academic research groups as well as pharmaceutical companies. In

addition, the widening threat of HIV epidemics, an alarming spread of tuberculosis around the world, and a global threat of antibiotic resistant bacteria in the last two decades remain only

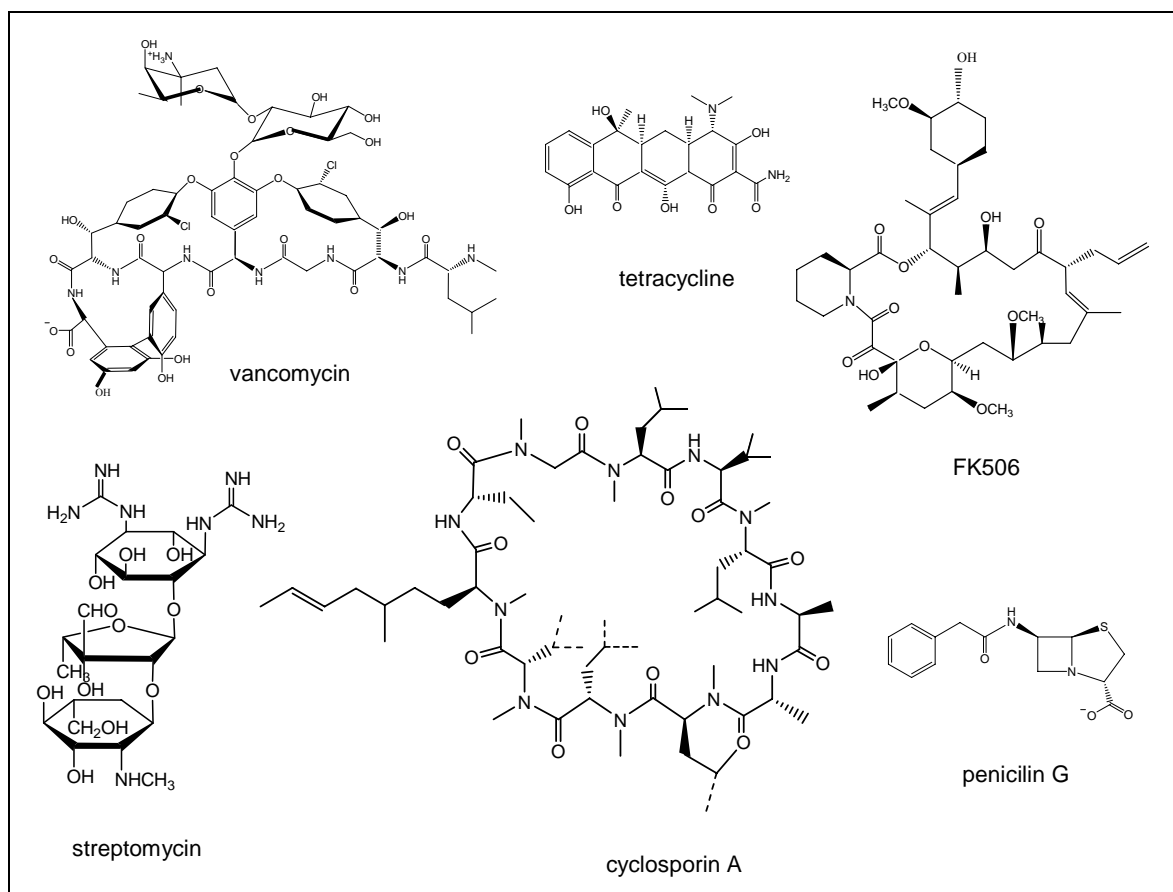


Figure 1: Examples of natural products in clinical use: antibiotics penicillin, vancomycin, streptomycin, tetracycline and immunosuppressants FK-506 and cyclosporine.

some of the hot issues that call for urgent development of new therapies to treat these diseases.^[4; 5] **Figure 2** illustrates some selected natural products which show promising anticancer and anti-HIV activities.

Today, natural products continue to play a vital role in the discovery and development of new drugs. This is evident from the fact that about 50% of all drugs that are currently in the clinical use are of natural product origin.^[6] A superior advantage of natural products in respect to their molecular counterparts obtained by combinatorial chemistry or diversity-oriented synthesis approaches generally include their greater structural complexity, higher abundance of stereogenic centers, great target specificity and higher water solubility.^[7] Such

characteristics are the outcome of a long evolutionary process that has conferred selective advantages on the producing organisms.

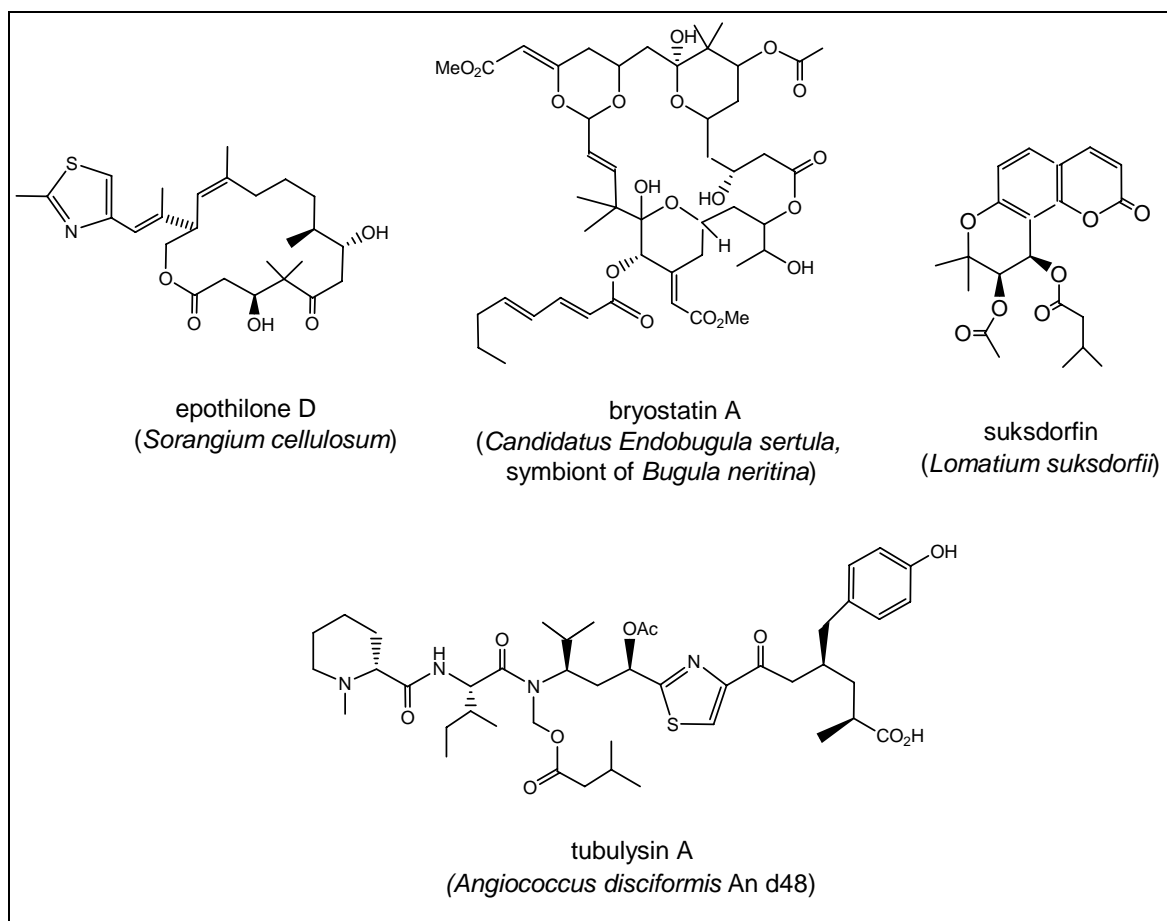


Figure 2. Natural products with potential of becoming anticancer and anti-HIV drugs: tubulysin A, bryostatin 1 and epothilone. The latter two are currently in phase II and III of clinical trials, respectively. Suksdorfin shows anti-HIV activity.

Because of these characteristics natural products are irreplaceable starting materials (leads) for the development of drugs with superior characteristics. The drug development generally aims at generating libraries of simplified structural analogues of the lead compound, e.g. lacking specific regions of the molecule or certain functional groups, in an effort to define the true pharmacophore region. A successful example of this approach is the bryostatin analogue A, which lacks the scaffolding regions (see **Figure 3**) but displays higher potency than bryostatin itself.^[8] Also, further modifications of the lead and its analogues through introduction of additional functional groups can be important for improving drug solubility

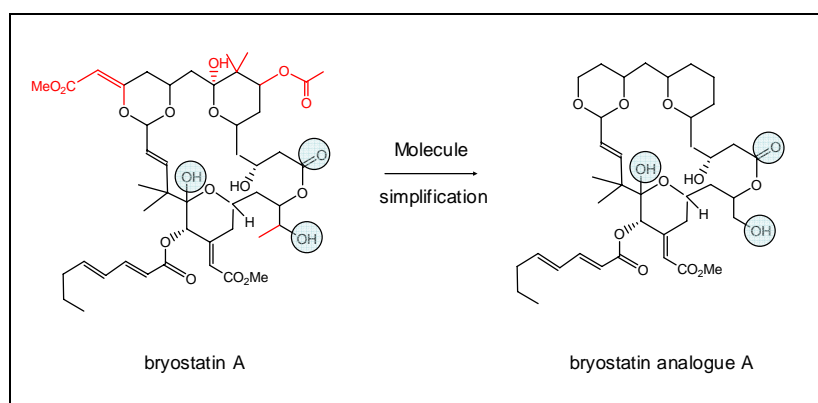


Figure 3. Simpler and more potent: A structurally simplified analogue of bryostatin A shows higher potency than the original natural product. "Omitted" functional groups are shown in red whereas the green circles indicate the functional groups essential for bryostatin activity.^[8]

and reactivity. In addition to the traditional organic synthetic efforts to new structures, some of the recent approaches utilize enzyme-directed tailoring as ways of producing new natural product variants. For example, in vitro-catalyzed modifications of aglycon libraries by glycosyltransferases from natural product biosynthetic pathways have proven as another elegant way of generating new potentially active molecules.^[9] Another approach to generate novel bioactive molecules is through reconstruction of the biosynthetic pathways leading to their assembly by using genetic engineering in their natural or in more suitable heterologous hosts. The latter two approaches require the use of molecular genetic methods for manipulation of the DNA as well as biochemical techniques required for enzyme expression and purification.^[10]

Natural product producers

Plants are prolific producers of natural products (NP) and as such have had the longest therapeutic applications dating back to the beginnings of the human civilization. Nevertheless, mapping of the genes governing NP production in plants is difficult due to their random distribution across the genome. In addition, complex organization of eukaryotic DNA makes the identification of genes dedicated to natural product biosynthesis extremely time

consuming.^[11; 12] Contrary to their more complex relatives, bacterial and fungal genes dedicated to production of secondary metabolites are generally found clustered in the chromosome. The best known producers of natural products within the bacterial kingdom are actinomycetes. This bacterial phylum has contributed with the highest number of clinically used antibiotics.

The search for new bioactive secondary metabolite producers also includes marine organisms. Coral reefs and deep sea floors are especially densely populated with organisms having sedentary life style which maintain their natural niches by chemical means of defense. It has been proposed that due to differences between marine and terrestrial habitats, the marine natural products may contribute with unique structural diversity.^[6] Besides cyanobacteria, a wide range of sponges, sea slugs, bryozoans and a variety of other marine organisms have been shown as valuable sources of highly cytotoxic compounds.^[12] Because of this marine organisms are becoming important sources of new compounds for the treatment of cancer. However, low levels of their recovery (often 1 mg/ 1-3 kg of tissue) and notorious difficulty, often inability to cultivate marine organisms, are one of the major limitations in the field of marine natural product research.

Attempts to identify genes responsible for their biosynthesis by creation of metagenomic libraries are starting to provide compelling evidence that the actual producers of these compounds are bacteria which have developed symbiotic coexistence with their higher eukaryotic hosts. For example, Piel presented evidence that the production of pederin, as well as its two structurally related compounds, thiopederin and onnamide, is governed by prokaryotic symbionts of their terrestrial and marine hosts, respectively.^[13; 14] In addition, an increasing number of examples of structural analogues are being isolated from both marine and terrestrial bacteria. These insights suggest that the genes responsible for secondary metabolism have been acquired very early in the evolution. Indeed, discovery of both marine

actinomycetes^[15] and marine myxobacteria^[16] raise the possibility that this "structural uniqueness" may have similar bacterial origins.

Myxobacteria as producers of natural products

In the past 30 years, myxobacteria have emerged as a new genus of natural product producers. The most intense research program in myxobacterial natural products has been carried out at the German Research Center for Biotechnology in Braunschweig (Germany), resulting in screening of about 7500 myxobacterial strains. These efforts have resulted in the structural elucidation of about 100 new compounds and ca. 500 structural derivatives.^[17; 18] Even though myxobacteria are understudied in comparison with actinomycetes, today they are recognized as one of the top producers of natural products in the bacterial kingdom. This has been reconfirmed by the recent analysis of *Myxococcus xanthus* genome, which has revealed a stunning 8.6% of the genome dedicated to secondary metabolite production. This percentage surmounts the two well-known secondary metabolite producers of *Streptomyces* family, *S. coelicor* and *S. avertimilis*, which dedicate 4.5% and 6.6% of their respective genomes to secondary metabolic activities.^[19]

Interest in myxobacterial secondary products continues to grow, at least partially due to the enormous success of epothilones, anticancer agents which are currently in the phase III of clinical trials. Epothilones show a similar mode of action to that of paclitaxel, another class of antitumor compounds isolated from the bark of the pacific yew.^[20] However, epothilons are also active on paclitaxel-resistant tumours, show better water solubility and can be produced from a more sustainable source than trees.^[21] Another promising anticancer agent is tubulysin A. Tubulysin A shows antiproliferative activity on several cancer cell lines, induces apoptosis of cancer, but not of healthy cells, and displays additional valuable antiangiogenic properties.^[22]

Myxobacteria produce a variety of compounds with uncommon mechanisms of action, such as soraphen, an inhibitor of fungal acetyl-CoA carboxylase.^[23] Disorazol and tubulysin cause depolymerization of microtubules and induce mitotic arrest,^[24; 25] whereas epothilones stabilize them.^[26] Rhizopodin and chondramide interfere with the actin system.^[27-29] Because of such remarkable diversity of compounds that target eukaryotic cells, many myxobacterial compounds exhibit high potential of becoming anticancer drugs or drug leads.

Furthermore, myxobacteria are one of the rare bacterial producers of steroids.^[30] Steroids are cyclic triterpenes, obtained by cyclization of a linear C30 epoxysqualene polymer consisting of six isoprenoid precursors (**Figure 4**). Whereas production of steroids is common in eukaryotes, up to date it has been documented in only two other bacterial species: proteobacterium *Methylococcus capsulatus*^[31] and more recently in the planctomycete *Gemmata obscuriglobus*.^[32] Whereas both *M. capsulatus* and *G. obscuriglobus* produce lanosterol, the basic precursor of cholesterol, myxobacteria reveal a wider potential for steroid biosynthesis. Among all myxobacteria, the most remarkable is the capacity of *Nanocystis* sp. to synthesize almost all precursors of mammalian-like cholesterol except for the final product. Furthermore, *Stigmatella aurantiaca* Sg a15 is the only known bacterium to produce a cycloartenol, a typical product of plants and algae.^[33] In addition to steroid biosynthesis, myxobacteria have also devised biosynthetic strategies to incorporate isoprenoid moieties into secondary metabolites of polyketide (PK) or polyketide/nonribosomal peptide (PK/NRP) origin. Such is the case with leupyrrins (produced by *Sorangium cellulosum*) which combine uncommon isoprenoid and carboxylic acids moieties together with traditional PK and NRP building units.^[34] Similarly, aurachins (secondary products of *S. aurantiaca* Sg a15) incorporate a farnesyl moiety^[35] (**Figure 4**).

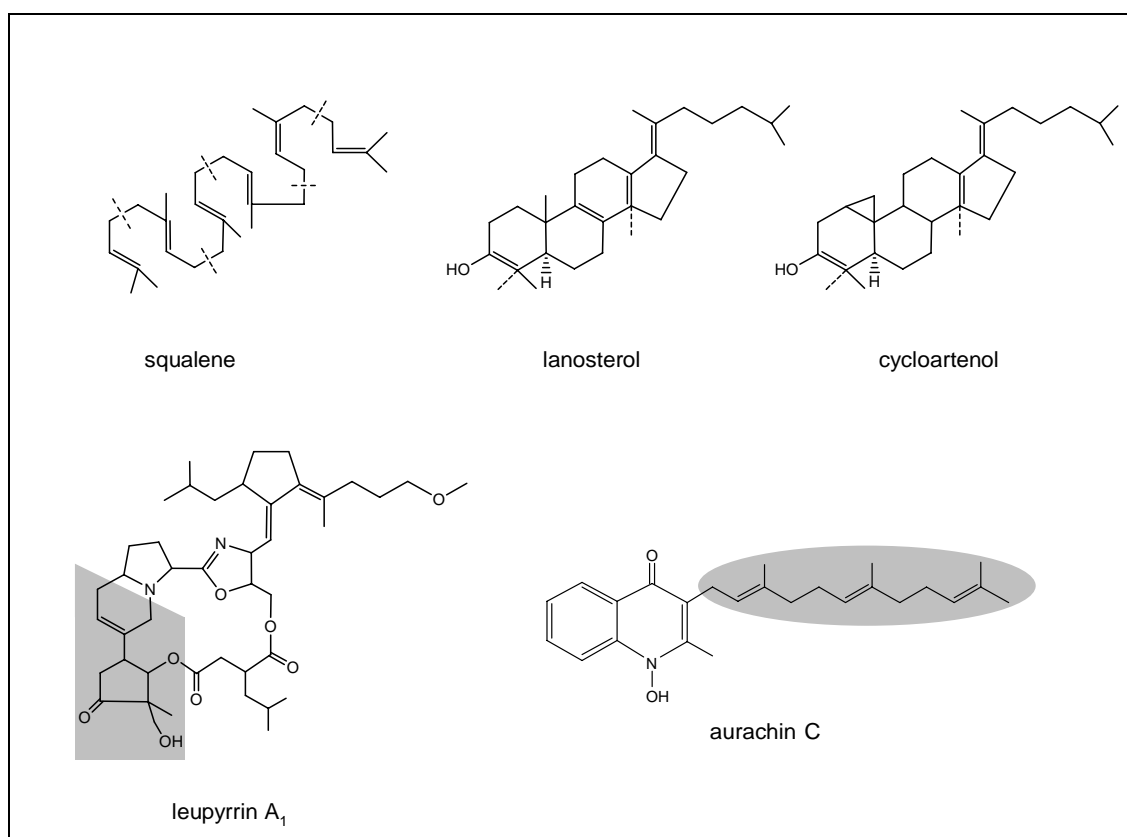


Figure 4. Top: Steroids are a class of tetracyclic lipids obtained by slightly different cyclizations of epoxisqualene, such as lanosterol and cycloartenol. Dashed lines indicated on squalene point out individual isoprenoid moieties. Bottom: Two natural products from myxobacteria, leupyrrins and aurachins, integrate isoprenoid-building blocks into their respective PKS/NRPS and PKS backbones.

Aside from the presence of an isoprenoid side chain, aurachins are also an example of rare bacterial quinoline alkaloids which use anthraniloyl-CoA as the starter unit. Soraphen also incorporates a very rare starter moiety, benzoyl-CoA,^[36] and uses a methoxymalonyl polyketide extender moiety, most likely derived from 1,3-bisphosphoglycerate.^[37] Ambruticin has a rarely observed methylcyclopropane ring.^[38] Moreover, the myxovirescin antibiotics, which are the topic of this thesis, contain atypical side chains originating from acetate and succinate.^[39; 40]

Furthermore, some natural products from myxobacteria show striking structural resemblance with those isolated from higher marine organisms. For example, chondramide B, produced by the genus *Chondromyces*^[41] is a structural cousin of jaspamide, a compound

isolated from the marine sponge *Jaspis splendens*^[42; 43] (**Table 1**). Further, saframycin Mx1 of *M. xanthus* Mx1^[44] shares a striking similarity with reinaramycin E isolated from another sponge - *Reniera* sp. - and the potent antitumor metabolite ecteinascidin ET-743 isolated from the Caribbean ascidian *Ecteinascidia turbinata*.^[12] For additional examples of structural analogues see **Table 1**. Taking into account the aforementioned limitations in the field of marine natural product research, the prospect of the availability of these compounds from the more easily accessible terrestrial myxobacterial hosts presents a unique advantage. Therefore, by circumventing the need for the construction of metagenomic libraries, a significant shortcut toward elucidation of their corresponding biosynthetic gene clusters and acceleration of their expressions in heterologous hosts can be achieved. An excellent example of this approach is the recently published biosynthetic gene cluster governing the biosynthesis of chondramide B.^[45]

Why do myxobacteria produce secondary metabolites?

In order to answer this question, a short introduction into myxobacterial physiology is required. Myxobacteria are soil, social, δ Proteobacteria that show an extraordinary capacity for adaptation towards different environmental conditions.^[46] In that respect, myxobacteria have developed an extremely complex network of sensory molecules and enzymes which functions as a highly sophisticated system dedicated to monitoring of their cellular number (quorum sensing), as well as their nutritional status. They move in swarms and prey on other microorganisms by releasing a powerful cocktail of proteolytic enzymes. Most myxobacteria feed on polypeptides. A notable exception is a cellulose degrading genus *Sorangium*. When faced with starvation, cells initiate an alternative life cycle visible as the directed and coordinated swarming movement of hundreds of thousands of cells that culminates in the formation of multicellular, three-dimensional structures called fruiting bodies. During this

extremely energetically demanding process, 90% of cells are sacrificed (lysed) and only the remaining 10% are packaged in fruiting bodies. The completion of the developmental process

Table 1. A list of currently known myxobacterial natural products which share high structural resemblance with those isolated from marine organisms.

Myxobacterial compound	Myxobacterial host	Structurally similar compound	Marine Invertebrate Source
saframycin ^[44]	<i>Myxococcus xanthus</i> Mx1	reinaramycin E ecteinascidin (ET 743) ^[12]	<i>Reniera</i> sp. (sponge) <i>Ecteinascidia</i> <i>turbinata</i> (ascidian)
chondramide ^[41]	<i>Chondromyces</i> <i>crocatus</i>	jaspamide ^[42; 43]	<i>Jaspis</i> sp. (sponge)
apicularen ^[47]	<i>Chondromyces robustus</i>	salicylhalamide ^[12]	<i>Haliclona</i> sp. (sponge)
rhizopodin ^[48]	<i>Myxococcus stipitatus</i>	sphinxolide ^[12]	<i>Neosiphonia superstes</i> (sponge)

occurs within the fruiting body and is marked with transformation of vegetative cells into dormant and desiccation resistant cells (spores).

Secondary metabolites are likely to play roles in both vegetative and developmental life cycle. During the vegetative cycle, these metabolites may be involved in killing or paralyzing other microorganisms by making them easy targets (substrates) for proteases. Another function may be in protecting the damaged and semilysed cells during early development from becoming preys of other organisms, or alternatively, they may be used as toxins to kill the sibling cells and therefore delay development. The latter situation has been described for *B. subtilis* which apparently releases the extracellular killing factor.^[49] The high potencies of myxobacterial secondary metabolites "speak" in favour of this hypothesis. Another evidence for the interdependence between primary and secondary metabolism is the identification of positive regulators of both secondary metabolite production and development. Regulator ChiR from *S. celulosum* is essential for both chivosazol production and development. Accordingly, disruption of *chiR* leads to the loss of both phenotypes.^[50]

Some secondary metabolites, like the yellow-pigmented DKxanthenes, are required for the formation of viable spores and therefore play an essential role in development.^[51] Addition of DKxanthenes to DKxanthene deficient cells partially restores this defect. These insights suggest that DKxanthenes may not have defensive, but rather structural or protective roles during late development of *M. xanthus*.

The genome of *M. xanthus* DK1622 reveals high potential for secondary metabolite production

Genes for secondary metabolism occupy a significant 8.6% of the *M. xanthus* DK1622 genome. A total of 18 biosynthetic gene clusters are localized in two chromosomal regions between 4.4 and 5.8 Mb and 1.5 and 3.5 Mb of the chromosome.^[19] Since *M. xanthus* DK1622 had not been subjected to extensive screenings for secondary metabolite production, release of the genome sequence has enabled DNA-based identification of secondary metabolic clusters. This approach has led to the identification of four biosynthetic gene clusters, homologues of which had previously been discovered in other myxobacterial species. These include biosynthetic gene clusters for myxalamides-yellow, lipophilic compounds previously isolated from *M. xanthus* Mx x12 and *Cystobacter fuscus*,^[52-54] myxochromides,^[55] another family of yellow, lipophilic compounds and the iron-chelators myxochelins.^[56] In addition to these three classes of secondary metabolites, which have been identified based on similarity with their biosynthetic gene clusters from *Stigmatella aurantiaca*, a putative myxovirescin gene cluster has been also detected^[57; 58] (**Figure 5**). Release of the genome sequence, in combination with targeted gene inactivation experiments, has facilitated identification of the third class of yellow compounds-DKxanthenes.^[51]

The availability of the genome has also set the stage for the study of global analysis of protein profiles in the whole cell mixtures by using powerful liquid chromatography-tandem mass spectrometry (LC-MS-MS). This approach has provided real time evidence for the

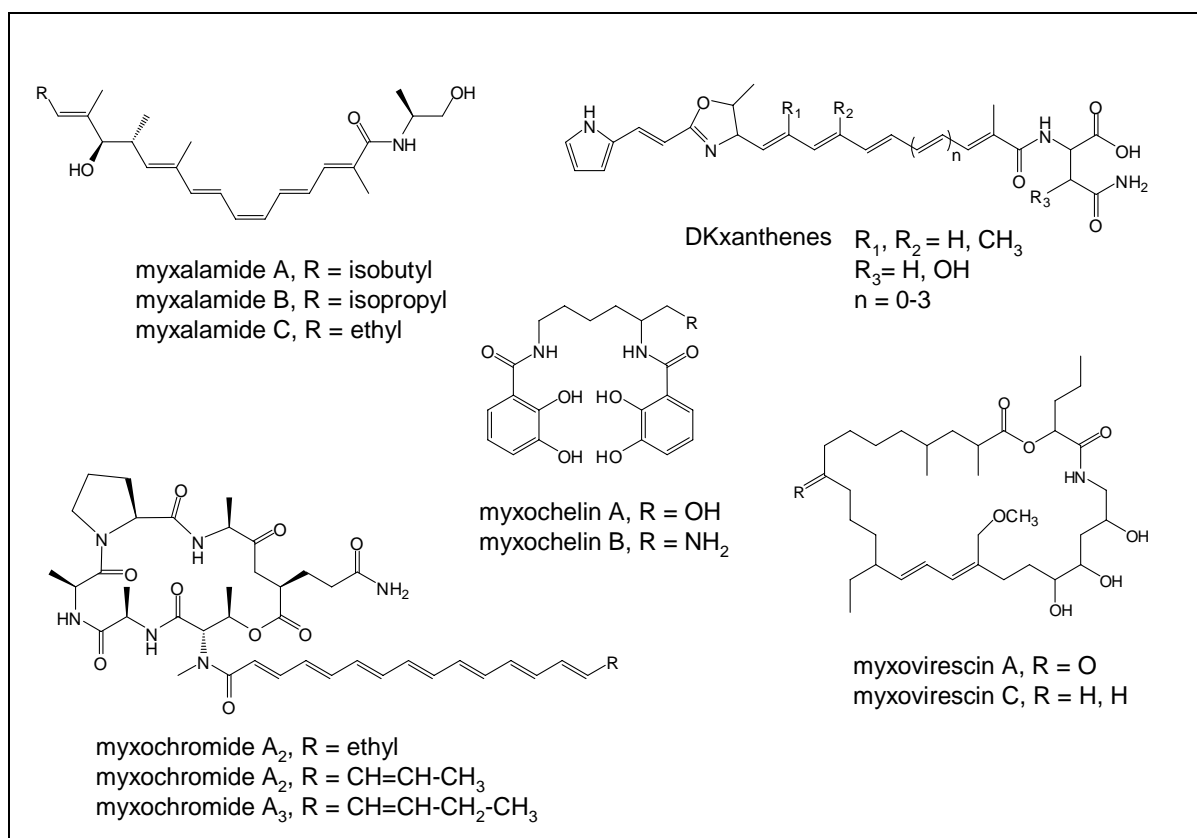


Figure 5. Structures of five known groups of secondary metabolites produced by *M. xanthus* DK1622.

expression of six out of thirteen cryptic secondary metabolic gene clusters that were previously suspected to be "silent." [59] These findings open up a new frontier directed toward identification of their chemical structures, biological activities and possible physiological roles.

The genome of *M. xanthus* DK1622 reveals extraordinary abundance of genes with putative functions in sensory transduction and regulation

Unlike other δ Proteobacteria, *M. xanthus* seems to have undergone lineage-specific duplications of genes encoding sensory transductions and regulations of DNA and protein interactions. A stunning 256 genes have been annotated to function as two component systems, 97 as serine/threonine protein kinases (STK) and 56 as σ^{54} enhancer binding proteins (EBPs).^[19]

EBPs are activator proteins required for the initiation (activation) of transcription from promoters recognized by RNA polymerase associated with the alternative σ^{54} factor. EBPs have modular organization and use their central ATPase domain to initiate transcription upon contact with the σ^{54} . In addition to the central ATPase domain,^[60] σ^{54} -specific activators usually also contain the N-terminal sensory domain involved in signal transduction plus a C-terminal DNA-binding domain.^[61] As EBPs bind the enhancer boxes located either upstream or downstream from the promoter, the interaction of EBPs with the σ^{54} -RNA polymerase (σ^{54} -RNAP) complex requires the looping of the DNA. Activation of transcription is powered by hydrolysis of ATP, which causes the essential conformational switch in σ^{54} ,^[60] resulting in the formation of an open complex.

In contrast to other bacteria in which σ^{54} functions as alternative transcription factors, in *M. xanthus* σ^{54} (RpoN) is essential.^[62] Therefore, the remarkable abundance of EBPs present in the genome only highlights the significance of σ^{54} -type regulation in gene expression of *M. xanthus*. Twelve *M. xanthus* EBPs contain fork head-associated (FHA) sensory domains which functions as phosphothreonine and phosphotyrosine binding epitopes.^[63] An even higher number of EBPs (24) are found located in the close proximity to serine threonine/tyrosine protein kinases (STKs).^[19] These observations raise the possibility that STKs activate gene transcription by coupling their sensory output to the FHA domains. In

addition, almost half of the EBPs neighbour histidine protein kinases (HPKs). HPKs architectures are also often complex and can include additional sensory modules, such as PAS domains, involved in sensing of redox states, or GAF domains, which may be involved in sensing and degrading cyclic adenosine or guanosine monophosphates (AMP or GMP).

Myxovirescins-structure elucidation and pharmacological applications

Myxovirescin A, also known as antibiotic TA, has been previously isolated from three different *Myxococcus* species: *Myxococcus xanthus* TA and ER15 and *Myxococcus virescens* Mx v48.^[64-66] Detailed analysis of its production in *M. virescens* Mx v48 has revealed a family of about 20 myxovirescin analogues, among which myxovirescin A is the most abundant product.^[40] Myxovirescins are macrolactone antibiotics which inhibit peptidoglycan biosynthesis of gram negative bacteria.^[67] In combination with their adhesive properties, myxovirescin A showed promising results in the treatment of gingivitis in humans.^[68-70] However, in spite of its good characteristics, myxovirescin A has not been developed for commercial production due to the high complexity of its total synthesis and low production titers in its natural myxobacterial hosts.

Outline of the dissertation-Biosynthesis and regulation of myxovirescin antibiotics in *M. xanthus* DK1622

This PhD dissertation focuses on the isolation, structural identification, biosynthesis and regulation of production of myxovirescin antibiotics by the developmental model strain *Myxococcus xanthus* DK1622. In the course of this study, the myxovirescin biosynthesis gene cluster has been identified on the basis of 99% DNA identity with the segment of Ta-1 polyketide synthase from a related *M. xanthus* TA.^[58] Based on this information, the identification of myxovirescin antibiotics by standard analytical procedures (HPLC-MS) was

performed, revealing the production of several myxovirescin antibiotics. Following a larger scale fermentation, the two main myxovirescin products were isolated and structurally analyzed by nuclear magnetic resonance (NMR).^[39] Based on these analyses, the most abundant form was assigned as myxovirescin A and its less abundant C-20 deoxy analogue myxovirescin C (**Figure 6**).

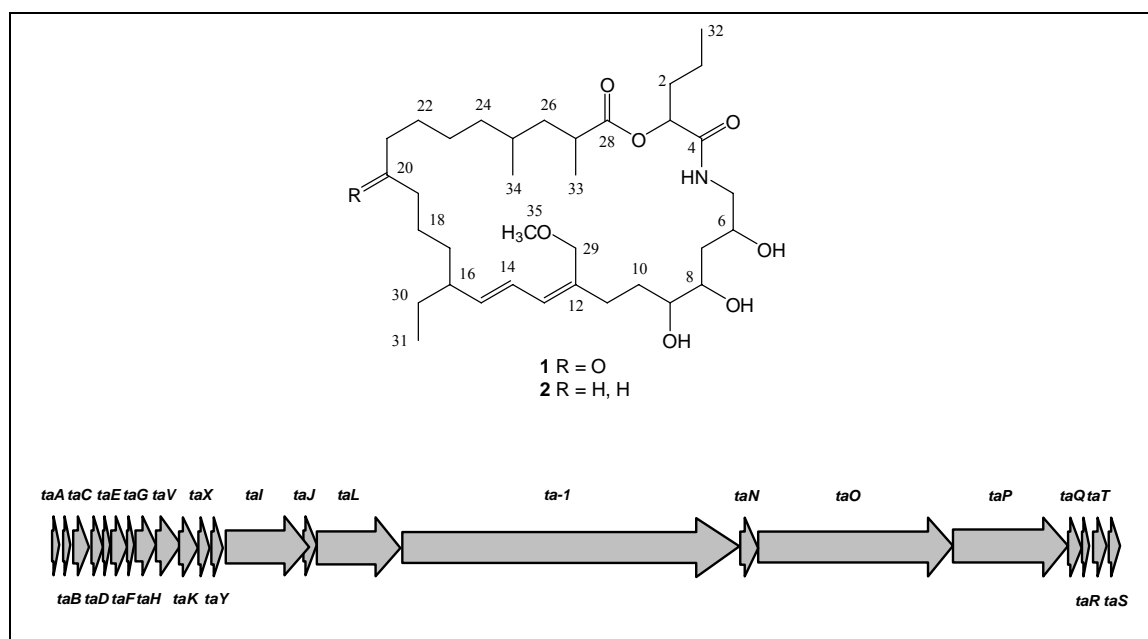


Figure 6. Top: two main forms of myxovirescin antibiotics produced by *M. xanthus* DK1622: myxovirescin A (**1**) and myxovirescin C (**2**). Bottom: Gene organization of the ca. 83 kb myxovirescin gene cluster.^[39]

The availability of the complete myxovirescin biosynthetic gene cluster in combination with the stable isotope labelling data of myxovirescin A provided the first opportunity for the reconstruction of myxovirescin biosynthesis. This analysis has revealed several intriguing features of the myxovirescin megasynthetase.^[39] Some of the most striking features included the absence of *cis*-acting acyltransferase domains within all multimodular polyketide synthase modules. Instead, two acyltransferase domains were found encoded by one gene, *taV*. The cluster also encodes more modules than could be theoretically anticipated to be required for myxovirescin A biosynthesis. This has led to the proposal that two PKSs,

TaI and TaL, may carry out the biosynthesis of the starter 2-hydroxyvaleryl-*S*-ACP precursor (**Figure 7**).

Besides discretely encoded acyltransferases, the cluster is rich with additional open reading frames (ORFs) encoding for monofunctional proteins (*taA-taY*). Among them the most intriguing is the presence of atypical cassette of genes consisting of two homologues of acyl carrier proteins (ACPs), 3-hydroxy-3-methylglutaryl-CoA (HMG-CoA) synthases and

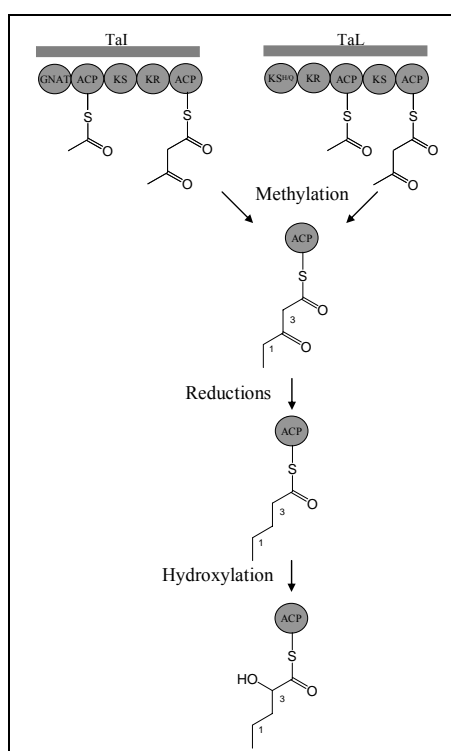


Figure 7. Precursor biosynthesis. Both TaI and TaL PKSs may catalyze the formation of acetoacetyl-*S*-ACP. In either case, acetoacetyl-*S*-ACP has to be further methylated at C1 position, reduced at C2 and hydroxylated at C3 position to form the presumed 3-hydroxyvaleryl-*S*-ACP starter intermediate.

enoyl-CoA hydratases (ECH), as well as one monofunctional β -ketoacyl synthase (KS) (**Figure 8 a**). These enzymes have been proposed to carry out the incorporation of C29 carbon, originating from the C2 acetate label and the ethyl group originating from C2-C3 of succinate, two times during formation of myxovirescin polyketide skeleton (**Figure 8 b**). Formation of these side chains was postulated to take place by condensation of acetate and propionate units onto the β -keto intermediates **2** and **6**, via two HMG-like condensing

enzymes TaC and TaF leading to hypothetical intermediates **3** and **7** (**Figure 8 c**). Following condensation, elimination of water and carbon dioxide would have to take place leading to methyl and ethyl groups attached to carbons C12 and C16 (intermediates **5** and **9**). Further modification of the C29 methyl group was postulated to take place via hydroxylation and subsequent *O*-methylation reactions to furnish the methoxymethyl group attached to C29, as observed in myxovirescin A (**1**).

In the course of the analysis of the DNA region located upstream of the myxovirescin biosynthetic gene cluster, two potential regulatory operons have been found (**Figure 9 a**). Some genes were found to encode for σ^{54} EBP and several other sensory and regulatory proteins exhibiting an intriguing modular organization (**Figure 9 b**). Due to their proximity to the myxovirescin biosynthetic genes, these have been postulated to regulate myxovirescin production (see also Chapter 5).

In order to critically evaluate hypotheses pertaining to the formation and regulation of the production of the myxovirescin macrolactam antibiotic, we decided to take advantage of the relatively fast doubling time of *M. xanthus* (5-6 hours) and reliable genetic tools available for its manipulation.^[71; 72] These techniques allow reproducible integrations, as well as excisions of plasmid DNA from the chromosome, resulting in gene knockouts or gene deletions. In the course of this PhD work, 14 markerless deletion mutants and 3 merodiploid mutants have been constructed and their effects on myxovirescin production described.^[39; 73] Four of these mutants have led to the production of three new myxovirescin analogues. In addition to the purification and structural characterization of two myxovirescins from the wild-type *M. xanthus* DK1622, three new myxovirescin analogues have been structurally characterized using nuclear magnetic resonance spectroscopy (NMR) analysis, or a combination of high resolution mass spectrometry and tandem mass spectrometry.

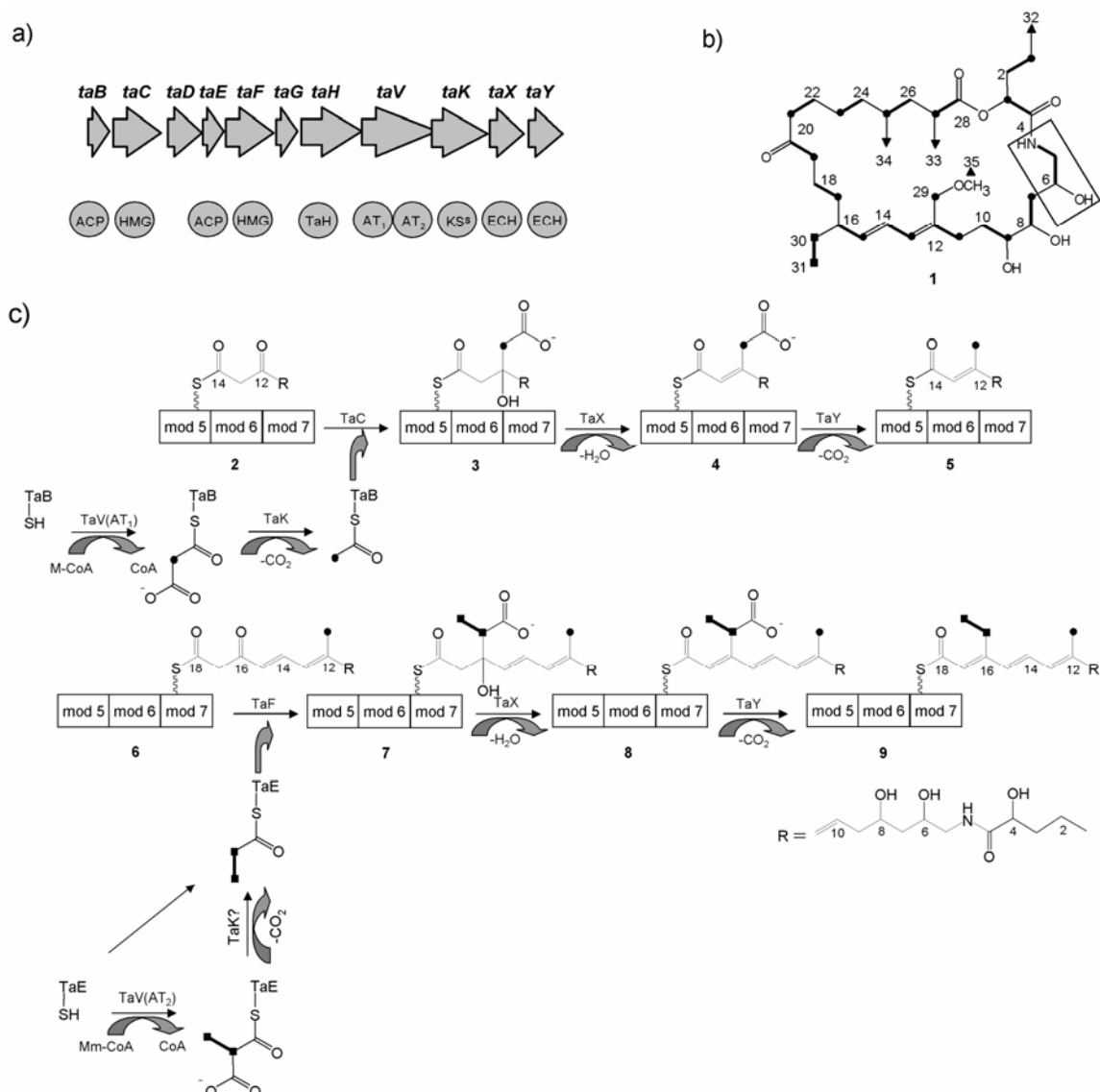


Figure 8. a) 10.9 kb fragment of the myxovirescin A biosynthetic gene cluster encoding for monofunctional enzymes. TaB and TaE are putative ACPs, TaC and TaF homologues of HMG-CoA synthases, TaK is a variant β -ketoacyl-ACP synthase (KS^S), TaX and TaY are homologues of enoyl-CoA hydratases (ECH), and TaH is a putative cytochrome P450. b) Structure of myxovirescin A (**1**) indicating the biosynthetic origin of its building units.^[40] Boxed carbons originate from glycine, black circles indicate C2 of acetate, triangles indicate methyl groups derived from methionine, and connected squares show the ethyl group originating from carbons 2 and 3 of succinate. c) A working model of myxovirescin A assembly depicts two rounds of modification reactions leading to the formation of C12 β -methyl and C16 β -ethyl side groups in myxovirescin scaffold. Two ATs encoded by TaV load malonyl-CoA (M-CoA) and methylmalonyl-CoA (Mm-CoA), respectively, onto their cognate ACPs (TaB and TaE), that become substrates of the decarboxylase TaK. Alternatively, propionyl-CoA may be directly loaded on TaE to give propionyl-S-TaE. Condensation of intermediate **2** with acetyl-S-TaB and intermediate **6** with propionyl-S-TaE catalyzed by the HMGs TaC and TaF, respectively, creates intermediates **3** and **7**. Removal of the carboxyl groups from intermediates **3** and **7** is a two step process involving dehydration by TaX (resulting in intermediates **4** and **8**), followed by their sequential decarboxylation to yield **5** and **9**. The carbon labelling pattern is described in b).

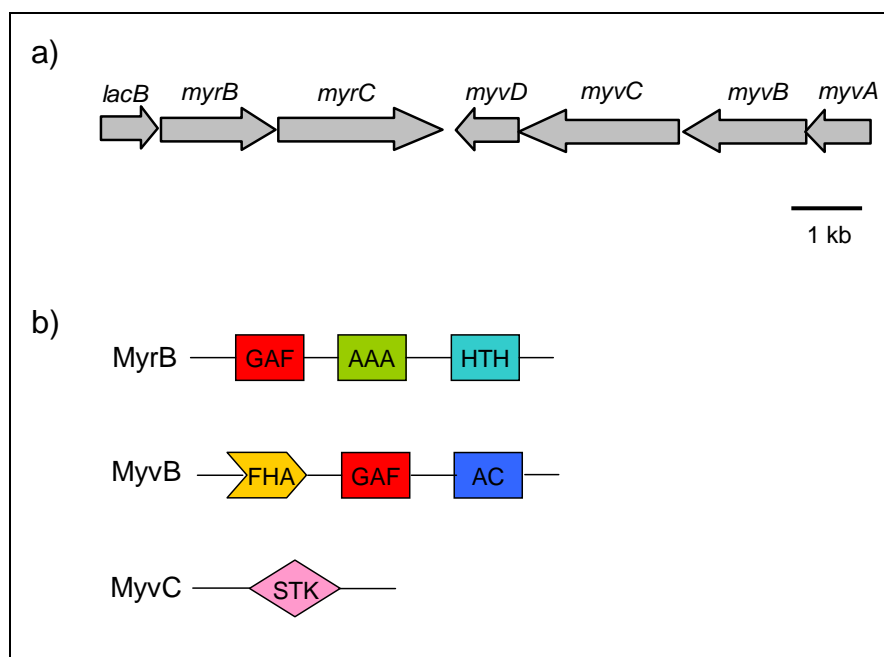


Figure 9. a) 10.9 kb of the myxovirescin regulatory region located upstream from *taA*. b) MyrB, an enhancer binding protein (EBP), encodes a GAF sensory domain.^[74] The AAA domain is an ATPase domain and the helix-turn-helix DNA binding motif is indicated as HTH. MyvC encodes for a serine threonine kinase (STK), while MyvB shows an interesting modular organization consisting of cGMP, GAF and FHA domains. The GAF domain may be involved in binding cAMP or cGMP molecules, while the cGMP module may carry out cyclization of AMP (GMP) (<http://pfam.janelia.org/browse.shtml>). The FHA domain functions as a universal phosphopeptide-binding module.^[63]

Biosynthetic Logic of Polyketide and Nonribosomal Peptides

The biosyntheses of three major classes of these products: polyketides, nonribosomally-made peptides and PK/NRPS hybrids has been studied in the considerable detail and the common logic of their assembly is relatively well understood. The underlying principle of their production is that consecutive condensations of monomer units bound as thioesters give rise to an oligomer. PKS assembly lines utilize acyl-CoA thioesters as monomer units, whereas NRPS assembly lines select from the pool of proteinogenic and nonproteinogenic amino acids as well as aryl acids.^[75]

Many PKSs (also known as type I PKS) and all NRPSs are large polypeptides organized into modules, where each module constitutes a compartment endowed with a set of

enzymatic domains needed for the incorporation and optional modification of (typically) only one extension unit into the oligomer. Accordingly, the processes governing both polyketide and non-ribosomally-made peptide biosyntheses conform to a general reaction scheme consisting of three basic steps: initiation, elongation and termination. Each initiation module usually requires two, each elongation module three and the termination module a minimum of four catalytic domains. In PK biosynthesis these include: acyltransferase (AT), acyl carrier protein (ACP) and ketosynthase (KS) domains and in NRP biosynthesis adenylation (A), condensation (C) and peptidyl carrier domains (PCP). A thioesterase (TE) domain is common to both pathways.

Initiation of PK and NRP biosynthesis

The initiation of polyketide biosynthesis commences on the loading module, which may entail a KS domain in addition to AT and ACP domains. When present, the KS domain is generally characterized by the active site His to Glu substitution (KS^Q), and functions as dedicated decarboxylase in converting (methyl)malonyl-S-ACP into propionate/acetate-S-ACP starters of polyketide biosynthesis. However, in many systems which lack the KS domain in the loading module (AT-ACP), the acyltransferase selects and loads acetyl-CoA/propionyl-CoA starter onto the first ACP (**Figure 10**). The loading module of NRPS assembly lines is comprised of an adenylation (A) domain and a PCP domain. A necessary requirement for product assembly in both PKS and NRPS assembly lines is posttranslational activation of acyl/peptidyl carrier proteins.

1) Transfer of the acyl/aminoacyl-adenylate moiety onto the 4' phosphopantetheine (Ppant) arm of the acyl carrier (ACP) or peptidyl carrier proteins (PCP)

In order for a PCP or ACP to accept the acyl/peptidyl extender unit, they have to be activated via posttranslational modification. This activation is catalyzed by Ppant transferases

and proceeds by covalent attachment of the Ppant arm of coenzyme A onto the conserved active site serine of the carrier protein (**Figure 10**).

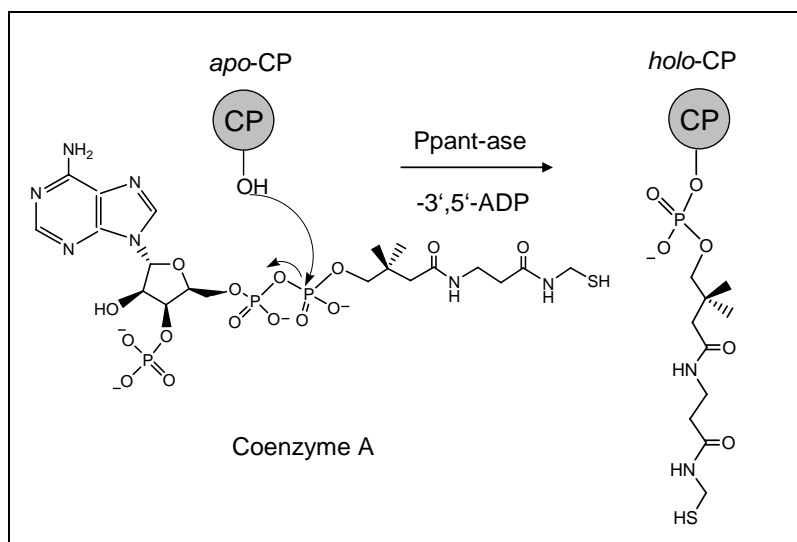


Figure 10. Posttranslational activation of carrier protein via phosphopantetheinyl transferase (Ppant-ase) catalyzed reaction.

In PK biosynthesis, the free thiol of the Ppant arm enables thioesterification (loading) of the acyl extender unit from the active site serine of the respective AT (acyl-*O*-Ser-AT) to form the acyl-*S*-ACP.^[76] Similarly, during NRP assembly, the free thiol of the Ppant arm enables the conversion of the aminoacyladenylate oxoester (aminoacyl-*O*-AMP) into the thioester (aminoacyl-*S*-PCP) by displacing the AMP.

2) Recognition and binding of the acyl-CoA (PKS) by acyltransferase (AT)/ recognition and activation of amino acid via adenylation (NRPS)

In PK biosynthesis selection of specific acyl-CoAs: acetyl, malonyl or methylmalonyl-CoA is carried out by a malonyl (methylmalonyl)-specific acyltransferase (AT). This enzyme loads the acyl-CoA onto the active site serine. This results in transient generation of a tetrahedral intermediate and ends with the release of CoA and the formation of the acyl-oxoester (**Figure 11 a and b**).

The first step of NRPS biosynthesis is catalyzed by an adenylation (A) domain. Following the recognition of the cognate amino acid, determined by the specific set of residues residing within the A4-A5 substrate binding conserved boxes,^[77] adenylation of the

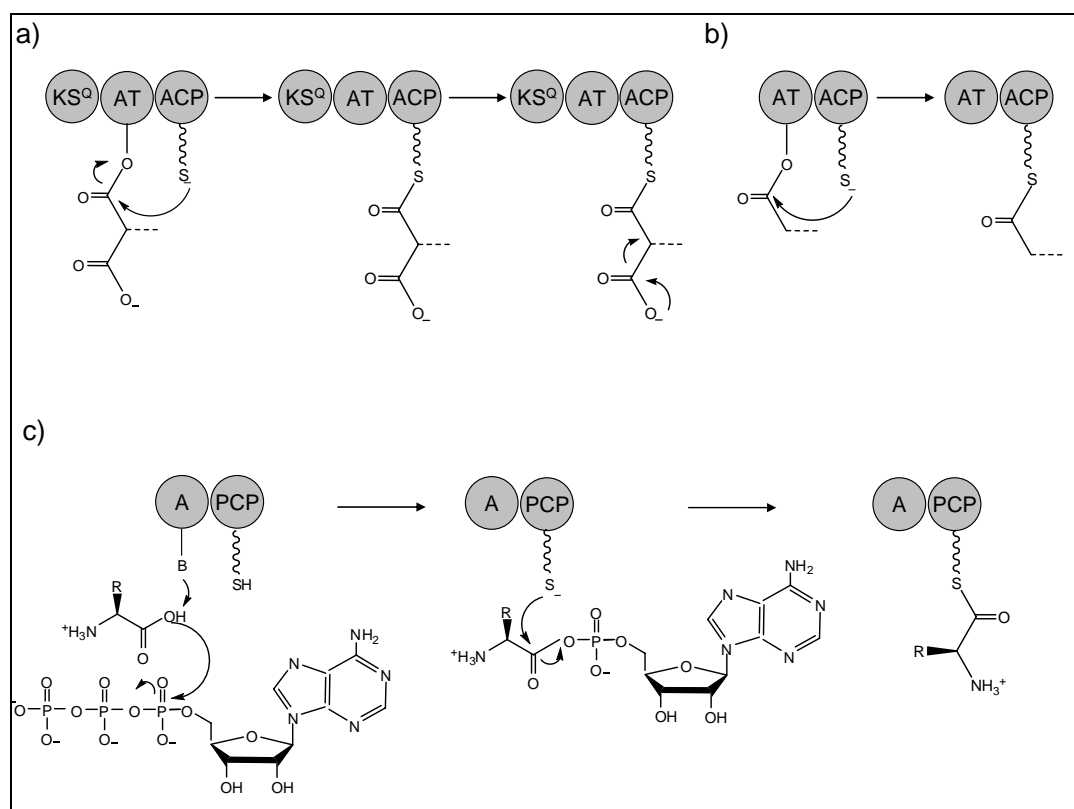


Figure 11. a) and b) Initiation mechanisms of polyketide and c) nonribosomally-made peptide biosynthesis. a) In PKS, the loading module may encode a KS^Q domain which functions as a decarboxylase during conversion of malonyl-S-ACP into acetyl-S-ACP. b) Alternatively, the AT loads an acetyl (propionyl)-CoA directly onto the first ACP. c) In NRP biosynthesis an amino acid first has to be activated as an oxoester adenylylate by the A domain before it is transferred onto the PCP. This process requires hydrolysis of ATP.

selected amino acid takes place at the expense of ATP (**Figure 11 c**). Even though the overall reaction of amino acid activation is similar to that performed by ribosomal aminoacyl-tRNA-synthetases, adenylation domains show lower substrate specificity.

Elongation of PK and NRP biosynthesis

Condensation of the acyl/aminoacyl monomer onto the downstream module

In PK biosynthesis, ketosynthase catalyzes decarboxylation of the downstream (methyl)malonyl-*S*-ACP and generates a thioester enolate nucleophile. Thioester enolate attacks the upstream acyl-*S*-ACP thioester resulting in the formation of a new C-C bond (**Figure 12 a**). However, in NRP biosynthesis the amine group of the downstream aminoacyl-*S*-PCP performs a nucleophilic attack onto the upstream aminoacyl-*S*-PCP thioesters and leads to the formation of a peptide (C-N) bond (**Figure 12 b**).

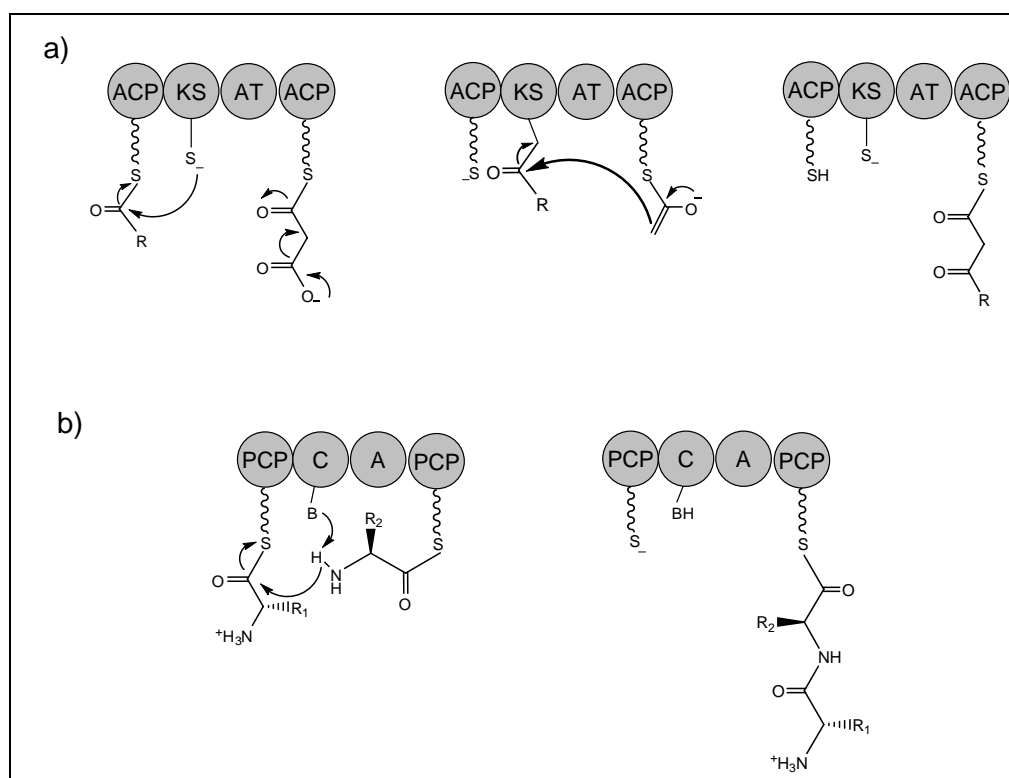


Figure 12. a) Elongation in PKS is catalyzed by KS domain and leads to C-C bond formation. b) In NRPS, the condensation is catalyzed by condensation domain (C), which governs peptide (C-N) bond formation. The thermodynamic driving force required for condensation reactions in both assembly lines comes from the energy-rich thioester-bound substrates.

Reduction of β -ketoacyl intermediates

In addition to the basic set of catalytic domains required for introduction and linking of the extender units, optional domains specialized in processing of the β -ketoacyl

intermediates can be present within modules. These include ketoreductase (KR), dehydratase (DH) and enoyl reductase (ER) domains, which result in β -hydroxyacyl, α,β -enoyl or fully reduced $\text{CH}_2\text{-CH}_2$ bonds (**Figure 13**).

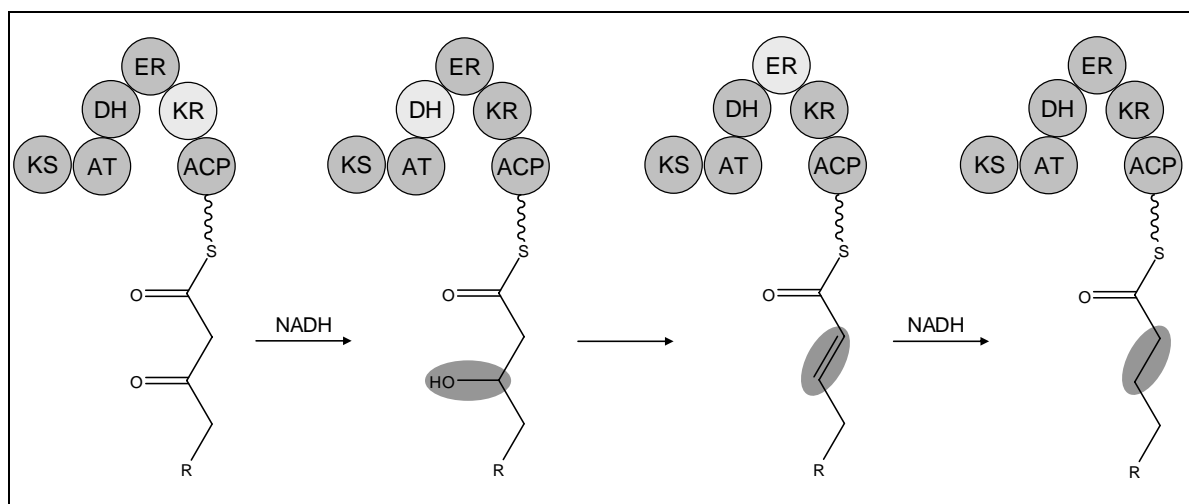


Figure 13. Optional modification of β -ketoacyl intermediates of variable chain length R can be achieved through ketoreduction, dehydration and (or) enoyl reduction. These reactions are catalyzed by ketoreductase (KR), dehydratase (DH) and enoyl reductase(ER) domains.

Termination of PKS and NRPS biosynthesis

In both PKS and NRPS assembly lines the fully extended acyl/aminoacyl-*S*-CP thioesters are usually released from the assembly line by the thioesterase (TE) domain. In this reaction, oxygen of the conserved serine (Ser-*O*-) performs a nucleophilic attack on the fully extended acyl/aminoacyl-*S*-ACP thioester by converting it into the corresponding oxoester. This intermediate may be hydrolyzed from the assembly line to yield the free acids, or may form cyclic lactone structures via nucleophilic capture by one of the side chain hydroxyl groups (**Figure 14**).

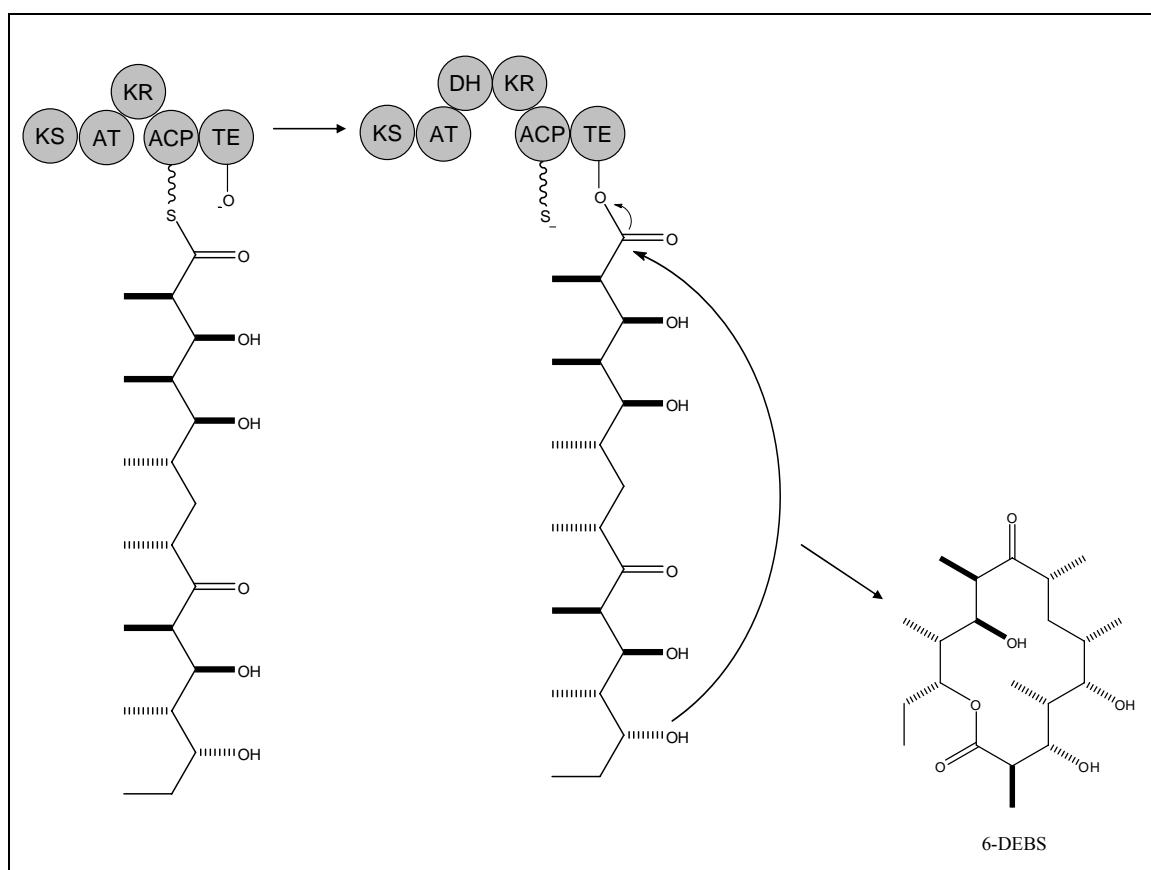


Figure 14. Release or termination of PKS and NRPS assembled products from the assembly line follows the same principle of conversion of thioester into oxoester. This figure illustrates the formation of the 6-deoxyerythronolide (DEBS) lactone (lactonization) by nucleophilic attack of a side hydroxyl group onto the oxoester.

The most simplistic and best studied system employing the above presented, so called type I paradigm of polyketide assembly, is the system which carries out the biosynthesis of 6-deoxyerythronolide B (DEBS), a precursor of erythromycin^[78]. The DEBS assembly line consists of seven modules encoded within three 200 kDa big polypeptides. **Figure 15** shows that each module contributes with one extension unit. Furthermore, the level of β -keto processing can be easily correlated with the presence of β -keto reducing domains present within each module, therefore allowing the structural prediction of the end product. This figure also illustrates an enormous potential of PK biosynthetic systems for the generation of structurally diverse compounds by optional recruitment of KR, DH, and ER domains.

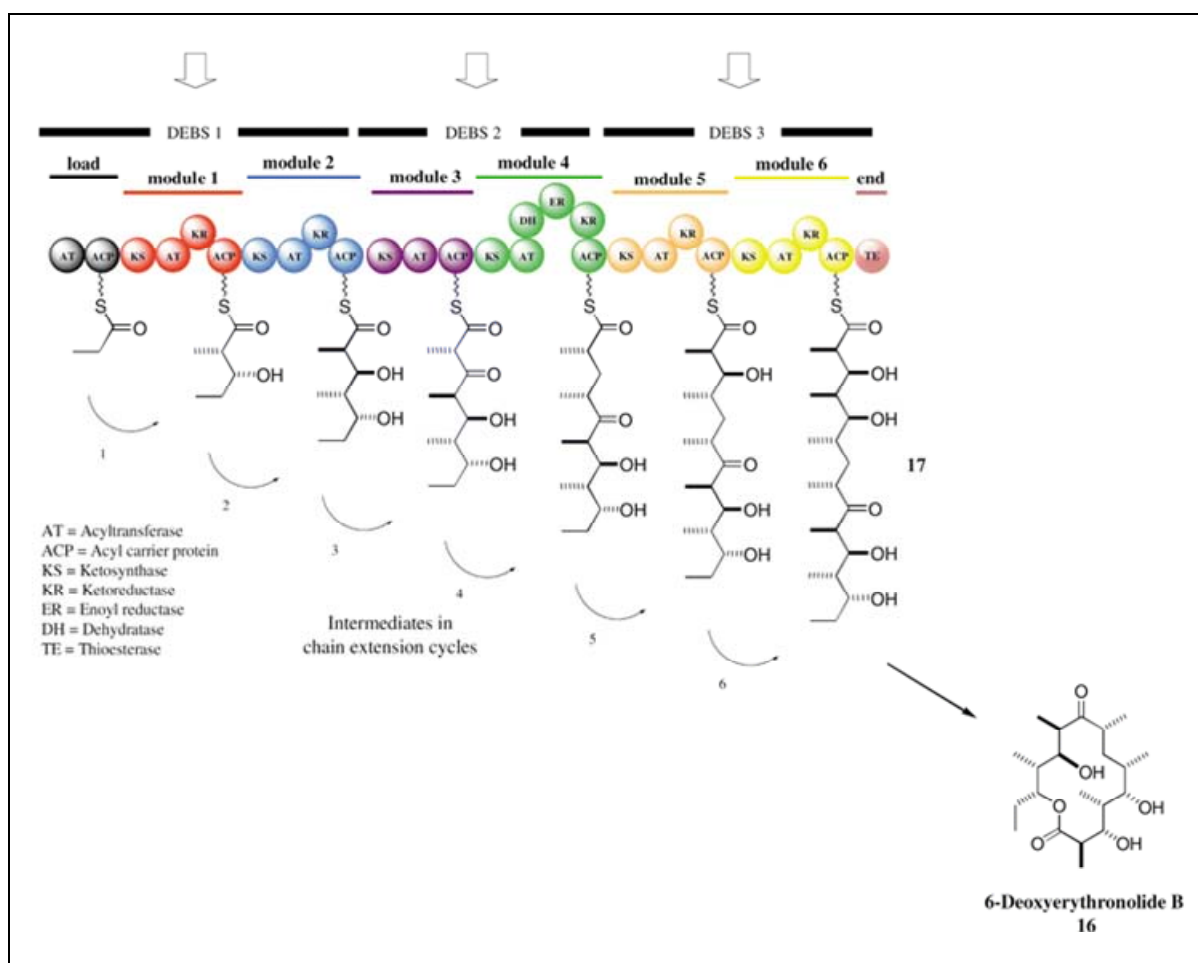


Figure 15. Example of a typical type I PKS assembly line-biosynthetic scheme for the assembly of (DEBS) (Figure is reproduced from).^[78]

Chapter 2

The following article has been published in the
ChemBioChem journal, Vol.7-No.8, August 2006,
Pages 1206-1220

Myxovirescin A Biosynthesis is Directed by
Hybrid Polyketide Synthases/Nonribosomal
Peptide Synthetase, 3-Hydroxy-3-
Methylglutaryl–CoA Synthases and *trans*-Acting
Acyltransferases

M.S.Vesna Simunovic, Dr. Josef Zapp, Dr. Shwan Rachid, Dipl-Chem. Daniel Krug,
Apotheker Peter Meiser and Prof. Dr. Rolf Müller

2006. Copyright John Wiley & Sons. Reproduced with permission.

DOI: 10.1002/cbic.200600075

Abstract

Myxococcus xanthus DK1622 is shown to be a producer of myxovirescin (antibiotic TA) antibiotics. The myxovirescin biosynthetic gene cluster spans at least 21 open reading frames (ORFs), covering a chromosomal region of approximately 83 kb. In silico analysis of myxovirescin ORFs, in conjunction with genetic studies, suggests the involvement of 4 type I PKSs (TaI, TaL, TaO and TaP), one major hybrid NRPS/PKS (Ta-1), and a number of monofunctional enzymes similar to the ones involved in type II fatty acid biosynthesis (FAB). Whereas deletion of either *taI* or *taL* causes a dramatic drop in myxovirescin production, deletion of both genes ($\Delta taIL$) leads to its complete loss. These results suggest that both TaI and TaL PKSs may act in conjunction with a methyltransferase, reductases and a monooxygenase to produce the 2-hydroxyvaleryl-*S*-ACP starter, proposed to act as the biosynthetic primer in the initial condensation reaction with glycine. Polymerization of the remaining 11 acetates required for lactone formation is directed by 12 modules of Ta-1, TaO, and TaP megasynthetases. All modules, except for the first module of TaL, lack cognate acyltransferase (AT) domains. Furthermore, deletion of a discrete tandem AT, encoded by *taV*, blocks myxovirescin production, suggesting their "*in trans*" mode of action. The assembly of the myxovirescin scaffold is proposed to switch two times during biosynthesis from PKS to HMG-CoA-like biochemistry to embellish the macrocycle with methyl and ethyl moieties. Disruption of the *S*-adenosyl methionine (SAM)-dependent methyltransferase TaQ shifts the production toward two novel myxovirescin analogues, designated myxovirescin Q_a and myxovirescin Q_c. NMR analysis of purified myxovirescin Q_a reveals the loss of the methoxy carbon atom. This novel analogue lacks bioactivity against *Escherichia coli*.

Introduction

Type I polyketide synthases (PKS), nonribosomal peptide synthetases (NRPS), and their hybrids (PKS/NRPS) are multifunctional, multidomain enzymes responsible for the production of natural products by incorporation of small building blocks in assembly-line-like fashion that is analogous to animal fatty-acid biosynthesis (FAB).^[1-2] In all three cases, the catalytic domains encoded within each module are responsible for the addition of one monomer unit to the growing chain, and its processing by various modification reactions. Typically, the fully extended product attached to the last module is dissociated from the megasynthetase to yield a free carboxylic acid or lactone structure, which undergoes further modifications by additional tailoring enzymes.

Whereas the unifying theme of PKS, NRPS, and FAB pathways is the catalytic flux of thioester-activated intermediates along the megasynthetase, differences in the choice of extender units and connecting bonds are reflected in the catalytic domains used to drive nonribosomal peptide (NRP), polyketide (PK), or fatty-acid (FA) chain elongation. For instance, formation of the peptide bond by NRPSs requires recognition and ATP-driven activation of two amino acids by their cognate adenylation domains (A), coupling of the respective adenyated amino acids onto their downstream peptidyl-carrier proteins (PCP), and their final condensation by the condensation domain (C).^[3] In PKS and FAB pathways, selection and loading of extender acyl units are executed by acyltransferases (AT). C-C bond formation between the two acyl groups attached to acyl carrier proteins (ACPs) is catalyzed by β -ketoacyl-ACP synthase (KS) by decarboxylative Claisen condensation. Unlike saturated FA biosynthesis, PKSs display greater variability in the level of β -ketothioester reduction, and can combine β -ketoacyl reductase (KR), β -hydroxyacyl dehydratase (DH), and enoyl reductase (ER). Additionally, PKSs might also perform methylations of carbon and oxygen^[4] with *S*-adenosylmethionine (SAM)-dependent methyltransferases (MT). Carbon-specific

methyltransferases couple the methyl group onto the activated α -carbon of the β -ketothioester intermediate, either during or post-assembly of the natural product.

In contrast to the multifunctional type I PKSs and animal FAB megasynthases, FA biosynthesis in bacteria and higher plants is governed by monofunctional, iteratively-acting enzymes that are encoded as separate ORFs; these are designated type II FAB.^[5] FAB in *E. coli* is initiated by KSIII (FabH), which performs the initial condensation of acetyl-CoA with malonyl-ACP to yield acetoacetyl-ACP. Two other β -ketoacyl-ACP synthases, KS I (FabF) and KAS II (FabB), carry out further elongation steps and show more specificity in their choice of substrates.^[2, 6-8]

A closer relationship between the type II FAB and PKS/NRPS-like natural product biosynthetic gene clusters came to light with the recent sequencing of pederin, mupirocin, and jamaicamide biosynthetic gene clusters.^[9-12] In these systems type II FAB enzymes appear to act in concert with the type I PKS and NRP megasynthases to create potent natural products.

Myxovirescins (also known as antibiotic TA) are wide-spectrum antibiotics that are active against Gram-negative bacteria, and have to date been exclusively found in the genus *Myxococcus*.^[13-16] In addition to their antimicrobial activity, myxovirescins are exceptionally adhesive to a variety of surfaces and dental tissues, which makes them good leads for the treatment of plaque and gingivitis in humans.^[17-19] The sequencing of several ORFs that belong to the myxovirescin biosynthetic cluster in the red-pigmented *Myxococcus xanthus* strain ER-15, has been carried out. However, these studies have led to a great underestimation of the size of the biosynthetic gene cluster^[20] and have failed to pinpoint the function of individual genes in myxovirescin biosynthesis, as polar effects of the described mutations could not be excluded.^[20-24]

This is the first report on the identification, isolation, and structure elucidation of myxovirescin antibiotics from *M. xanthus* strain DK1622. Furthermore, based on the genome sequence of *M. xanthus* DK1622, we present the annotation of the complete myxovirescin biosynthetic gene cluster, propose its biosynthetic assembly, and by performing a series of in-frame gene deletions provide the first unambiguous genetic evidence for the involvement of certain genes in myxovirescin assembly. Finally, we demonstrate that *M. xanthus* DK1622 is a valuable genetic system for biosynthetic studies and genetic engineering of PKS/NRPS pathways, as disruption of the SAM-dependent methyltransferase, TaQ, leads to the production of two novel desmethyl analogues of myxovirescin.

Results

M. xanthus DK1622 produces myxovirescin antibiotics

The first hint that *M. xanthus* DK1622 could be a myxovirescin producer arose when we analyzed its genome for the presence of secondary-metabolite biosynthetic genes.^[25] The genome was analyzed by performing a BLAST search with the previously reported PKS/NRPS fragment from *ta-1* from *M. xanthus* ER-15, which has been shown to be responsible for myxovirescin biosynthesis. The search revealed the presence of an almost identical gene in strain DK1622. Additionally, Ta-1 was identified by MALDI-TOF analysis in one of the fractions obtained in the membrane-separation experiments.^[26] To find out whether *M. xanthus* DK1622 is indeed a myxovirescin producer, HPLC and MS analyses were carried out. These revealed two characteristic peaks with a UV maximum at 239 nm (Figure 1 A) and masses diagnostic of myxovirescin antibiotics.^[27] Due to the fact that more than 30 myxovirescin analogues have been described from the related strain *M. virescens* Mx v48, we set out to perform a detailed chemical analysis of the two substances from strain DK1622.

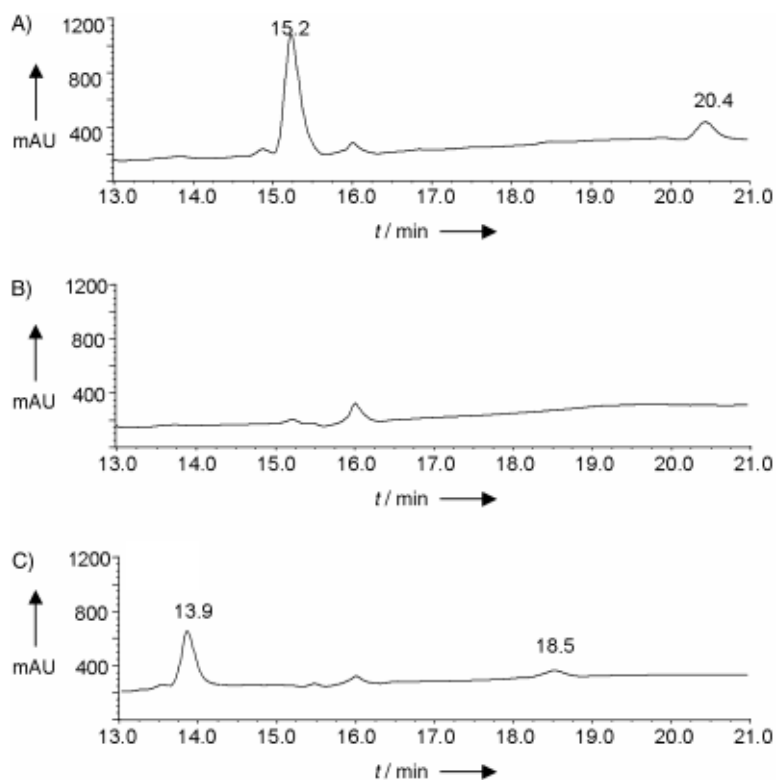


Figure 1. HPLC chromatogram traces of A) wild-type *M. xanthus* DK1622 strain, B) tandem acyltransferase mutant ΔtaV (VS1017), and C) methyltransferase mutant *taQ* (VS1016) measured at 239 nm; 1 and 2 elute at 15.2 min and 20.4 min, respectively. *M. xanthus* VS1016 produced two novel metabolites with retention times of 13.9 and 18.5 min.

Structural analysis of myxovirescins produced by *M. xanthus* DK1622

According to high-resolution mass spectroscopy data and NMR analysis (Supporting Information), the two substances that showed retention times of 15.2 and 20.4 min (Figure 1 A) were identified as compounds **1** and **2** (Figure 2 A); NMR measurements were performed in CD₃OD.

Analysis of the myxovirescin biosynthetic gene cluster

The myxovirescin biosynthetic gene cluster spans approximately 83 kb (Figure 2 B). It is dominated by four ORFs that encode type I PKSs (TaI, TaL, TaO, and TaP) and one major PKS/NRPS hybrid, Ta-1. Type I PKSs are flanked from both sides with various individual ORFs (*taA-taY* and *taQ-taS*), which show similarity to enzymes involved in type II FAS

systems (*taV*, *taB-C*, *taE-F*, *taK*, *taX*, and *taY*). The closest homologues of myxovirescin ORFs were found in the biosynthetic gene clusters of pederin, mupirocin, and leinamycin (Table 1).^[10-11, 28]

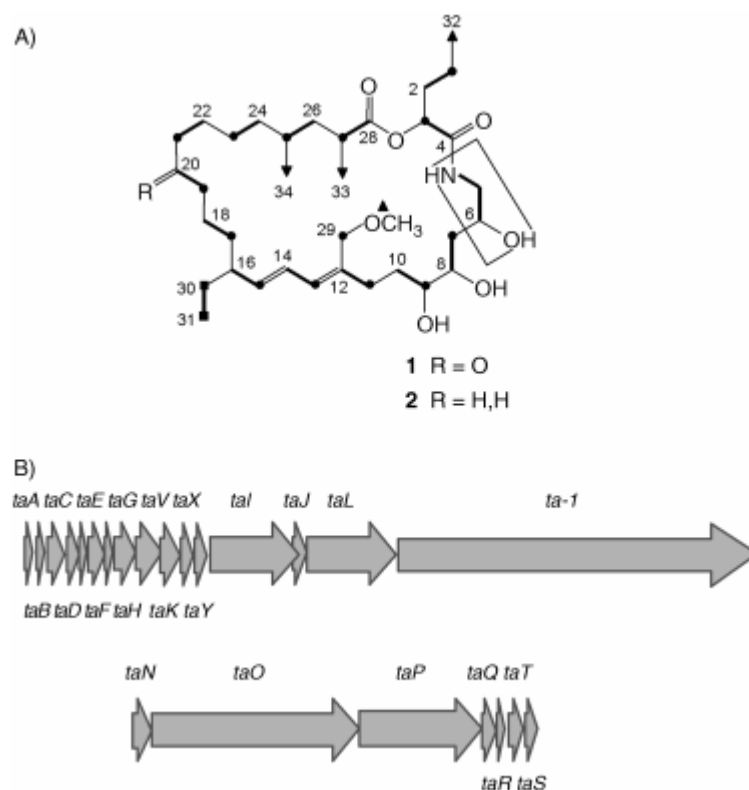


Figure 2. A) Stable isotope labeling of myxovirescin A, adopted from.^[16] Myxovirescin C (2), the second major product, lacks the oxygen at C20. Boxed carbons originate from glycine, ■ carbons indicate C2 of acetate, ▲ indicate methyl groups derived from methionine, and ◆ show the ethyl group that originates from succinate. B) Map of the 82.8 kb myxovirescin biosynthetic gene cluster.

Analysis of domains that comprise the myxovirescin megasynthetase

β-Ketoacyl synthases (KS): The myxovirescin biosynthetic gene cluster encodes 16 KS domains (Figure 3 A), 13 of which are conserved in the active-site Cys (box 1) and two His residues (boxes 2 and 3 in Figure 3 A).^[29] Two KSs, *TaL_KS1* (the first one found in *TaL*) and *KS3*, display a His to Gln substitution in the conserved box 2. However, *TaK*, the only discretely encoded *β*-ketoacyl-ACP synthase, carries a Cys to Ser substitution in the active site (Figure 3 A).

Table 1. List of myxovirescin ORFs and their protein homologues.

ORF	Protein/ gene	Size [Da/bp]	Putative function/homologue	Origin	Similarity/ Identity [%]	Accession number of the protein homologue
1	TaA/ <i>taA</i>	18406/507	transcription antiterminator	<i>Bacteriodes thetaitotaomicron</i>	29/50	AAO77992.1
2	TaB/ <i>taB</i>	9270/252	ACP	<i>Bacillus subtilis</i> subsp. <i>subtilis</i> strain 168	53/77	NP_570904.1
3	TaC/ <i>taC</i>	44851/1239	HMG-CoA synthase PksG	<i>Bacillus subtilis</i> subsp. <i>subtilis</i> strain 168	66/80	NP_389595.2
4	TaD/ <i>taD</i>	34534/930	unknown			
5	TaE/ <i>taE</i>	9170/252	ACP	<i>Streptomyces atroolivaceus</i>	41/67	AAN85525.1
6	TaF/ <i>taF</i>	46134/1263	HMG-CoA synthase	<i>Streptomyces atroolivaceus</i>	62/75	AAN85526.1
7	TaG/ <i>taG</i>	19599/516	lipoprotein signal peptidase II	<i>Clostridium tetani</i> E88	35/57	NP_782221.1
8	TaH/ <i>taH</i>	53110/1428	cytochrome P450- dependent enzyme	<i>Polyangium celulosum</i>	38/56	CAD43453.1
9	TaV/ <i>taV</i>	71444/1974	acyltransferase MmpIII	<i>Pseudomonas fluorescens</i>	43/58	AAM12912.1
10	TaK	43880/1254	KS I/II PksF	<i>Bacillus subtilis</i> subsp. <i>subtilis</i> strain 168	54/72	NP_389594.1
11	TaX	29229/789	enoyl-CoA hydratase/isomerase	<i>Burkholderia mallei</i> ATTC 23344	56/71	YP_105854.1
12	TaY	24880/666	enoyl-CoA hydratase/isomerase PksI	<i>Bacillus subtilis</i> subsp. <i>subtilis</i> strain 168	65/79	NP_389597.1
13	TaI	229067/6267	Pks type I	symbiont bacterium of <i>Paederus fuscipes</i>	37/51	AAR19304.1
14	TaJ	43715/1179	oxygenase OnnC	symbiont bacterium of <i>Theonella swinhoei</i>	64/79	AAV97871.1
15	TaL	235874/6549	Pks type I	<i>Bacillus subtilis</i> subsp. <i>subtilis</i> strain 168	47/65	NP_389602.2
16	Ta-1/ <i>ta-1</i>	978123/27 135	OnnI PKS	symbiont bacterium of <i>Theonella swinhoei</i>	44/60	AAV97877.1
17	TaN/ <i>taN</i>	53325/1458	dioxygenase MmpIII	<i>Pseudomonas fluorescens</i>	54/74	AAM12912.1
18	TaO/ <i>taO</i>	547875/15318	Pks type I	<i>Bacillus subtilis</i> subsp. <i>subtilis</i> strain 168	47/65	NP_389602.2
19	TaP/ <i>taP</i>	330422/9114	PksM polyketide synthase	<i>Bacillus subtilis</i> strain 168	35/53	NP_389601.2
20	TaQ/ <i>taQ</i>	35468/951	SAM-dependent methyltransferase	<i>Mycobacterium tuberculosis</i>	38/54	NP_217468.1
21	TaT/ <i>taT</i>	37567/1041	unknown, containing DTW repeat domain	<i>Bdellovibrio Bacteriovorus HD 100</i>	33/51	CAE79280
22	TaS/ <i>taS</i>	333/999	radical SAM methyltransferase	<i>Clostridium beijerinckii</i>	31/50	AAS91673

	box 1	box 2	box 3
A)			
KS8	ETACSSS 171	VEAHGTG 307	NIGHLMT 348
KS6	DTACSSS 166	VEMHGTG 304	SIGHTSA 343
KS12	DTACSSS 167	VEAHGTG 303	NLGHATAT 354
KS9	ETACSSS 173	IEAHGTG 309	NIGHLEL 347
KS11	ETACSSS 173	VEAHGTG 309	NIGHLEL 357
KS10	ETACSSS 173	IEAHGTG 309	NIGHLEL 357
KS5	ETACSSS 173	IEAHGTG 309	NIGHLEL 357
KS2	DTMCSSS 178	LEAHGTG 314	NIGHLEA 355
KS4	DTACSSS 162	VEAHGTG 298	NIGHLEA 339
KS7	DTMCSSS 179	VEAHGTG 315	NIGHCES 356
TaI_KS1	DTACSSS 167	IEAHGTG 303	NIGHLEA 349
KS3	NTMCSSA 165	IEAOGMA 302	LTGHMES 349
TaL_KS1	NTMCSSA 171	IEAOGMG 308	MMGHMHS 355
TaL_KS2	DTACSSA 169	VEAHGVS 305	CIGHGEL 351
KS1	HTNCSSS 177	VEAHGTG 313	NLGHLDT 355
TaK	GGASASG 171	VNPHGSG 312	ITGHGLS 346
B)			
KR1	SGGTGALARL 15	APK(X) ₂₃ S(X) ₁₂ YAA 144	
KR4	TGGGGVAVARL 15	APK(X) ₂₃ S(X) ₁₂ YAA 165	
KR8	SGGAGRLGLR 15	WPK(X) ₂₃ S(X) ₁₂ YAA 151	
KR10	TGGAGGLGKR 15	APK(X) ₂₃ S(X) ₁₂ YAA 150	
KR6	TGGLGGLGMI 15	EPK(X) ₂₃ S(X) ₁₂ YAT 151	
TaI_KR1	TGGLGVPVEQ 15	AAK(X) ₂₃ S(X) ₁₂ YGY 151	
KR12	IGGAGGLGG- 14	AAK(X) ₂₃ S(X) ₁₂ YAA 145	
KR2	TGGTGGIGLE 15	APK(X) ₂₃ S(X) ₁₄ YAM 145	
TaL_KR1	VGGGALGLA 13	APK(X) ₂₃ S(X) ₁₂ YAA 145	
C)			
PedD	VAGHSLG 89	SGAFHSRY 196	
PksC	VAGHSLG 89	SGAFHSRY 196	
PksE	AAGHSLG 86	SGAFHSRY 191	
TaV_2	VAGHSLG 85	RAPFHSRY 190	
MmpIII_2	VLGHSLG 74	SAPFHSRY 179	
LnmG	LAGHSLG 90	SAAFHSRH 195	
Lkn_ORF15	LTGHSLG 90	SGAFHSRH 195	
TaV_1	VVGASMG 96	RYPFHSRH 199	
MmpIII_1	VLCSSLG 94	NRPFHSRH 197	
D)			
MT1	VRILEIG GTG 77		
MT2	LRVLEIGAGTG 57		
TaQ	REVLEVGCGRG 118		
E)			
TaC	SACYS 108	AFHTP 244	VGNIM 288
TaF	QACYA 124	AMHTP 252	VGNLC 296
HMG_CoAS	EACYA 113	CFHVP 235	VGNIY 275

Figure 3. Clustal W alignments of the catalytic and conserved domains of: A) β -ketoacyl-ACP synthases (KS), B) β -ketoacyl-ACP reductases (KR), C) acyltransferases (AT), D) methyltransferase (MT), and E) 3-hydroxy-3-methylglutaryl-CoA (HMG-CoA) synthases. The active-site residues are shown in light gray, active-site substitutions are highlighted in dark gray, conserved residues are shown as white letters and are highlighted in dark gray, and similar amino acids are presented as white letters on a black background. The numbers indicate amino-acid positions within sequences and (X)_n indicates the number of amino acids that separate the active-site residues. The accession numbers of acyltransferase homologues are given in parentheses: PedD from *Pederus beetles* (AAS47563), PksC and PksE from *B. subtilis* (NP_389591 and CAB13584), MmpIII from *Pseudomonas fluorescens* (AAM12912), LnmG from *Streptomyces atroolivaceus* (AAN85520), and ORF15 from *Streptomyces rochei* (NP_851437). The accession number of *Staphylococcus aureus* HMG-CoA synthase is AAG02422.

Ketoreductase (KR): Three ketoreductases, KR1, KR2, and KR4, display slight alterations in the Rosmann fold (GxGxxG), which is required for NADP(H) binding (Figure 3 B). However, all nine KR domains contain the completely conserved Lys-Ser-Tyr catalytic triad that is necessary for ketoreduction.^[30]

Dehydratases (DH): All seven DH domains encoded in the cluster contain a conserved His (X)₁₃ Glu signature, in which His and Glu form a catalytic diad that is required for enzymatic activity.^[29]

Enoyl reductases (ER): The myxovirescin cluster encodes two ER domains. Both of these show high identity with Zn-dependent alcohol dehydrogenases (Conserved domain search: COG1064), as well as with enoyl reductases from other systems. Whereas both ERs possess the conserved catalytic Tyr and Lys residues,^[29] they occupy unusual positions within PKS modules (see below).

Acyl-carrier proteins (ACP): All ACPs encoded in the cluster show the conserved catalytic Ser residue.

Acyltransferases (AT): The myxovirescin cluster has only one atypical AT domain encoded within its functional modules (see below). Two more acyltransferases (AT1 and AT2; Table 2) are encoded discretely on the same open reading frame designated *taV*. Both AT1 and AT2 contain a conserved active-site Ser, as well as a His residue that is specific for the binding of malonyl-CoA.^[31] In a BLAST search, TaV showed the highest similarity to AT domains found in pederin, mupirocin, leinamycin, and lankacidin clusters (Figure 3C). All these biosynthetic gene clusters lack ATs as integral part of their modules and are referred to as "AT-less" or "*trans*-AT" type I PKSs,^[32] instead, they contain separately encoded ATs that

Table 2. List of myxovirescin biosynthetic enzymes containing PKS/NRPS domains.

Protein	Size(Da)	Encoded domains with coordinates in the protein sequence	
TaV	71444		AT1 (1-330), AT2 (363-658)
TaK	43880		KS ^S
TaI	229067		GNAT (559-629), ACP (767-808) KS (839-1263), KR (1694-1875), ACP (2014-2079)
TaL	235874		KS (32-460), KR (1091-1248), ACP (1344-1410)
Ta-1	978123	NRPS module	C (98-538), A (537-1041), PCP (1063-1125)
		Module 1	KS1 (1154-1582), KR1 (1932-2109), ACP1 (2200-2257)
		Module 2	KS2 (2300-2737), KR2 (3357-3543), ACP2 (3668-3724)
		Module 3	KS3 (3759-4181), ACP3 (4391-4443)
		Module 4	KS4 (4474-4893), KR4 (5547-5730), ACP4 (5823-5880)
		Module 5	KS5 (5929-6365), ACP5 (6621-6680)
		Module 6	KS6 (6736-7155), DH6 (7360-7511), KR6 (7819-8002), ACP6 (8097-8152)
		Module 7	KS7 (8198-8634), ACP7 (8938-8997)
TaO	547875	Module 8	ER8 (58-356), KS8 (409-831), DH8 (1041-1179), KR8 (1474-1662), ACP8 (1759-1812)
		Module 9	KS9 (1873-2309), DH9 (2500-2666), ACP9 (2830-2886)
		Module 10	KS10 (2945-3381), DH10 (3564-3736), KR10 (4027-4226), ACP10 (4327-4384), KS10 (4458-4893)
TaP	330422	Module 11	MT11 (101-382), ACP11 (399-446)
		Module 12	KS12 (502-922), KR12 (1615-1799), MT12 (2008-2280), ACP12 (2294-2345), ER12 (2294-2345), TE12 (2756-2919)

are thought to act iteratively. Recently, myxobacterial biosynthetic gene clusters responsible for the production of disorazol and chivosazol have also been reported to have such gene organization.^[33-34] Nevertheless, only mupirocin and myxovirescin biosynthetic gene clusters contain two AT domains that are encoded as one ORF.

Methyltransferases (MT): Even though feeding studies with ¹³C-labeled precursors indicate the incorporation of four methyl groups (derived from methionine) into myxovirescin^[16] (Figure 2 A), only three putative SAM-dependent MT domains are found to be encoded in the cluster. Two of these MT domains, MT11 and MT12, are located within modules 11 and 12 of TaP (Table 2). The third putative SAM-dependent MT is encoded by

taQ, which is immediately downstream of *taP*. All three MTs contain the conserved SAM-binding motif, V(I)LEV(I)GXG^[35] (Figure 3 D). The only candidate that can carry out the fourth methylation is TaS, and the corresponding gene is located at the 3' end of the cluster, about 2.7 kb downstream of *taQ* (Figure 2 A).

HMG-CoA synthases/β-ketoacyl-ACP synthase III (FabH): The *taC* and *taF* gene products show similarity to HMG-CoA synthases and β-ketoacyl-ACP synthases III (FabH). The closest homologues of TaC are putative HMG-CoA synthases (PksG) from *Bacillus subtilis* subsp. *subtilis* strain 168 (66% identity, 80% similarity) and JamH from *Lyngbya majuscula* (64% identity, 77% similarity). TaF shares the highest similarity with the putative HMG-CoA synthases LnmM from *Streptomyces atroolivaceus* (62% identity, 75% similarity), and CurD from *L. majuscula* (47% identity, 65% similarity). Furthermore, both TaC and TaF share the conserved Cys-His-Asp catalytic triad with numerous HMG-CoA synthases that are involved in the mevalonate pathway, including that from *Streptococcus aureus* (Figure 3 E).^[36]

Genetic analysis of the myxovirescin biosynthetic gene cluster

To elucidate the function of individual genes in myxovirescin biosynthesis, large regions of *taV* that encode the AT1 and AT2 domains, as well as large regions of *taI* and *taL* PKSs, were deleted in-frame to ensure the absence of polar effects on downstream ORFs (Tables 2 and 3). In addition, the putative methyltransferase, *taQ*, which is located at the very end of the gene cluster (Figure 2 B), was disrupted by plasmid insertion. Wild-type DK1622 and mutant cells that were fermented with XAD adsorbent resin were extracted with methanol (see Experimental Section) and analyzed by HPLC. Unlike wild-type *M. xanthus* DK1622, which produces myxovirescins A and C (Figure 1A), both ΔtaV (VS1017) and *taQ* (VS1016) mutant extracts showed loss of myxovirescin production (Figure 1 B and C). In addition, the

Table 3. List of plasmids and strains used in the study.

Plasmid	Description of construction
pVS23	639 bp PCR product amplified by using primer pair taV1 and taV2, which contained <i>NotI</i> and <i>SpeI</i> restriction sites, respectively, and cloned into pCR2.1-TOPO
pVS26	662 bp PCR product amplified by using primer pair taV3 and taV4, which contained <i>SpeI</i> and <i>SacI</i> sites, respectively, and cloned into pCR2.1-TOPO
pVS27	1295 bp fragment derived by ligating the 639 bp insert from pVS23 (digested with <i>NotI</i> and <i>SpeI</i>) with the 662 bp insert from pVS26 (digested with <i>SpeI</i> and <i>SacI</i>); product was cloned into the <i>NotI</i> and <i>SpeI</i> sites of pSWU41
pVS50	580 bp PCR product generated by using primer pair taI1 and taI2, which contained <i>XbaI</i> and <i>BamHI</i> sites, respectively, and cloned into pCR2.1-TOPO
pVS51	578 bp PCR product generated by using primer pair taI3 and taI4, which contained <i>BamHI</i> and <i>SpeI</i> sites, respectively, and cloned into pCR2.1-TOPO
pVS52	1152 bp fragment derived by ligating the 580 bp insert from pVS50 (digested with <i>XbaI</i> and <i>BamHI</i>) and the 578 bp insert from pVS51 (digested with <i>BamHI</i> and <i>SpeI</i>); product was cloned into the <i>XbaI</i> and <i>SpeI</i> sites of pSWU41
pVS48	564 bp PCR product generated by using primer pair taL1 and taL2, which contained <i>XbaI</i> and <i>BamHI</i> sites, respectively, and cloned into pCR2.1-TOPO
pVS49	563 bp PCR product generated by using primer pair taL3 and taL4, which contained <i>BamHI</i> and <i>SpeI</i> sites, respectively, and cloned into pCR2.1-TOPO
pVS61	1121 bp fragment derived by ligating the 564 bp insert from pVS48 (digested with <i>XbaI</i> and <i>BamHI</i>) and the 563 bp insert from pVS49 (digested with <i>BamHI</i> and <i>SpeI</i>); product was cloned into the <i>XbaI</i> and <i>SpeI</i> sites of pSWU41
pVS16	450 bp PCR product amplified by using the taQ_knock_frw and taQ_knock_rev primer pair, and cloned in pCR2.1-TOPO
pVS75	824 bp PCR product amplified by using taOseq_up and taOseq_down primer pair, and cloned into pCR2.1-TOPO
<i>M. xanthus</i> strains	Genotype description
DK1622	Wild type
VS1017 (ΔtaV)	Δ 1455 bp encoding for AT1 and AT2
VS1024 (ΔtaI)	Δ 4044 bp encoding for ACP-KS-KR-ACP domains
VS1025 (ΔtaL)	Δ 2382 bp encoding for ACP-KS-ACP domains
VS1029 ($\Delta taLL$)	Δ 4044 bp encoding for ACP-KS-KR-ACP of <i>taI</i> and Δ 2382 bp encoding for ACP-KS-ACP of <i>taL</i>
VS1016 (<i>taQ</i>)	merodiploid mutant created by homologous recombination of pVS16 into the genome of <i>M. xanthus</i> DK1622

taQ knockout produced two novel metabolites with retention times of 13.9 and 18.5 min (Figure 1 C); these were found to be in the same 5:1 ratio as **1** and **2** in the wild-type cells.

Investigation of ΔtaI and ΔtaL mutant extracts by HPLC-MS revealed that both *M. xanthus* strains VS1024 and VS1025 display a dramatic drop in antibiotic production compared to the wild-type cells (Figure 4 A-C). In order to determine their exact concentrations, we developed a quantitative HPLC-MS method that can quantify **1** down to 1 ng mL⁻¹ (Experimental Section). Using this method, we measured an approximately 100000-

fold drop in myxovirescin production in both ΔtaI and ΔtaL mutants, in comparison to wild-type production levels (data not shown). To test whether myxovirescin production persists in the absence of both TaI and TaL PKSs, a double $\Delta taIL$ mutant was created (VS1029) and analyzed in the same fashion. Deletion of large regions of both genes in strain VS1029 clearly led to complete abolishment of myxovirescin production (Figure 4 D).

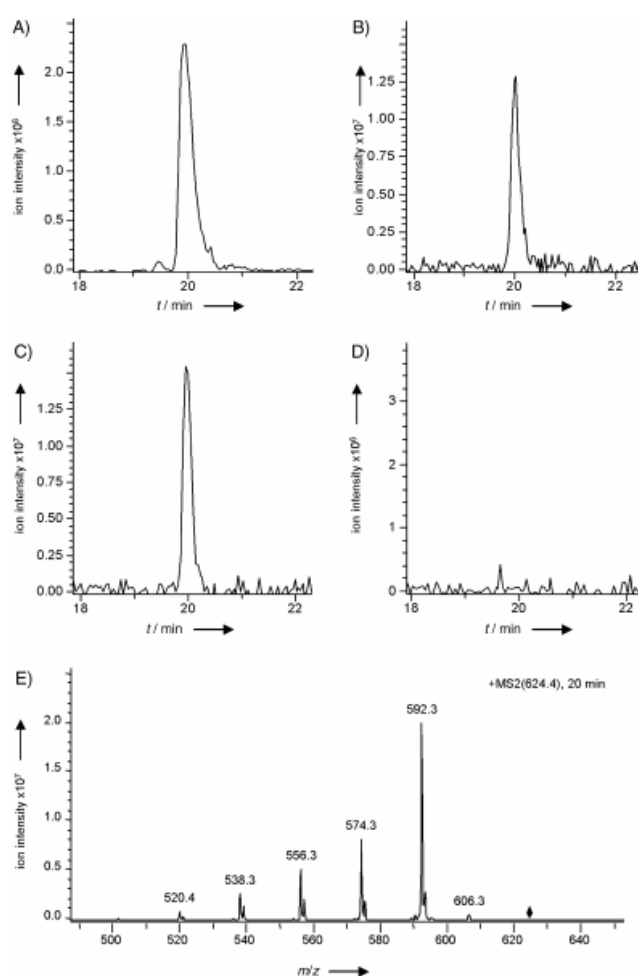


Figure 4. Extracted ion-mass chromatograms (EIC) of myxovirescin A from A) wild-type DK1622, B) ΔtaI PKS (VS1024), C) ΔtaL PKS (VS1025), and D) $\Delta taIL$ double PKS mutant (VS1029). The high detection ability of the HPLC/MS analysis revealed miniscule levels of **1** in ΔtaI and ΔtaL mutants (see Experimental Section). Nevertheless, deletion of both PKS-encoding genes in $\Delta taIL$ mutants led to complete abolishment of myxovirescin production. E) MS-MS fragmentation pattern of **1**.

TaQ is an *O*-methyltransferase specific for the C29 oxygen

To elucidate the role of *taQ* methyltransferase, the novel product with the 13.9 min retention time (Figure 1 C; exact mass of 610.43248 $[M+H]^+$ and molecular formula $C_{34}H_{60}NO_8$) was purified from XAD-adsorbent beads that were cofermented with *M. xanthus* VS1016 culture (8 L), and used for detailed NMR analysis (Table 4).

MS analysis confirmed the postulated loss of m/z 14 expected for the loss of one methyl group. In addition, 1H and ^{13}C NMR spectroscopy data of **3** (Scheme 1A and Table 4) were similar to those observed for myxovirescin A,^[37] and revealed C20 and C4 ketones ($\delta_C =$

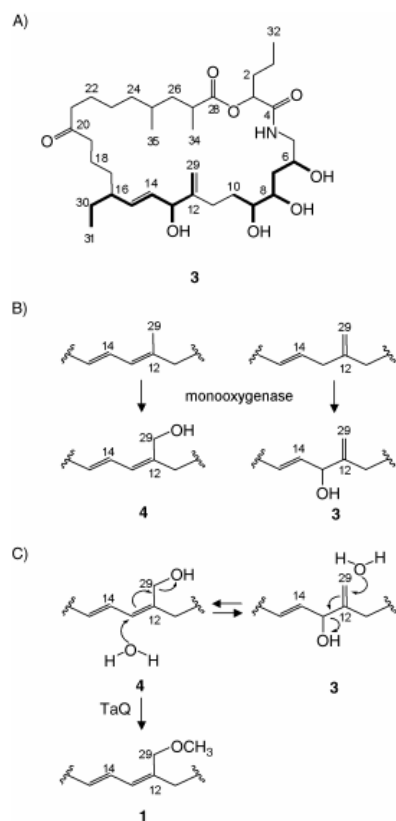
Table 4. NMR data of **3** in $CDCl_3$.

Carbon	^{13}C	1H J (Hz)	m	Carbon	^{13}C	1H J (Hz)	m
1	18.1	1.36	m	18	21.8	1.69 1.34	m m
2	34.2	1.82	m	19	42.9	2.40 2.22	m m
3	73.2	5.24	m	20	212.5	-	-
4	171.6	-	-	21	42.4	2.39	m
5	44.8	3.5	m	22	23.5	1.53	m
6	69.8	3.96	m	23	26.5	1.24 1.14 (7)	s d
7	37.4	2.12 1.48	m m	24	36.6	1.34 1.06	m m
8	71.8	3.6	m	25	30.2	1.24	s
9	80.0	3.3	m	26	41.2	1.63 1.28	m m
10	29.4	2.09 1.37	m m	27	36.8	2.60	m
11	31.9	2.5 2.26	m m	28	175.8	-	-
12	146.4	-	-	29	108.3	4.79 4.77	s s
13	80.6	4.21 (9)	d	30 *	34.2	1.82	m
14	129.2	5.50 (15/8)	dd	31	12.0	0.84 (7)	t
15	139.7	5.30 (15/11)	dd	32	13.7	0.92 (7)	t
16	45.1	1.89	m	33	17.4	1.14 (7)	d
17 *	34.11	1.41 1.09	m m	34	20.0	0.85 (7)	d

* indicate interchangeable carbons

212.5 and $\delta_C = 171.6$, respectively), a C28 ester ($\delta_C = 175.8$), and a secondary amide ($\delta_H = 6.78$), together with four secondary alcohols specific to carbons C3, C6, C8, and C9. Overall,

the upper part of **3** was found to be in good agreement with that of **1**, whereas the lower part of the molecule (C5-C15, including C29) indicated structural changes. In addition, the spectra of **3** lacked signals for a methoxy group. Moreover, an additional resonance specific for a secondary alcohol connected to C13 appeared at $\delta_{\text{C}} = 80.6$ and $\delta_{\text{H}} = 4.21$. Another deviation between the two compounds was specific to the positions of two double bonds. Whereas **1** displays a conjugated, disubstituted system specific to C12 and C14 in the macrocycle, careful analysis of the chemical shifts of **3** revealed two isolated double bonds; one of them comprised an *exo*-methylene group made of a quaternary carbon C12 ($\delta_{\text{C}} = 146.4$), and C29 ($\delta_{\text{C}} = 108.3$; $\delta_{\text{H}} = 4.79$ and 4.77 , both broad s).



Scheme 1. A) Structure of a novel desmethyl analogue of myxovirescin A (**3**) elucidated by NMR spectroscopy. The bonds shown in bold indicate two fragments deduced from ^1H , ^1H COSY and HSQC correlations. B) Hydroxylations of two postulated intermediates that result from PKS/HMG-CoA reactions. According to the first possibility, hydroxylation at C29 of the diene-containing myxovirescin precursor produces intermediate **4**, whereas hydroxylation at C13 of the *exo*-methylene-like myxovirescin precursor yields **3**. C) Hypothetical conversion of **3** into **4** and vice versa, which could take place either by enzymatic or nonenzymatic isomerization, might explain the existence of **3** as the main structure revealed by NMR

spectroscopy. In wild-type cells, **4** acts as a substrate for TaQ to yield mature myxovirescin A (**1**).

The structure of the C5-C15 fragment, which includes C29, was deduced from ^1H , ^1H COSY and HSQC spectra. This allowed the construction of the two fragments shown in bold in Scheme 1 A. The first fragment (C12-C16) contains two double bonds separated by a secondary-alcohol function at C13. In the ^1H , ^1H COSY, two *exo*-methylene protons of C29 showed long-range couplings to the broad doublet of the methine proton of C13, which showed further vicinal correlation to the olefinic proton of C14 at $\delta_{\text{H}} = 5.50$. The other olefinic proton ($\delta_{\text{H}} = 5.30$) showed the same neighbourhood as in **1** and was therefore assigned to C15. The ^1H , ^1H COSY of the second fragment (C5-C11) indicated a complete conservation of the connectivity in this part of the molecule. The confirmation of the

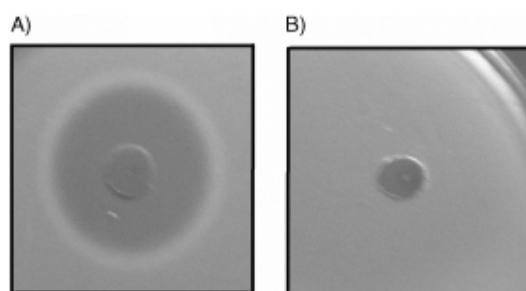


Figure 5. A) Antibiotic-activity test performed with myxovirescin A (10 μg) and B) its desmethyl analogue **3**, which were spotted on a filter disc and layered on the lawn of *E. coli* XL-1 blue cells. The lack of inhibition by **3** suggests the indispensability of *O*-specific methylation for the antimicrobial activity of the myxovirescin antibiotic.

structure for **3** was performed by using NMR prediction tools, which calculated similar resonance values for the respective carbon and hydrogen atoms. To our surprise, the *O*-desmethyl analogue of **1** failed to inhibit *E. coli* growth in the standard antibiotic assay (Figure 5).

Proposed biosynthesis of myxovirescin A

The myxovirescin gene cluster belongs to the "*trans*-AT" type of natural product

biosynthetic gene clusters

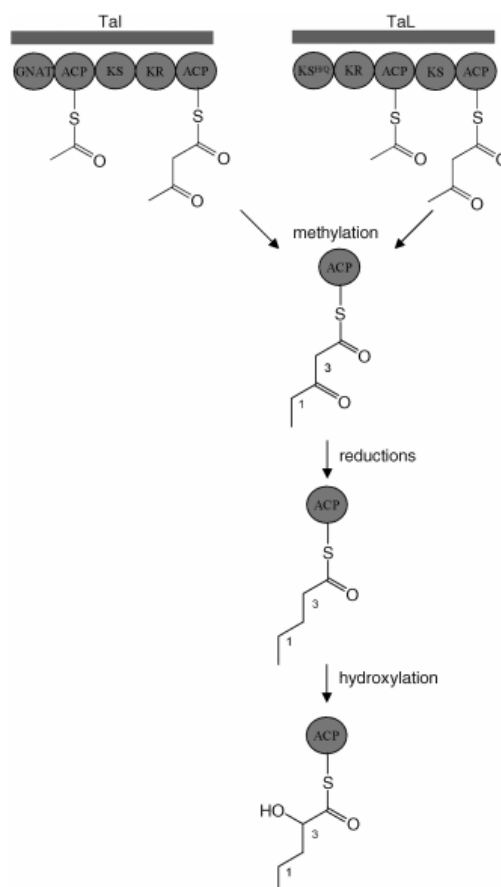
All modules of the myxovirescin biosynthetic gene cluster-with the exception of the first module of TaI-lack AT domains. Instead, two acyltransferase domains are encoded by *taV* (Table 2). Based on the biochemical evidence that indicates the "*trans*" activity of acyltransferase LnmG of the leinamycin system, which is shown to load malonyl-CoA on every ACP of leinamycin megasynthetase,^[38] we assumed a similar function for TaV. This hypothesis was confirmed by an in-frame deletion of *taV*, which led to a myxovirescin-negative phenotype (Figure 1B).

Starter biosynthesis

Feeding studies and the overall organization of the myxovirescin gene cluster suggest that biosynthesis of the myxovirescin starter unit takes place by fusion of an acetyl-S-ACP with malonyl-S-ACP. This is followed by subsequent methylation of the C1 carbon, reductions of C2, and hydroxylation of C3 (Scheme 2). The likely candidates for the first biosynthetic step are one or both of the first two modular PKSs, TaI and TaL.

TaI contains a peculiar GNAT domain (see below), followed by ACP-KS-KR-ACP domains. The GNAT superfamily of acetyltransferases perform nitrogen-specific acetylation reactions on a wide range of substrates, including glycosides, either to achieve antibiotic resistance,^[39] or to tolerate their own phytotoxins.^[40] The GNAT domain of the myxovirescin gene cluster shows close similarity to such domains found in the onnamide, pederin, and curacin A biosynthetic systems.^[9, 41, 42] However, the function of GNAT domains in these systems remains obscure. Although the GNAT domain in myxovirescin biosynthesis

could catalyze the transfer of the starter moiety to the nitrogen atom of glycine, a more likely candidate for this reaction is the C domain of the NRPS module of Ta-1 (see below).



Scheme 2. Two possible routes to starter biosynthesis. Both TaI and TaL could catalyze the first biosynthetic reaction of fusing acetyl-*S*-ACP with malonyl-*S*-ACP to yield acetoacetyl-*S*-ACP. Acetoacetyl-*S*-ACP would have to undergo methylation at C1, followed by reductions of C2, and final hydroxylation at C3 to yield the C3-hydroxyvaleryl-ACP starter.

Starter biosynthesis could be initiated by loading of CoA-activated acetate and malonate onto the two ACPs of TaI by the TaV "*trans*-ATs," each of which might be responsible for transferring one substrate. Next, the TaI KS might catalyze their decarboxylative condensation to form an acetoacetyl-*S*-ACP (Scheme 2).

The other PKS, TaL, consists of KS-KR-ACP-KS-ACP domains. The first KS domain of TaL (TaL-KS1) contains a His to Gln substitution in the conserved box 2 (Figure 3 A), which most likely renders it inactive as a condensing enzyme.^[29] This mutant KS, referred to

in the text as KS^{H/Q}, should be distinguished from KS^Q synthase mutants which have characteristic active-site Cys to Gln substitutions.^[43, 44] The KS^{H/Q} mutation, also observed in KS1 of MmpA of the mupirocin biosynthetic gene cluster, was shown to be indispensable for mupirocin production, both by deletion of the whole KS domain and by point mutation of the active-site Cys to Ala. El-Sayed et al. proposed that KS^{H/Q} might act as a pseudo-loading module that either enables the transfer of an intermediate from MmpD to MmpA or loads the starter on MmpD.^[11] Whereas KS^{H/Q} could help to load the acetyl-CoA onto TaL-ACP1, KS^{H/Q}-mediated transfer of intermediates from TaI to TaL is not plausible because it would increase the length of the presumed starter unit from 4 to 6 carbons. Finally, TaL-KS2 might catalyze decarboxylative condensation of acetyl-S-ACP and malonyl-S-ACP to yield acetoacetyl-ACP.

Irrespective of whether TaI or TaL performs the first biosynthetic step of fusing acetyl-S-ACP with malonyl-S-ACP, both PKSs lack adequate biosynthetic domains that are needed for the full reduction of the C2 carbon. This suggests an additional interplay of "trans"-acting reductive domains in starter assembly. SAM-derived methylation at the C1 position might be carried out by TaS (Table 1) early during starter biosynthesis, whereas oxygenation of C3 could be carried out by the TaJ monooxygenase, the gene for which is found to be transcriptionally coupled to *taL* (Scheme 2).

To find out which PKS carries out the first biosynthetic step, we have separately deleted ACP-KS-KR-ACP coding regions of *taI* and ACP-KS-ACP coding regions of *taL* (Table 3), and analyzed production of **1** in the resulting mutants. To our surprise, quantitative HPLC-MS analysis of both ΔtaI and ΔtaL extracts indicated approximately 100000-fold reduction in myxovirescin production compared to the wild-type strain. To further clarify whether precursor biosynthesis is dependent on the presence of TaI and TaL PKSs, channeled

from the metabolic pool, or simply a product of another PKS encoded in the genome, a double *ΔtalL* mutant was created (Table 3). The complete loss of myxovirescin production in *ΔtalL* mutants (Figure 4 D) rules out the second and third possibility and indicates the direct involvement of TaI and TaL PKSs in starter biosynthesis. Furthermore, basal levels of **1** in *Δtal* and *ΔtalL* and its absence in *ΔtalL* mutants argue that either PKS (TaI or TaL) is adequate for starter biosynthesis and myxovirescin production, and eliminates the possibility of transfer of an intermediate from TaI to TaL during biosynthesis. Moreover, involvement of TaI and TaL in later steps of polyketide assembly seems equally unlikely due to the good agreement of the proposed biosynthetic pathway with the enzymatic functions of Ta-1, TaO, and TaP (see below). Finally, the dramatic reductions of myxovirescin production in *Δtal* and *ΔtalL* mutants suggests that both TaI and TaL are required for wild-type levels of antibiotic production- possibly by adding to the structural stability of the myxovirescin megasynthetase.

Assembly of myxovirescin A combines HMG-CoA synthase and PKS/NRPS enzymology

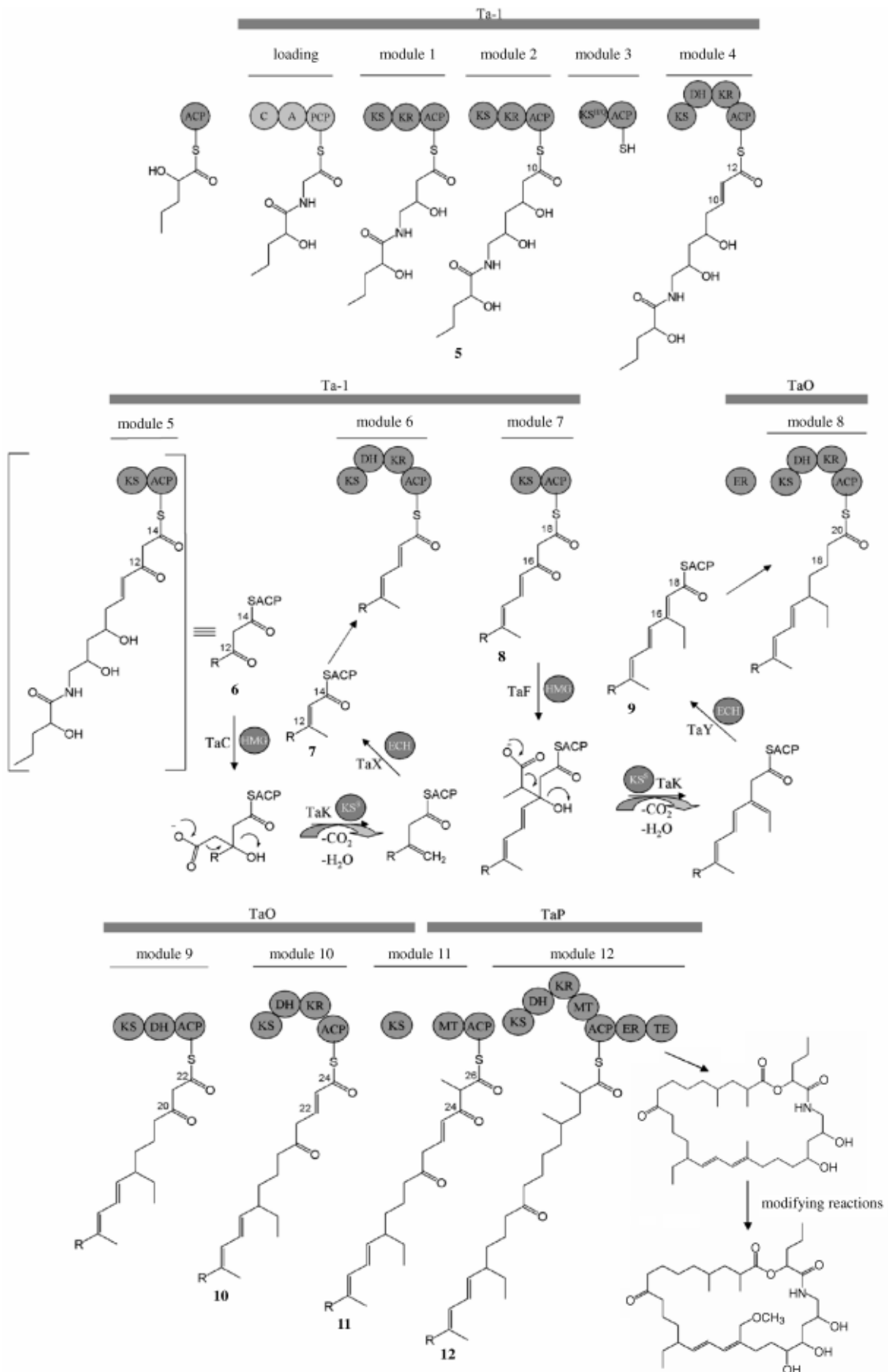
Following biosynthesis of the putative starter moiety, 2-hydroxyvaleryl-S-ACP, the NRPS module located at the N terminus of Ta-1 extends this molecule with glycine. The adenylation domain shows a very good agreement with the conserved core region that is specific for activation of glycine (DILQLGMIWK)^[45] This confirms the results obtained from isotope-labeling experiments.^[27] Consistent with **1**, modules 1 and 2 are expected to follow typical PKS assembly-line logic to yield intermediate **5** (Figure 6).

Module 3 consists of an ACP with the conserved active-site Ser, and a KS^{H/Q} β-ketosynthase, which is thought to be capable of binding the intermediate to the active-site Cys, but which is defective in decarboxylation of the substrate required for elongative condensation (see above). Even though module 3 is not likely to be involved in the extension of **5**, it might be involved in the transfer of the acyl chain to module 4 either through KS3^{H/Q}

and ACP3, or directly through ACP3. Mutagenesis studies performed on KS1^{H/Q} of the mupirocin system have shown that its active-site Cys is essential for mupirocin production.^[11] In addition, the above hypothesis is also supported by extensive studies of the PikAIV PKS that harbors the last module (module 6) of the pikromycin PKS. This module was thought to be skipped when the shorter, 10-deoxymethynolide hexaketide was produced instead of the heptaketide narbonolide. However, contrary to expectations, active-site mutagenesis (KS, AT, and ACP) of module 6 proved essential, leading to a model that proposed transacylation of the product by KS6 and ACP6 without its subsequent elongation.^[46] TaK KS^S carries out the second round of decarboxylation and dehydration reactions, while the second enoyl-CoA hydratase/isomerase, TaY, performs the final isomerization to yield intermediate **9**. If it is not

Figure 6. The proposed biosynthesis pathway of myxovirescin A switches two times from PKS to HMG-CoA synthase biochemistry. The enzymatic domains are: KS: β -ketosynthase, KS^{H/Q}: nonfunctional KS, AT: acyltransferase, KR: ketoreductase, DH: dehydratase, ER: enoylreductase, MT: methyltransferase, ACP: acyl-carrier protein, TE: thioesterase, C: condensation domain, A: adenylation domain, PCP: peptidyl-carrier protein, HMG: 3-hydroxy-3-methylglutaryl synthase, ECH: enoyl-CoA hydratase, KS^S: decarboxylase. Intermediate **6** attached to ACP5 is shown in abbreviated form to accentuate its resemblance to acetoacetyl-CoA. During the first round of "HMG-box" reactions, TaC is predicted to add acetate onto the β -keto position of **6**, while the KS^S, TaK, performs sequential decarboxylation and dehydration. The modified product undergoes final isomerization by the TaX enoyl-CoA hydratase to yield intermediate **7**. Intermediate **7** is then subjected to two more rounds of PKS extensions directed by modules 6 and 7 to form intermediate **8**. In the second round of HMG-box reactions, TaF adds propionyl-CoA onto the β -keto position of **8**, TaK KS^S carries out the second round of decarboxylation and dehydration reactions, while the second enoyl-CoA hydratase/isomerase TaY performs the final isomerization to yield intermediate **9**.

Chapter 2



transferred by module 3, **5** might alternatively be moved directly from ACP2 to KS4 and thereby completely bypasses module 3. An example for such a mechanism was recently found in the NRPS system that encodes for myxochromide S, in which module 4 was shown to be completely skipped during biosynthesis.^[47]

Following transfer of **5** to KS4, module 4 is proposed to contribute with another extension unit while performing β -ketoreduction and dehydration on C10, whereas minimal module 5, which consists of only KS and ACP domains, leads to the formation of intermediate **6**. The isotope labeling scheme, which indicates the addition of a C2 atom of acetate at carbon C12 (Figure 2 A), and structural analogy of intermediate **6** with acetoacetyl-CoA (Figure 6), suggest that intermediate **6** might be the substrate of a HMG-CoA synthase-like enzyme.

HMG-CoA synthases perform Claisen condensation by mediating the attack of acetyl-CoA on the β -keto group of acetoacetyl-CoA.^[36] Following addition of acetate at the C12 keto carbon of **6**, sequential decarboxylation, water elimination (possibly involving activation of the hydroxyl group), and isomerization reactions would be required to obtain intermediate **7**. In our model, TaC HMG-CoA synthase is depicted to add acetate, TaK β -keto synthase with the Cys to Ser active-site substitution (KS^S) would carry out the decarboxylation, and the enoyl-CoA hydratase (ECH), TaX, would perform the isomerization reactions (Figure 6). The assignment of TaK as decarboxylase was based on biochemical studies of Cys to Ser KS point mutants in *E. coli*. For instance, a Cys to Ser mutant of KSI was shown to bind and decarboxylate myristic acid. However, the enzyme's ability to perform condensation was severely compromised.^[48] In addition, a Cys to Ser mutant of *E. coli* KSIII exhibited a 425% higher decarboxylation activity than the wild type.^[49] Decarboxylation enzymes such as KS^S might be needed to compensate for the

presence of a poor leaving group, such as hydroxyl, which is found in the proposed intermediate (Figure 6). In the mevalonate pathway this situation is circumvented by activation of the hydroxyl by phosphorylation.^[50] However, no gene encoding for a hypothetical kinase could be found in the myxovirescin gene cluster.

Modules 6 and 7, which encode the same repertoire of catalytic domains as modules 4 and 5, are expected to yield compound **8**. This intermediate, which is attached to the ACP located at the C terminus of the Ta-1 megasynthetase, is presumed to act as a nucleophile in the second reaction catalyzed by a HMG-CoA synthase; the latter now uses propionyl-CoA instead of acetyl-CoA as substrate (see below). Addition of propionyl-CoA onto C16 by HMG-CoA synthase (TaF) followed by sequential decarboxylation (TaK), water elimination, and isomerization (TaY) are hypothesized to give rise to intermediate **9**.

Conclusive data confirming the incorporation of propionate rather than acetate at carbon C16 came from the analysis of ¹³C NMR spectra obtained from myxovirescin-producing *M. virescens* strain Mx v48 that were fed with [2,3-¹³C₂]-succinate. This experiment indicated incorporation of an intact [2,3-C₂]-succinate-derived unit into **1**, which was likely achieved by conversion of succinyl-CoA into propionyl-CoA.^[16]

KS^S and ECH homologues have been found in all natural product biosynthetic gene clusters that harbor HMG-CoA synthases,^[11-12, 28, 42, 51] and HMG-CoA synthase-based mechanisms for the incorporation of methyl groups have been proposed for mupirocin and pederin biosynthesis.^[10-11] However, myxovirescin is the first system where a HMG-CoA synthase (TaF) is postulated to act upon a substrate other than acetyl-CoA, and to contain two HMG-CoA synthases (TaC and TaF) and two enoyl-CoA hydratases (TaX and TaY). Nevertheless, only one decarboxylative enzyme KS^S (TaK) is present in the cluster and is

depicted to act after both HMG-CoA synthases. Similar to models published recently by Gerwick's group for curacin and jamaicamide biosynthesis,^[12, 42] the two isomerization reactions are thought to be carried out by TaX and TaY enoyl-CoA hydratases/isomerases.

After the second round of HMG-CoA-like modifications, biosynthesis switches back to PKS biochemistry. Intermediate **8**, which is attached to ACP7 of Ta-1, is further reduced by the ER domain of TaO and transferred to module 8 where another extension with malonyl-*S*-ACP, keto reduction, and dehydration is performed. The ER domain encoded prior to module 8 is expected to complete this set of reductive reactions. Module 9 (KS-DH-ACP) is predicted to extend the polyketide with one more malonyl-*S*-ACP unit. Although DH9 contains the conserved active site, it is unlikely to act without a KR domain. This observation is consistent with the intact keto functionality at C20 of myxovirescin A. Further, module 10 (KS-DH-KR-ACP) introduces the next malonyl-*S*-ACP unit followed by β -ketoreduction at C22.

Module 11 is physically split between TaO and TaP PKSs (Figure 6) and the KS domain of TaP is most likely complemented with MT and ACP domains of TaO to create a functional module 11. To eliminate the possibility of a frame shift due to errors in sequencing, a 0.84 kb region covering the end of *taO* and beginning of *taP* was cloned and resequenced (Experimental Section). The results confirmed the validity of the sequence. Furthermore, this module lacks reductive domains that are expected to saturate C24.

Finally, module 12 has the full reductive capacity to saturate the C26 keto group, while the MT domain is most likely responsible for methylation of C27. In the last step, the linear product attached to ACP12 undergoes cyclization by nucleophilic attack of the C3 hydroxy oxygen onto the C28 carbonyl to generate the basic myxovirescin lactone fold.

Reductive reactions

Three out of nine ketoreductase domains contain alterations in the Rosmann fold (GxGxxG). KR1 and KR4 contain a conserved Gly to Ala substitution (GxGxxA), which is also present in KR1 and KR2 of avermectin.^[52] KR2 has a nonconserved Gly to Arg substitution, which judging from several KRs with the identical substitution, is also most likely to be active.^[53, 54]

The myxovirescin gene cluster harbors only two out of the five expected ER domains, and three double bonds, C10=C11, C16=C17, and C22=C23, as well as the C24 keto group, require reduction (Figure 6). It is interesting to notice that the two ERs take unusual positions within PKS modules; one ER, for example, precedes KS8. Taking into account that, typically, the start of a module is defined with a KS and its end with an ACP or TE domain, this ER cannot be functionally assigned to either module 7 (KS-ACP) or module 8 (KS-DH-KR-ACP), to which it translationally belongs. However, our hypothetical scheme suggests a need for enoylreductase within both modules 7 and 8. Accordingly, the first enoyl reduction would saturate the C16=C17 double bond of intermediate **9**, while the second reduction would occur after extension of **9** by module 8 and aid KR8 and DH8 in the full reduction of the C18 ketone. Therefore, the ambiguous positioning of the ER domain at the interface of modules 7 and 8, along with our proposed assembly scheme, raises the possibility that this ER is actively shared by two modules that are encoded on two proteins.

Further, analysis of modules 10 and 11 suggests that module 10 “lacks” an ER domain that is needed for saturating the C22=C23 double bond. Furthermore, the “split” module 11, in TaO and TaP PKSs, “lacks” a complete reductive loop that is expected to saturate the C24 ketone. However, the last module (module 12) contains all three reductive domains, with the ER unusually positioned between the ACP and TE domains. We postulate

that all the above-mentioned reductive reactions take place on intermediate **12** within module 12. This model would explain the physical separation of the ER from the KR and DH domains within this module, and would allow the domain to act iteratively and independently of the other two reductive domains. Alternatively, intermediates **10** and **11** would have to skip from their respective modules to module 12 and back, in order to achieve the expected reductions before the intermediates are passed to module 12 for the final cycle of extension and modification.

Split modules and shared domains

Besides the presence of HMG-CoA synthases, KS^S and ECH (HMG-CoA box), and irregularly distributed reductive domains, the complexity of myxovirescin programming is also evident in the occurrence of modules that appear on two proteins and, therefore, can be classified as "split." This situation is encountered in module 11 where the KS domain encoded at the C terminus of TaO is likely complemented with MT and ACP domains of TaP. Split modules are encountered rather frequently in myxobacterial natural product clusters.^[33-34, 55]

Module 7 can also be considered as split as it consists of KS and ACP domains, which are presumably complemented by the HMG box, and finally reduced by the ER domain of TaO. In this particular case, the need for a split module is well rationalized with the proposed reaction mechanism, which suggests the interference of the HMG-CoA box in product assembly, and therefore requires an intact acetoacetyl-S-ACP-like intermediate. However, the "irregular" positioning of the ER domain at the interface of modules 7 and 8 can also be regarded as a "shared" domain.”

Auxiliary modifications

In addition to the required oxygenation at the C3 position- most likely carried out by the TaJ monooxygenase- two more oxidative enzymes, TaH cytochrome P450-dependent oxygenase and TaN dioxygenase (Table 1), are expected to perform hydroxylations at C9 and C29. MT11 and MT12, encoded within the TaP PKS, are expected to methylate carbons C25 and C27.

By inactivating *taQ* in *M. xanthus* DK1622, we were able to demonstrate a shift in the production of **1** and **2** toward two novel metabolites (Figure 1 C). Furthermore, NMR analysis of the novel compound with m/z 610 $[M+H]^+$ has revealed the loss of the methoxy group specific to C29. Therefore, this provides clear evidence that TaQ functions as the *O*-methyltransferase (Scheme 1 A). However, contrary to the predicted hydroxyl functionality connected to C29, NMR analysis of **3** revealed an *exo*-methylene specific to this position, whereas the hydroxyl group was found to be attached to carbon C13 (Scheme 1 A).

Since either an *exo*-methylene or a diene intermediate might be produced by the HMG-CoA-dependent addition of the methyl group (Figure 6), two options that lead to myxovirescin A biosynthesis can be envisioned (Scheme 1 B). The first possibility is that hydroxylation of the diene-containing intermediate at C29 yields **4**, which serves as a substrate for TaQ to yield myxovirescin A. The second scenario postulates hydroxylation of the *exo*-methylene intermediate at C13 to yield structure **3**, which was defined by NMR spectroscopy. Intermediate **3** could be isomerized to **4** and methylated by TaQ (Scheme 1C). The second pathway suggests a dual role for TaQ as both isomerase and methyltransferase. Therefore, **3** might be a natural precursor of myxovirescin A. Alternatively, **3** can be formed by enzymatic or nonenzymatic transformation of **4** in the absence of TaQ methyltransferase.

Finally, the methylation at C1 could be attributed to TaS-the enzyme that shows homology with members of the radical SAM-protein superfamily. This superfamily encompasses a wide range of enzymes, some of which function as methyltransferases.^[56] The involvement of *taS* in myxovirescin production remains to be proven in further experiments.

Conclusion

Myxovirescin megasynthetase shows a number of unusual features such as a dual pathway dedicated to starter biosynthesis, multimodular AT-less megasynthetases with "*trans*"-acting acyltransferases, lack of reductive domains, "split" modules, and a thioesterase that is not directly preceded by an ACP. In addition, the gene cluster is comprised of a number of noncanonical PKS enzymes and domains (GNAT, HMG-CoA synthases, and enoyl-CoA hydratases) and a β -ketosynthase that has a Cys to Ser point mutation. All these features challenge our previous knowledge pertaining to the organization of PKSs, their colinearity, and classification.

The myxovirescin biosynthetic gene cluster belongs to the novel family of natural-product gene clusters that is comprised of pederin, mupirocin, onnamide, curacin A, and jamaicamide. All clusters within this family appear to have acquired a novel variation in natural-product assembly by combining PKS/NRPS assembly lines with HMG-CoA synthase-type biochemistry. Elucidation of the biosynthetic logic that governs PKS/NRPS/HMG-CoA-orchestrated assembly of natural products will not only enrich the lexicon of natural-product biochemistry with another chapter, but more importantly, pave the way to designing novel antitumor and antibiotic analogues by using the HMG-CoA toolbox. The myxovirescin system of *M. xanthus* provides an excellent molecular-genetic platform for such studies.

Experimental Section

Growth media: *M. xanthus* strain DK1622 was grown in casitone yeast extract (CYE) medium that consisted of casitone (10%; Difco), yeast extract (5%; Difco), MgSO₄·7 H₂O (0.1%), and 3-morpholinopropanesulfonic acid buffer (MOPS; 10 mM) at pH 7.6.

Myxovirescin production was assayed in MD-1 medium that consisted of casitone (0.3%), CaCl₂·2 H₂O (0.07%), and MgSO₄·7 H₂O (0.2%); vitamin B12 (5×10^{-4} μg L⁻¹) was added after cooling. For cloning purposes *E. coli* strain DH5α was grown in Luria-Bertani (LB) medium^[57] and supplemented with standard amounts of antibiotic as required.

Annotation of the myxovirescin biosynthetic gene cluster: The complete sequence of the myxovirescin gene cluster was obtained from TIGR (<http://www.tigr.org/tdb>). Further annotation of the catalytic domains was performed by using the PKS-NRPS program kindly provided by Jacques Ravel (<http://jhunix.hcf.jhu.edu/~ravel/nrps//index2.html>). Annotation of the nitrogen-specific acetyltransferase (GNAT) and ACP domains of TaI, KR, and TaL were carried out by using the Pfam search engine (<http://pfam.wustl.edu>). MT domains were defined by using the natural-product biosynthetic gene database (www.npbio gene.com).

Construction of in-frame deletion mutants of *taV*, *taI*, *taL*, and *taII*: Construction of in-frame deletion mutants was carried out by amplifying approximately 600 bp regions on each side of the desired deletion area with Taq polymerase. Each fragment was subcloned into the pCR2.1[®]-TOPO vector (Invitrogen; see Supporting Information for the list of primers used). Following sequencing of the cloned regions, the corresponding amplification products were cut out of the pCR2.1-TOPO vector by using the restriction sites indicated (Table 3). The fragments were then gel purified and cloned into the pSWU41 vector, which carries a neomycin phosphotransferase (*nptII*) and levansucrase (*sacB*) gene cassette. The final constructs were electroporated into *M. xanthus*,^[58] and kanamycin-resistant, sucrose-

sensitive clones were checked for proper integration of the plasmid by PCR amplification. One transformant which showed the correct genotype was grown in CYE medium for three days with daily dilutions. On the third day, $0.2\text{-}2.0 \times 10^8$ cells were mixed with CYE-soft agar (0.75%; 3 mL) and poured onto CYE-agar plates that contained sucrose (5%), and incubated at 30°C for four days. Well-isolated colonies were picked and transferred onto CYE-agar containing sucrose (5%), and grown at 30°C for two days before being transferred onto CYE-agar containing kanamycin ($40 \mu\text{g mL}^{-1}$). After two days of growth at 30°C, colonies that were kanamycin sensitive and sucrose resistant were subjected to chromosomal-DNA extraction and their genotypes were confirmed by PCR amplification. In one PCR reaction a primer pair was used that recognized sequences outside of the region that was initially amplified. This yielded a product that was shorter than the desired deletion. As a negative control, the second PCR reaction was performed with a primer that bound outside of the amplified region in combination with a primer specific for the deletion area. To create a double $\Delta taII$ mutant, plasmid pVS61 was electroporated into *M. xanthus* VS1024 (ΔtaI). The excision of the plasmid resulted in *M. xanthus* VS1029.

Construction of the *taQ* mutant: To construct a *taQ* knockout, an internal 450 bp of *taQ* was amplified by using Taq polymerase and the primer pair taQ_knock_for and taQ_knock_rev. The former primer contained a base-pair insertion (Supporting Information) that created a stop codon. The PCR product was cloned into pCR2.1-TOPO and sequenced. The resulting plasmid, pVS16, was then electroporated into *M. xanthus* DK1622.^[58] Transformants were grown in CYE medium supplemented with kanamycin, and their genomic DNA was analyzed for integration of the plasmid in *taQ* by using PCR amplification. The primers used were taQ_knock_for (specific for *taQ*) and 21down (specific for pCR2.1-TOPO). The *taQ* knockout mutant was named VS1016.

Analysis of the *taO-taP* intergenic region: To eliminate the possibility of frame-shift error(s), 0.824 kb that covered the region near the 3' end of *taO* and the 5' region of *taP*, was PCR amplified by using Pfu Turbo polymerase (Stratagene) and primers taOseq_up and taOseq_down (Supporting Information). Following gel purification of the blunt-ended PCR product, A overhangs were added to it by using Taq polymerase, and the modified PCR product was cloned into pCR2.1-TOPO to create plasmid pVS75. The sequenced region was analyzed for ORFs by using FramePlot 3.0beta software (<http://watson.nih.gov/~jun/cgi-bin/frameplot-3.0b.pl>).

Fermentation and extraction conditions: Typically, MD-1 medium (100 mL) that contained amberlite XAD-16 (1%; Rohm & Haas, Frankfurt/Main, Germany) was inoculated with *M. xanthus* (1.5×10^8 cells mL⁻¹). After 3 days at 30°C, the cells and XAD beads were centrifuged for 15 min at 10000 g. The combined pellet of cells and XAD beads was extracted with methanol (3×50 mL). The total extract was resuspended in methanol (2 mL) and concentrated into 200 µL.

Antibiotic assay: In order to test inhibitory activity, *E. coli* XL-1 blue (0.1 mL) at 0.1 OD₆₀₀ were mixed with LB-soft agar (3 mL) and plated on a LB-agar plate. Purified antibiotics (10 µg and 50 µg) were spotted on the filter disk, dried, and placed on the soft agar. The plate was incubated at 30°C for 24 h.

Purification of myxovirescins from *M. xanthus* DK1622: To purify myxovirescins from wild-type *M. xanthus* DK1622, cells (8 L) were grown in a fermentor (Biostat V, Braun) under the conditions described above. At the end of the fermentation, XAD-adsorbent resin was removed by filtration through a 0.2 mm sieve (Retsch, Haan, Germany), and antibiotics were extracted from the resin by using methanol (3×400 mL). The total methanol extract

was then applied to a Sephadex LH-20 column (100 cm×2.5 cm) and eluted with methanol. Fractions that tested positive for myxovirescins were concentrated, dissolved in dichloromethane: methanol (15:1; 3 mL), applied to a silica-gel column (780×23 mm), and eluted by using the same solvent system. Fractions that contained myxovirescins were further concentrated, dissolved in methanol, and purified by preparative HPLC by using a Nucleosil 100-7 C-18 column (250×21 mm; Macherey & Nagel, Düren, Germany). Myxovirescins A and C were purified by sequential preparative HPLC (see above) by using different MeOH/H₂O mixtures. The final yields of myxovirescins A and C were 3 and 5 mg, respectively.

Purification of myxovirescin Q_a from the *taQ* mutant, VS1016: In order to isolate myxovirescin Q_a, *taQ* mutant cells (9 L) were grown in MD-1 medium until the late stationary phase was reached. After centrifugation, cells and XAD were extracted with methanol (3×400 mL). The total extract was concentrated and separated on a Sephadex LH-20 column. Fractions that tested positive for myxovirescin Q_a ($R_f = 0.375$) were collected, concentrated, and applied to preparative HPLC as described for the purification of myxovirescins A and C, and yielded a total of 2 mg of pure compound.

Myxovirescin A detection and quantification: Detection of myxovirescins by TLC was carried out by using a dichloromethane/methanol (15:1) solvent system. Myxovirescins were detected as a dark spot under 254 nm ultraviolet light ($R_f = 0.26$).

Additional detection by analytical reversed-phase HPLC was carried out by using the Dionex P680 pump unit coupled to PDA-100 DAD on a RP 125×2 mm/3 μm Nucleodur C-18 column (Macherey & Nagel). Solvent A: H₂O with formic acid (0.1%); solvent B: acetonitrile with formic acid (0.1%); flow rate 0.4 mL min⁻¹, and the following program: 0-2

min, 5 % B; 2-17 min to 95 % B; 17-20 min, 95 % B; 20-23 min, 5 % B. Under these conditions, myxovirescin A showed a retention time of 15.0 min and a characteristic UV_{\max} absorption at 239 nm.

Liquid chromatography/mass spectrometry (LC/MS) and quantification of

myxovirescin A by ion-trap MS: LC/MS measurements were performed on an Agilent 1100 series system equipped with a photodiode-array detector, and coupled to a Bruker HCT plus mass spectrometer operated in positive-ionization mode at a scan range from m/z 100 to 1100. Myxovirescin A showed a characteristic m/z 624.3 $[M+H]^+$.

In order to quantify myxovirescin A, combined cell and XAD extracts were separated by RP-HPLC on a 125×2 mm/3 μ m Nucleodur C-18 column by using an Agilent 1100 series solvent-delivery system and a flow rate of 0.4 mL min⁻¹. The gradient employed the same solvents as used for HPLC-MS and consisted of 0-1 min 70% B, 1-6 min to 95% B. Under these conditions myxovirescin A displayed a retention time of 3 min. Quantitative analysis was done on a coupled ESI ion-trap MS machine (Bruker HCTplus) operated in the manual MS(n) mode. Ions of m/z 624 $[M+H]^+$ were collected and subjected to fragmentation. The intensities of the three fragment ions (592, 574, and 556 $[M+H]^+$) were summed up and peak integration was carried out by utilizing the Bruker QuantAnalysis v1.5 software package. The calibration curve consisted of a series of dilutions of the purified myxovirescin A. Samples under investigation were diluted as required to fit the dynamic range of the method utilized.

NMR analysis: NMR analysis was performed in CD₃OD by using a Bruker Advance 500 instrument. ¹H NMR spectra were measured at 500 MHz. ¹³C spectra, ¹H, ¹H COSY, gradient spectroscopy HSQC, and HMBC data were obtained at 125 MHz. Distortionless

enhancement by polarization transfer (DEPT) spectrum was measured at 135°.

Acknowledgements

We would like to thank Jacques Ravel for supplying us with the PKS-NRPS software for the analysis of catalytic domains, and Helge B. Bode for helpful comments and critical reading of the manuscript. This work was supported by BMB+F and DFG research grants to R.M.

References

- [1] J. Staunton, K. J. Weissman, *Nat. Prod. Rep.* 2001, **18**, 380-416.
- [2] C. T. Walsh, *Science* 2004, **303**, 1805-1810.
- [3] S. A. Sieber, M. A. Marahiel, *Chem.Rev.* 2005, **105**, 715-738.
- [4] B. Silakowski, H. U. Schairer, H. Ehret, B. Kunze, S. Weinig, G. Nordsiek, P. Brandt, H. Blöcker, G. Höfle, S. Beyer, R. Müller, *J.Biol.Chem* 1999, **274**, 37391-37399.
- [5] S. Smith, A. Witkowski, A. K. Joshi, *Prog.Lipid Res.* 2003, **42**, 289-317.
- [6] J. L. Garwin, A. L. Klages, J. E. Cronan, Jr., *J.Biol.Chem.* 1980, **255**, 11949-11956.
- [7] Y. Ohashi, H. Okuyama, *Biochim.Biophys.Acta* 1986, **876**, 146-153.
- [8] K. Magnuson, S. Jackowski, C. O. Rock, J. E. Cronan, Jr., *Microbiol.Rev.* 1993, **57**, 522-542.
- [9] J. Piel, D. Hui, G. Wen, D. Butzke, M. Platzner, N. Fusetani, S. Matsunaga, *Proc.Natl. Acad.Sci.U S A* 2004, **101**, 16222-16227.
- [10] J. Piel, *Proc.Natl.Acad. Sci.USA* 2002, **99**, 14002-14007.
- [11] A. K. El-Sayed, J. Hothersall, S. M. Cooper, E. Stephens, T. J. Simpson, C. M. Thomas, *Chem.Biol.* 2003, **10**, 419-430.
- [12] D. J. Edwards, B. L. Marquez, L. M. Nogle, K. McPhail, D. E. Goeger, M. A. Roberts, W. H. Gerwick, *Chem.Biol.* 2004, **11**, 817-833.
- [13] E. Rosenberg, S. Fytlovitch, S. Carmeli, Y. Kashman, *J.Antibiot. (Tokyo)* 1982, **35**, 788-793.
- [14] K. Gerth, H. Irschik, H. Reichenbach, G. Höfle, *J. Antibiot.* 1982, **35**, 1454-1459.
- [15] W. Trowitzsch, K. Gerth, V. Wray, G. Höfle, *J. Chem.Soc.Chem.Commun.* 1983, 1174-1175.
- [16] W. Trowitzsch Kienast, K. Schober, V. Wray, K. Gerth, H. Reichenbach, G. Höfle, *Liebigs Ann.* 1989, 345-355.
- [17] A. Manor, I. Eli, M. Varon, H. Judes, E. Rosenberg, *J.Clin. Periodontol.* 1989, **16**, 621-624.
- [18] I. Eli, H. Judes, M. Varon, A. Manor, E. Rosenberg, *Refuat Hashinayim* 1988, **6**, 14-15.
- [19] A. Manor, M. Varon, E. Rosenberg, *J.Dent.Res.* 1985, **64**, 1371-1373.

- [20] Y. Paitan, E. Orr, E. Z. Ron, E. Rosenberg, *FEMS Microbiol.Lett.* 2001, **203**, 191-197.
- [21] Y. Paitan, E. Orr, E. Z. Ron, E. Rosenberg, *Gene* 1999, **228**, 147-153.
- [22] Y. Paitan, G. Alon, E. Orr, E. Z. Ron, E. Rosenberg, *J.Mol.Biol.* 1999, **286**, 465-474.
- [23] Y. Paitan, E. Orr, E. Z. Ron, E. Rosenberg, *J.Bacteriol.* 1999, 181, 5644-5651.
- [24] Y. Paitan, E. Orr, E. Z. Ron, E. Rosenberg, *FEMS Microbiol.Lett.* 1999, 170, 221-227.
- [25] H. B. Bode, R. Müller, *Angew Chem Int Ed* 2005, in press.
- [26] V. Simunovic, F. C. Gherardini, L. J. Shimkets, *J.Bacteriol.* 2003, **185**, 5066-5075.
- [27] W. Trowitzsch-Kienast, K. Schober, V. Wray, K. Gerth, H. Reichenbach, G. Höfle, *Liebigs Ann.Chem.* 1989, 345-355.
- [28] G. L. Tang, Y. Q. Cheng, B. Shen, *Chem.Biol.* 2004, **11**, 33-45.
- [29] S. W. White, J. Zheng, Y. M. Zhang, Rock, *Annu.Rev.Biochem.* 2005, **74**, 791-831.
- [30] R. Reid, M. Piagentini, E. Rodriguez, G. Ashley, N. Viswanathan, J. Carney, D. V. Santi, C. R. Hutchinson, R. McDaniel, *Biochemistry* 2003, **42**, 72-79.
- [31] C. D. Reeves, S. Murli, G. W. Ashley, M. Piagentini, C. R. Hutchinson, R. McDaniel, *Biochemistry* 2001, **40**, 15464-15470.
- [32] S. J. Moss, C. J. Martin, B. Wilkinson, *Nat.Prod. Rep.* 2004, **21**, 575-593.
- [33] M. Kopp, H. Irschik, S. Pradella, R. Müller, *ChemBioChem* 2005, **6**, 1277-1286.
- [34] O. Perlova, K. Gerth, A. Hans, O. Kaiser, R. Müller, *J. Biotechnol.* 2005, **121**, 174-191.
- [35] R. M. Kagan, S. Clarke, *Arch. Biochem. Biophys.* 1994, **310**, 417-427.
- [36] N. Campobasso, M. Patel, I. E. Wilding, H. Kallender, M. Rosenberg, M. N. Gwynn, *J. Biol. Chem.* 2004, **279**, 44883-44888.
- [37] W. Trowitzsch, V. Wray, K. Gerth, G. Höfle, *J.Chem. Soc.Chem.Commun.* 1982, 1340-1341.
- [38] Y.-Q. Cheng, G.-L. Tang, B. Shen, *Proc.Natl.Acad.Sci.USA* 2003, **100**, 3149-3154.
- [39] J. Davies, G. D. Wright, *Trends Microbiol.* 1997, **5**, 234-240.
- [40] H. He, Y. Ding, M. Bartlam, F. Sun, Y. Le, X. Qin, H. Tang, R. Zhang, A. Joachimiak, J. Liu, N. Zhao, Z. Rao, *J. Mol. Biol.* 2003, **325**, 1019-1030.
- [41] J. Piel, G. P. Wen, M. Platzer, D. Q. Hui, *ChemBioChem* 2004, **5**, 93-98.

- [42] Z. Chang, N. Sitachitta, J. V. Rossi, M. A. Roberts, P. Flatt, J. Jia, D. H. Sherman, W. H. Gerwick, *J.Nat.Prod.* 2004, **67**, 1356-1367.
- [43] A. Witkowski, A. K. Joshi, Y. Lindqvist, S. Smith, *Biochemistry* 1999, **38**, 11643-11650.
- [44] C. Bisang, P. Long, J. Cortes, J. Westcott, J. Crosby, A.-L. Matharu, R. Cox, T. Simpson, J. Staunton, P. Leadlay, *Nature* 1999, **401**, 502-505.
- [45] T. Stachelhaus, H. D. Mootz, M. A. Marahiel, *Chem.Biol.* 1999, **6**, 493-505.
- [46] B. Beck, Y. Yoon, K. Reynolds, D. Sherman, *Chem.Biol.* 2002, **9**, 575-583.
- [47] S. Wenzel, P. Meiser, T. Binz, T. Mahmud, R. Müller, *Angew.Chem.Int.Ed.* 2005., **45**, 2296-2301.
- [48] K. A. McGuire, M. Siggaard-Andersen, M. G. Banger, J. G. Olsen, P. von Wettstein-Knowles, *Biochemistry* 2001, **40**, 9836-9845.
- [49] C. Davies, R. J. Heath, S. W. White, C. O. Rock, *Structure Fold Des.* 2000, **8**, 185-195.
- [50] G. Michal, *Biochemical Pathways, Vol. 1*, Spektrum Akad. Verlag, Heidelberg, 1999.
- [51] F. Kunst, N. Ogasawara, I. Moszer, A. M. Albertini, G. Alloni, V. Azevedo, M. G. Bertero, P. Bessieres, A. Bolotin, S. Borchert, R. Borriss, L. Boursier, A. Brans, M. Braun, S. C. Brignell, S. Bron, S. Brouillet, C. V. Bruschi, B. Caldwell, V. Capuano, N. M. Carter, S. K. Choi, J. J. Codani, I. F. Connerton, A. Danchin, et al., *Nature* 1997, **390**, 249-256.
- [52] H. Ikeda, T. Nonomiya, S. Omura, *J. Ind. Microbiol.Biotechn.* 2001, **27**, 170-176.
- [53] K. Nakajima, A. Yamashita, H. Akama, T. Nakatsu, H. Kato, T. Hashimoto, J. Oda, Y. Yamada, *Proc.Natl.Acad.Sci.U S A* 1998, **95**, 4876-4881.
- [54] M. Fisher, S. E. Sedelnikova, W. Martindale, N. C. Thomas, J. W. Simon, A. R. Slabas, J. B. Rafferty, *Acta Crystallogr.D.Biol.Crystallogr.* 2000, **56 (Pt 1)**, 86-88.
- [55] B. Silakowski, G. Nordsiek, B. Kunze, H. Blöcker, R. Müller, *Chem.Biol.* 2001, **8**, 59-69.
- [56] H. J. Sofia, G. Chen, B. G. Hetzler, J. F. Reyes-Spindola, N. E. Miller, *Nucleic Acids Res.* 2001, **29**, 1097-1106.
- [57] J. Sambrook, E. F. Fritsch, T. Maniatis, 2 ed., Cold Spring Harbor Laboratory Press, Cold Spring Harbor, NY, **1989**.
- [58] K. Kashefi, P. L. Hartzell, *Mol.Microbiol.* 1995, **15**, 483-494.

Supporting Information

for

Myxovirescin A Biosynthesis is Directed by Hybrid Polyketide
Synthases/Nonribosomal Peptide Synthetase, 3-Hydroxy-3-
Methylglutaryl CoA Synthases and *trans*-Acting Acyltransferases

V. Simunovic, J. Zapp, S. Rachid, D. Krug, P. Meiser and Rolf Müller*

2006. Copyright John Wiley & Sons. Reproduced with permission.

DOI: 10.1002/cbic.200600075

Table S1. List of primers used in the study.

Primer name	Sequence 5'→3'
taV1	ACAGCGGCCCGCACCATCGCGCGGACCTGTGG
taV2	ATGACTAGTGACAGCGTCCGGCTGGATA
taV3	TACTACTAGTCATGACAACGTGGTGCAG
taV4	GATGAGCTCGATAGGCTGCTTGCATCAGC
tal1	GCTCTAGAC AGACATTTCAGTTCCTTCTGCACCG
tal2	CGGGATCCC GATGTCGCTCGAAGAGCTCCTG
tal3	CGGGATCCCT CGGTCTCCGTGGACGCCAC
tal4	GGACTAGT AGTACCCTCAGGGCCAACCTGGTGCT
tal1	GCTCTAG AGGTCCACAGGCGAGATCGAATGGCA
tal2	CGGGATCC ACGTTGGTGCAGCGGGGCGCGA
tal3	CGGGATCCCC GAGCGTCAGCATCGACCG
tal4	GGACTAGT AGTGGGCGCGGGAAGCACGG
taQ_knock frw	GCGACCAC <u>T</u> AAGGCGGTGGAT
taQ_knock_rev	CGGTGAACTGAGGCGTTTCCT
taOseq_up	GCGAGCGCGTTCGTTGAAGAA
taOseq_down	TGCAGGTGTTTCCTCACGGGA
21down	CGACGGCCAGTGAATTGTAATA
taV5	GGAATTCGTTGGATGGCGAACTGCTGCG
taV6	GGGGTACCCACGCCCCGTCTTCAGCCTGG
tal 6	CGTGTGGAGCATCAAGGAGA
tal5	GCACTGGAGCGGCTGGAGCG
tal7	GCTGATGTTCTCCGCGCCCC
tal6	TCCCTCATCGCCTCCAATGG
tal7	GTATTGGCTCGCGTCTGGCT
tal5	CTTGCCGGGTCGAAATCTGG

Bold letters indicate restriction sites and underlined base pair insertion

Table S2. NMR data for myxovirescins A (left) and C (right) obtained in CD₃OD.

Carbon	¹³ C	¹ H J (Hz)	<i>m</i>	¹³ C	¹ H J (Hz)	<i>m</i>
1	19.5	1.42	m	19.5	1.43	m
2	35.1	1.77	m	35.2	1.77	m
3	74.9	4.95 (8/5)	dd	74.9	4.93 (8/5)	dd
4	173.3	-	-	173.3	-	-
5	46.3	3.31	m	46.4	3.31	m
6	68.4	3.92	m	68.3	3.92	m
7	37.3	1.51	m	37.2	1.52	m
8	72.5	3.73	m	72.5	3.72	m
9	76.0	3.46 (10/3)	dt	76.0	3.47 (10/3)	dt
10	31.7	1.70 1.50	m m	31.9	1.71	m
11	32.4	2.34 2.15	m m	32.5	2.32 2.15	m m
12	136.9	-	-	136.5	-	-
13	130.2	6.07 (11)	d	130.4	6.08 (11)	d
14	127.5	6.36 (15/11)	dd	127.1	6.32 (15/11)	dd
15	140.1	5.40 (15/9)	dd	140.6	5.39 (15/9)	dd
16	46.2	1.93	m	46.5	1.92	m
17	35.9	1.43 1.21	m m	36.3	1.41 1.22	m m
18	23.4	1.56 1.47	m m	n.a.	n.a.	n.a.
19	43.8	2.45 2.33	m m	n.a.	n.a.	n.a.
20	214.4	-	-	n.a.	n.a.	n.a.
21	43.0	2.42	m	n.a.	n.a.	n.a.
22	25.0	1.51	m	n.a.	n.a.	n.a.
23	27.5	1.25	m	n.a.	n.a.	n.a.
24	37.6	1.33 1.10	m m	37.8	1.36 1.10	m m
25	31.5	1.49	m	31.6	1.49	m
26	41.8	1.56 1.34	m m	42.0	1.57 1.36	m m
27	38.5	2.62 (14/7)	dd	38.5	2.62	m
28	177.9	-	-	177.9	-	-
29	71.3	4.10 (12) 4.06 (12)	d d	71.2	4.09 (12) 4.07 (12)	d d
30	29.5	1.29 1.43	m m	n.a.	n.a.	n.a.
31	12.18	0.86 (7)	t	12.28	0.85 (7.3)	t
32	14.0	0.94 (7)	t	14.1	0.95 (7)	t
33	17.7	1.15 (7)	d	17.6	1.14 (7)	d
34	20.0	0.86 (7)	d	20.1	0.86 (7)	d
OCH ₃	58.0	3.29	s	58.0	3.29	s

n.a. in the table indicates the carbons which could not be assigned due to the small amount of fatty acid impurity.

Chapter 3

The following article has been published in the
ChemBioChem journal; Vol. 8-No.5, March 2007

Pages 497-500

3-Hydroxy-3-Methylglutaryl-CoA-like Synthases Direct the Formation of Methyl and Ethyl Side Groups in the Biosynthesis of the Antibiotic Myxovirescin A

M.S. Vesna Simunovic and Prof. Dr. Rolf Müller

2007. Copyright John Wiley & Sons. Reproduced with permission.

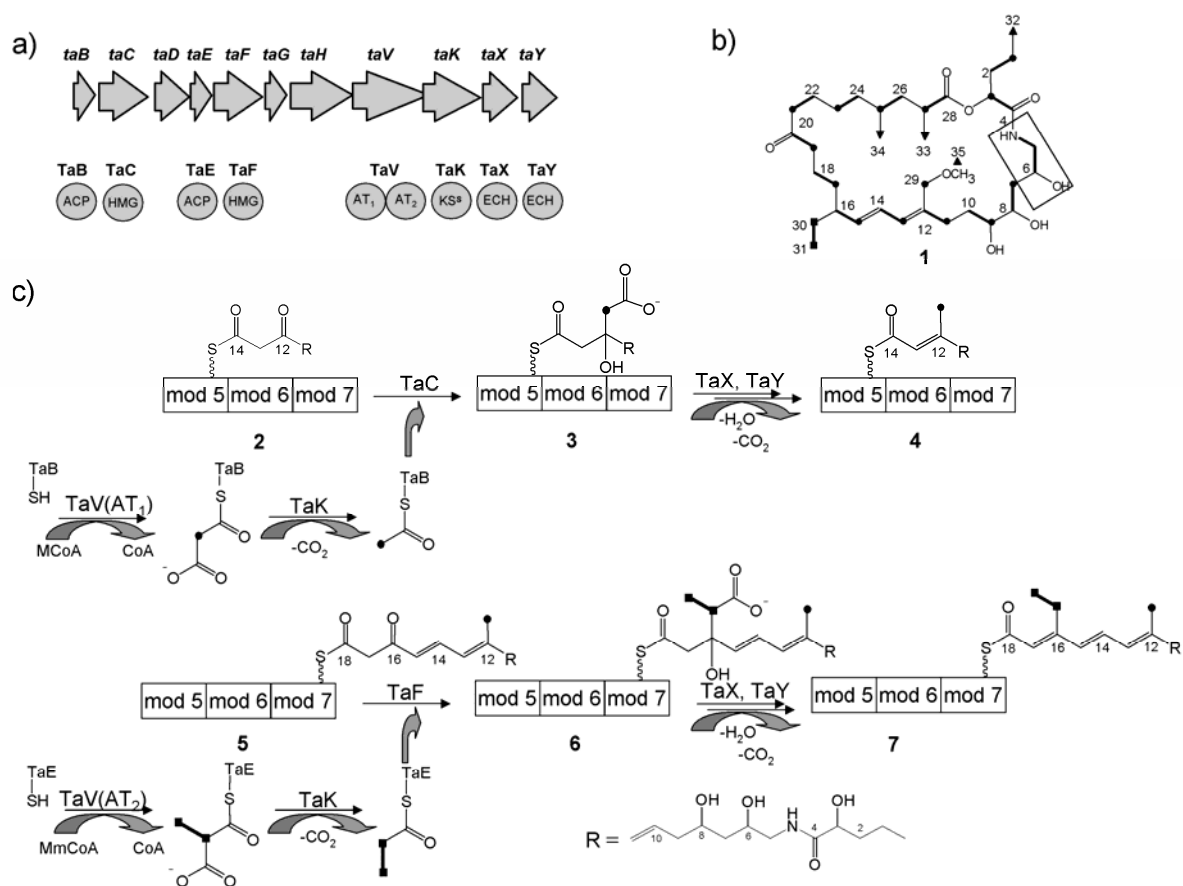
10.1002/cbic.200700017 DOI

Polyketides (PK), nonribosomal peptides (NRP) and their hybrids (PK/NRP) are classes of secondary metabolites whose members exhibit valuable activities with high potential for therapeutic applications. The program governing PK/NRP assembly is typically encoded within modular megasynthetases on which consecutive condensations of activated short-chain carboxylic acids (catalyzed by polyketide synthases; PKS) or amino acids (performed by nonribosomal peptide synthetases; NRPS) take place through a thiotemplated mechanism.^[1]

Annotations of several PKS/NRPS gene clusters, including bacillaene, curacin and mupirocin,^[2-8] indicated that a novel type of Claisen condensation mechanism is used in such natural product biosynthesis. Strikingly, all six biosynthetic gene clusters revealed (a) free-standing homologue(s) of 3-hydroxy-3-methylglutaryl-CoA synthase (HMGS), generally surrounded by a set of genes encoding an acyl carrier protein (ACP), a mutant KS with a Cys-to-Ser active site substitution (KS^S) and two homologues of the enoyl-CoA hydratase (ECH) family.^[4, 7] HMG-CoA synthases are known to couple acetyl-CoA (Ac-CoA) onto the β -keto group of acetoacetyl-CoA to yield 3-hydroxy-3-methylglutaryl-CoA (HMG-CoA).^[9] It was therefore proposed that the above gene products condense Ac-CoA with structurally similar β -ketoacyl-S-ACP intermediates of polyketide origin to eventually result in the addition of the C2 acetate carbon in their respective structures.^[2, 4-6] This hypothetical scheme has been recently revised following in vitro reconstitution of the bacillaene enzyme homologues of *B. subtilis*^[7, 8] (cf. Scheme 1 C). In comparison with other gene clusters,^[4, 7] the myxovirescin cluster contains two free-standing ACPs (TaB and TaE) and two HMG synthases (TaC and TaF; Scheme 1 A). Curiously, the myxovirescin-labelling scheme indicates two atypical pendant groups branching from the basic polyketide backbone, the methylene group derived from the C2 portion of acetate attached to carbon C12, and the C2-C3 fragment derived from

succinyl-CoA (Succ-CoA) at carbon C16^[10] (Scheme 1 B). Accordingly, the proposed biosynthetic scheme for myxovirescin assembly envisions two HMGS-like catalyzed reactions that would “intersect” the classical PK biochemistry by modifying ACP-bound intermediates **2** and **5** (Scheme 1 C). After each round of reactions, polyketide biosynthesis would be resumed and carried out by multimodular PKSs. The first one of these reactions is postulated to be carried out by the HMG-like synthase TaC by condensation of Ac-S-TaB with the C12 β -keto group of substrate **2** to yield **3** (Scheme 1 C). In the second reaction, HMG-like synthase TaF should catalyze the condensation of propionyl-S-TaE (Pp-S-TaE) with the C16 β -keto group of intermediate **5** to yield **6**. In analogy to the KS^S PksG of *B. subtilis*,^[7] KS^S TaK is thought to act twice during the biosynthesis by cleaving carboxyl groups from both malonyl-S-TaB (M-S-TaB) and methylmalonyl-S-TaE (Mm-S-TaE) in order to supply TaC and TaF, respectively, with their cognate substrates. The Mm-CoA is presumably a product of the Mm-CoA mutase-catalyzed conversion of Succ-CoA.^[10] Similarly, based on in vitro data,^[7, 11] two enoyl-CoA hydratases TaX and TaY dehydrate and decarboxylate intermediates **3** and **6** to yield **4** and **7**, respectively (Scheme 1 C).

Even though PksG, the TaC homologue of *B. subtilis*, has been shown to catalyze the formation of HMG-S-ACP in vitro,^[7] there has been no in vivo proof for the function of any HMGS in PKS/NRPS biosynthesis. Such evidence is especially needed given that, in most systems, HMGS homologues are predicted to form much more complex products than HMG-S-ACP.^[7] For instance, TaC and TaF are predicted to act on carbons chains 15 and 19 atoms long while tethered to the ACPs of the giant 995-kDa PKS Ta-1, and to utilize atypical substrates, such as Pp-S-ACP, in addition to Ac-S-ACP.^[6]



Scheme 1. A) 10.9-kb fragment of the myxovirescin A biosynthetic gene cluster encoding for monofunctional enzymes. TaB and TaE are putative ACPs, TaC and TaF homologues of HMG-CoA synthases, TaK is a mutant β -ketoacyl-ACP synthase (KS^S), and TaX and TaY are homologues of the crotonase family of enoyl-CoA hydratases. B) Structure of myxovirescin A (1) indicating the biosynthetic origin of its building units.^[10] Boxed carbons originate from glycine, black circles indicate C2 of acetate, triangles indicate methyl groups derived from methionine, and connected squares show the ethyl group originating from carbons 2 and 3 of succinate. C) A working model of myxovirescin A assembly, based on refs.^[6, 7, 11] depicts two rounds of modification reactions involving HMGS-like and ECH enzyme homologues taking place on the polyketide/nonribosomal peptide intermediates **2**, **3**, **5** and **6**. Two ATs encoded by *taV* load malonyl-CoA (M-CoA) and methylmalonyl-CoA (Mm-CoA) onto their cognate ACPs (TaB and TaE), which become substrates of the decarboxylase TaK. Acetyl-S-TaB and propionyl-S-TaE serve as second substrates for TaC and TaF HMGS-like synthases, respectively. The carbon-labelling pattern is described in (B). The C16=C17 double bond of intermediate **7** is presumably reduced by TaO PKS.

In an effort to provide such in vivo evidence, we have attempted to delete the HMGS homologues (*taC* and *taF*) and to analyze the engineered strains for the possible modifications these mutations would impose on the antibiotic structure. Consistent with the proposed working model, we envisioned three possible effects these deletions would have on

myxovirescin biosynthesis. 1) The loss of TaC or TaF would not halt the myxovirescin biosynthetic machinery but only prevent condensation of the Ac (Pp) unit with the PKS/NRPS scaffold, therefore leading to the production of myxovirescin analogues carrying a ketone in the place of a methoxymethyl or ethyl group at the C12 and C16 positions, respectively (cf. Scheme 1 B). In the case of loss of TaC, we assumed that this modification would also disrupt the C12-C14 diene system. 2) Antibiotic production would be blocked either by jamming of the reaction intermediates on the assembly line, or disruption of the megasynthetase complex. 3) Antibiotic production would be circumvented by complementation of function supplied by the other HMG-like synthase encoded in the gene cluster. Hence, in the case of loss of TaC, TaF would rescue antibiotic assembly by installing a Pp unit on both the C12 and C16 β -keto positions of intermediates **2** and **5** to produce myxovirescin analogues with two ethyl groups at respective positions. The ethyl group at C12 might be further modified into a hydroxyethyl or methoxyethyl group. Conversely, in the case of loss of TaF, TaC would attach two Ac groups onto intermediates **2** and **5**. After additional modification reactions on the C12 methyl carbon, a novel analogue of **1** carrying a methyl instead of an ethyl group at C16 would be formed.

Following construction of two HMGS-like mutant strains, *M. xanthus* VS1011 (ΔtaC) and VS1012 (ΔtaF), the wild-type and mutant extracts were analyzed by HPLC-MS. Production of **1** was abolished in both VS1011 and VS1012 (data not shown). Masses of the predicted modified products could not be detected with a ΔtaC background. However, a unique, novel peak of $[M+H]^+ = 610$ with shorter retention time than **1** was apparent in the VS1012 extracts.

Evidence that the novel metabolite is a myxovirescin analogue was provided by tandem MS analysis. In addition, the UV_{\max} absorption at 239 nm of the novel myxovirescin

ΔF suggested the same chromophore as in **1**. However, in comparison to the production of **1** by the wild-type strain, production of myxovirescin ΔF in VS1012 was reduced tenfold.

The high-resolution mass spectrum (HRMS) of myxovirescin ΔF (m/z 610.4287) suggested the molecular formula $C_{34}H_{60}NO_8^+$, and thus indicated the loss of one methylene group relative to **1**. In order to find out at which carbon position this modification occurred, myxovirescin ΔF was purified and subjected to NMR analysis (see the Supporting Information). Comparative analysis of 1H NMR spectra of myxovirescins A and ΔF indicated changes specific to the aliphatic region (Figure 1 A). The spectrum of myxovirescin ΔF lacked a triplet at $\delta_H = 0.86$ ppm assigned to the C31 methyl group of **1**. Instead, a new methyl group was visible as a doublet at $\delta_H = 1.00$ ppm ($J = 7$ Hz). 1H , 1H COSY and HMBC

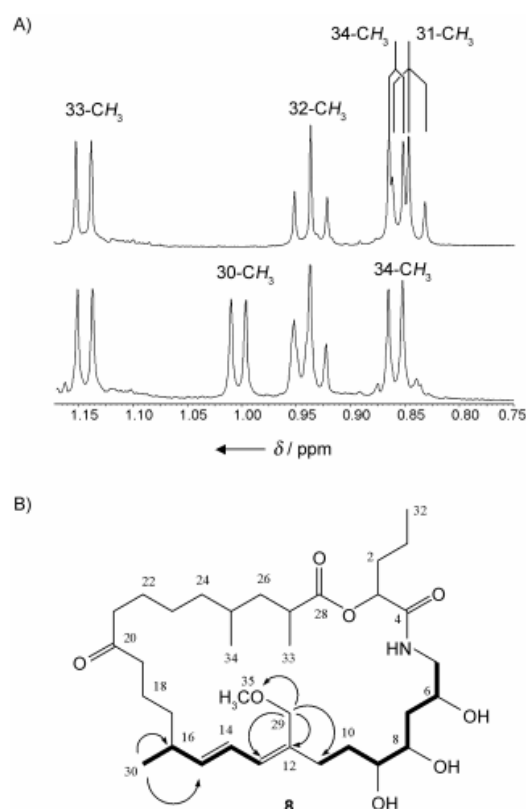


Figure 1. A) 1H NMR spectral expansions of the aliphatic regions of myxovirescin A (upper) and the novel myxovirescin analogue ΔF (lower). B) The NMR-deduced structure of myxovirescin ΔF (**8**) reveals the presence of a methyl rather than ethyl group at C16. Bold lines indicate selected 1H , 1H COSY and arrows show important HMBC correlations.

analysis showed this new methyl group to be connected to the C16 methine group ($\delta_C = 38.3$ ppm, $\delta_H = 2.19$ ppm); this led to the assignment **8** (Figure 1 B). Therefore, NMR analysis provided unambiguous evidence for the presence of a methyl, instead of an ethyl group, at C16 of **8**.

To evaluate whether another HMGS, besides TaC, could be directing production of **8**, the *M. xanthus* DK1622 genome was screened for genes encoding HMGS homologues. This search revealed only one candidate, MvaS (E value = 10^{-48}), the HMGS of the mevalonate pathway.^[12] Unlike in some other bacteria, disruption of *mvaS* in *M. xanthus* does not cause any growth defects, due to the efficient incorporation of leucine, as alternative precursor to HMG-CoA, and subsequently isoprenoids by a second pathway.^[12-13] Similarly, analysis of the ΔtaF and the *mvaS::neo*, ΔtaF double mutant (strain VS1044) extracts showed equal production of **8** (data not shown).

Isotope-labelling data for **1** (Scheme 1 B) demonstrate that both C30 and C31 (the ethyl group at C16) originate from Mm-CoA. Therefore, the appearance of a methyl group at C16 of **8** suggests that, in the absence of TaF, the megasynthetase fails to incorporate Mm-CoA. The absence of the ethyl moiety in **8** is also supported by the observation that addition of vitamin B₁₂ to VS1012 fermentations does not stimulate the production of **8**; this is in contrast to the observed two- to threefold increase it causes in the production of **1** by the wild-type strain DK1622 (data not shown). This argues for a role of vitamin B₁₂ in the production of Mm-CoA, which takes place through a vitamin B₁₂-dependent Mm-CoA mutase-catalyzed conversion of Succ-CoA into Mm-CoA. Indeed, evidence that TaF is directly involved in the formation of the ethyl group at C16 is also supported by the complete loss of production of **1** and appearance of **8** in the ΔtaF background.

Furthermore, the tenfold reduction in the production of **8** in comparison to **1** indicates severe impairment of the metabolic flux through the megasynthetase upon removal of TaF, with only 2 mg of **8** being produced from 45 L of VS1012 culture (Supporting Information). In contrast, elimination of myxovirescin accessory enzymes, such as the methyltransferase TaQ,^[6] and one of the oxygenating enzymes (V.S. and R.M., unpublished data) results in production of the respective desmethyl and deoxy analogues of **1** at 80-100 % of the wild-type yield. In addition, loss of TaC abolishes myxovirescin production. Taken together, these results support the part of our biosynthetic model that depicts TaC and TaF acting directly on the “assembly line” rather than after assembly of the antibiotic scaffold.^[6] Moreover, these insights back the in vitro studies performed with the HMGS homologue PksG of *B. subtilis*.^[7]

Therefore, having excluded the involvement of the primary metabolic HMGS MvaS in the addition of the C30 methyl group of **8**, our results argue for a model in which, in the absence of TaF, TaC rescues myxovirescin assembly by installing two Ac building blocks, one at the C12 and the other one at the C16 β -keto positions of intermediates **2** and **5**, respectively. This results in a novel antibiotic endowed with two methyl groups, one of which is further oxygenated and methylated (**8**; Figure 1 B). It appears that this rather discrete complementation by TaC in the ΔtaF background and the failure of TaF to complement TaC in the ΔtaC background highlight the differences between the TaC and TaF HMG-like synthases, probably not only in the choice of their cognate substrates, but also in the specificity of their docking interactions with the other enzymes comprising the megasynthase complex. Alternatively, incorporation of the larger ethyl group early in biosynthesis might result in the rejection of the modified intermediate at later biosynthetic steps.

In summary, this work provides one of the first in vivo studies (related work on the mupirocin system was reported at a recent conference; T. J. Simpson, personal

communication) directed toward the elucidation of a novel pathway leading to PKS/NRPS natural product assembly, which takes place by a Claisen condensation mechanism previously thought to be specific only to HMG-CoA synthases of the primary metabolism. In contrast to the *S*-adenosylmethionine (SAM)-dependent methyltransferases (MT), which use an electrophilic substrate (SAM) to methylate the activated C2 carbons of the β -ketoacyl-*S*-ACP intermediate,^[9] HMGSs use nucleophilic substrates to methylate the C3 carbon of the same type of substrate.^[7] Due to enzymatic differences between HMGSs and SAM-dependent MTs, introduction of the C30 methyl group onto the C16 carbon by SAM MT appears mechanistically unfeasible. HMGSs, in combination with the set of enzymes mentioned above, can form methyl or ethyl groups, which may be further processed into methylmethoxy,^[6] *exo*-methylene,^[14] cyclopropyl^[4] or vinyl chloride groups.^[5] Knowledge gained from these and further studies might benefit future biocombinatorial efforts directed towards rational redesigning of known or the discovery of novel molecules with therapeutic potential.

Acknowledgements

The authors would like to thank Prof. Dr. H. G. Floss and Drs. H. B. Bode and S. C. Wenzel for their critical reading of this manuscript. We acknowledge Dr. J. Zapp for help with the NMR analysis. Research in R.M.'s laboratory was financed by grants from the Deutsche Forschungsgemeinschaft (DFG) and the Ministry of Education and Research (BMB+F).

References

- [1] M. A. Fischbach, C. T. Walsh, *Chem.Rev.* 2006, **106**, 3468-3496.
- [2] A. K. El-Sayed, J. Hothersall, S. M. Cooper, E. Stephens, T. J. Simpson, C. M. Thomas, *Chem.Biol.* 2003, **10**, 419-430.
- [3] J. Piel, *Proc.Nat. Acad.Sci. USA.* 2002, **99**, 14002-14007.
- [4] Z. Chang, N. Sitachitta, J. V. Rossi, M. A. Roberts, P. Flatt, J. Jia, D. H. Sherman, W. H. Gerwick, *J.Nat.Prod.* 2004, **67**, 1356-1367.
- [5] D. J. Edwards, B. L. Marquez, L. M. Nogle, K. McPhail, D. E. Goeger, M. A. Roberts, W. H. Gerwick, *Chem.Biol.* 2004, **11**, 817-833.
- [6] V. Simunovic, J. Zapp, S. Rachid, D. Krug, P. Meiser, R. Müller, *ChemBioChem.* 2006, **7**, 1206-1220.
- [7] C. T. Calderone, W. E. Kowtoniuk, N. L. Kelleher, C. T. Walsh, P. C. Dorrestein, *Proc.Natl.Acad.Sci.U S A.* 2006, **103**, 8977-8982.
- [8] X. H. Chen, J. Vater, J. Piel, P. Franke, R. Scholz, K. Schneider, A. Koumoutsi, G. Hitzeroth, N. Grammel, A. W. Strittmatter, G. Gottschalk, R. D. Süssmuth, R. Borriss, *J.Bacteriol.* 2006, **188**, 4024-4036.
- [9] G. Michal, *Biochemical Pathways, Vol. 1*, Spektrum Akad. Verlag, Heidelberg, 1999.
- [10] W. Trowitzsch Kienast, K. Schober, V. Wray, K. Gerth, H. Reichenbach, G. Höfle, *Liebigs Ann.* 1989, 345-355.
- [11] L. Gu, J. Jia, H. Liu, K. Hakansson, W. H. Gerwick, D. H. Sherman, *J.Am.Chem.Soc.* 2006, **128**, 9014-9015.
- [12] H. B. Bode, M. W. Ring, G. Schwär, R. M. Kroppenstedt, D. Kaiser, R. Müller, *J.Bacteriol.* 2006, **188**, 6524-6528.
- [13] H. B. Bode, B. Zeggel, B. Silakowski, S. C. Wenzel, H. Reichenbach, R. Müller, *Mol.Microbiol.* 2003, **47**, 471-481.
- [14] J. Piel, G. P. Wen, M. Platzer, D. Q. Hui, *ChemBioChem.* 2004, **5**, 93-98.

Supporting Information

for

3-Hydroxy-3-Methylglutaryl-CoA-like Synthases Direct the Formation of
Methyl and Ethyl Side Groups in the Biosynthesis of the Antibiotic
Myxovirescin A

V. Simunovic and R. Müller

2007. Copyright John Wiley & Sons. Reproduced with permission.

10.1002/cbic.200700017 DOI

Table 1. List of primers used in the study.

Primer	Primer Sequence (5'-3')
Mvi1	CAGGGATCCGCGCTGGAGCTTCATCGTC
Mvi2	TGCGTCGACGAGTTCTTCAGCGGCGTCATC
Mvi3	CTCGTCGACGGTGACCAGGAGCTCGATG
TaFSpeI	GACTAGTCAACGTGAAGATGCGCGAGG
TaF1	TCCACGTAGTTGCCCAACG
TaF2	CGTGCGACGTGGACGAAAT
TaF3	GGCTCATCTACTTCGCGTCG
Mvi5	GTCGGATCCGATTTCGCTGCCGAAGTTGTAC
Mvi6	TGCGTCGACGAGTTCTTCAGCGGCGTGG
Mvi7	CTCGTCGACAGCCACCAGCAGCTCGATG
Mvi8	CGGAAGCTTTGGAGGTGAGCGCCGAGC
taC1	AGGCTCTCGTTCGACTTGCCG
taC2	GTCGCCGTGGTTCGATGGTCCC
taC3	TATCTGCGGGTGGGGCAGCGC
Mx619r	GGAATTCGCATCCGCCGGCAGCTTCATCAG
21down	CGACGCCAGTGAATTGTAATA

Table 2. List of plasmids and strains used in the study.

Plasmid name	Description	Reference
pVS1	0.6 kb upstream from <i>taF</i> amplified with Mvi1 and Mvi2 primer pair carrying <i>Bam</i> HI and <i>Sal</i> I restriction sites, respectively, cloned in pCR2.1-TOPO vector	This study
pVS22	0.6 kb downstream from <i>taF</i> amplified with primers Mvi3 and TaFSpeI containing <i>Sal</i> I and <i>Spe</i> I sites, respectively, cloned in pCR2.1-TOPO vector	This study
pVS3	0.6 kb upstream from <i>taC</i> amplified with primers Mvi5 and Mvi6 carrying <i>Bam</i> HI and <i>Sal</i> I restriction sites respectively, cloned in pCR2.1-TOPO vector	This study
pVS4	0.6 kb downstream from <i>taC</i> amplified with primers Mvi5 and Mvi6 carrying <i>Sal</i> I and <i>Hind</i> III restriction sites respectively, cloned in pCR2.1-TOPO vector	This study
pVS7	1.2 kb fragment obtained by ligation of the <i>Bam</i> HI/ <i>Sal</i> I and <i>Sal</i> I and <i>Spe</i> I-containing inserts from pVS1 and pVS22, respectively, ligated in <i>Bam</i> HI and <i>Spe</i> I sites of pBJ113 vector	This study
pVS23a	1.2 kb fragment obtained by ligation of the <i>Bam</i> HI/ <i>Sal</i> I and <i>Sal</i> I and <i>Hind</i> III -containing inserts from pVS3 and pVS4, respectively, ligated in <i>Bam</i> HI and <i>Hind</i> III sites of pSWU41 vector	This study
p619-1	766 bp internal fragment of MXAN_4267 amplified with Mx619f and Mx619_r primer pair; cloned in pCR2.1-TOPO vector	[1]
<i>M. xanthus</i> strains		
DK1622	Wild type strain	[2]
VS1011	<i>ΔtaC</i>	This study
VS1012	<i>ΔtaF</i>	This study
VS1044	Merodiploid mutant created by homologous recombination of p619-1 in the chromosome of <i>M. xanthus</i> VS1012	This study

Table 3: NMR data for **8** obtained in CD₃OD.

Carbon	$\delta^{13}\text{C}$ [ppm]	$\delta^1\text{H}$ [ppm]	<i>multiplicity</i> J[Hz]
1	19.5	1.42 (2H)	m
2	35.1	1.77 (2H)	m
3	74.9	4.95	dd (8/5)
4	174.0 ^[a]	-	-
5	46.4	3.30	m
6	68.4	3.92	m
7	37.3	1.50 (2H)	m
8	72.5	3.72	m
9	75.9	3.44	dd (4/3)
10	31.7	1.70	m
		1.49	m
11	32.4	2.33	m
		2.16	m
12	137.0	-	-
13	130.4	6.05	d (11)
14	125.8	6.36	dd (15/11)
15	141.5	5.52	dd (15/9)
16	38.3	2.19	m
17	37.6	1.24	m
		1.27	m
18	23.4	1.46	m
		1.59	m
19	43.7	2.46	m
		2.34	m
20	n.d. ^[b]	n.d.	n.d.
21	43.0	2.43 (2H)	m
22	25.0	1.51 (2H)	m
23	27.4	1.27 (2H)	m
24	37.7	1.35	m
		1.12	m
25	31.6	1.48	m
26	41.9	1.57	m
		1.34	m
27	38.5	2.62	dq (14/7)
28	179.0 ^[a]	-	-
29	71.2	4.07 (2H)	s
30	21.3	1.00 (3H)	d (7)
31	-	-	-
32	14.0	0.93 (3H)	t (7)
33	17.7	1.14 (3H)	d (7)
34	20.1	0.86 (3H)	d (7)
35	58.0	3.28 ^[a]	* ^[b]

^[a] Values taken from HMBC

^[b] n.d.- not detected

* ^[b] not detected due to the overlap with the multiplet signal arising from the CD₃OD solvent peak

Experimental Section

Mutant construction: Deletions of *taC* and *taF* were carried out using the same strategy as reported previously,^[3] except that the fragments employed for the deletion of *taC* were cloned into the pBJ113 vector. Upon integration of the resulting vector pVS7 in strain DK1622, plasmid excision was carried out on galactose (1%).^[4]

In order to disrupt the 3-hydroxy-3-methylglutaryl-CoA synthase of the mevalonate pathway (*mvaS*) in the ΔtaF background, plasmid p619-1 (**Table 2**) was electroporated into VS1012 cells.^[5] A novel, kanamycin resistant mutant *M. xanthus* VS1044 was confirmed in a PCR reaction using the Mx619r and 21down primer pair.

Fermentation of *M. xanthus* VS1012 and purification of myxovirescin ΔF : To purify myxovirescin ΔF , *M. xanthus* VS1012 cells were inoculated in MD-1 medium lacking vitamin B₁₂ at 1.5×10^8 cells \times mL⁻¹ and cultivated with Amberlite XAD-16 resin (1%; Fluka) for 4 days at 30°C. Fermentations (45 L total) were carried out in batches of 5 L Erlenmeyer flasks containing 1.5 L of medium.^[3] Following the extraction of the XAD-16 resin with methanol, the total extract was purified on a Sephadex LH 20 column. A fraction enriched in myxovirescin ΔF was further separated on a silica gel using dichloromethane: methanol (25:1) as solvent system. Final purification was carried out by preparative HPLC using a combination of gradient and isocratic conditions and different water/methanol mixtures.^[3] The pure compound (2 mg) was dissolved in CD₃OD and subjected to NMR spectroscopy as described.^[3]

High resolution MS of **8** was performed on Bruker MicrO TOF instrument (Bruker, Bremen, Germany).

References

- [1] H. B. Bode, M. W. Ring, G. Schwär, R. M. Kroppenstedt, D. Kaiser, R. Müller, *J.Bacteriol.* 2006, **188**, 6524-6528.
- [2] H. Chen, I. M. Keseler, L. J. Shimkets, *J.Bacteriol.* 1990, **172**, 4206-4213.
- [3] V. Simunovic, J. Zapp, S. Rachid, D. Krug, P. Meiser, R. Müller, *ChemBioChem* 2006, **7**, 1206-1220.
- [4] B. Julien, A. D. Kaiser, A. Garza, *Proc Natl Acad Sci U S A* **2000**, *97*, 9098-9103.
- [5] K. Kashefi, P. L. Hartzell, *Mol.Microbiol.* 1995, **15**, 483-494.

Chapter 4

The following article has been published in the
ChemBioChem journal, Vol 8, July 2007

Mutational Analysis of the Myxovirescin Biosynthetic Gene Cluster Reveals
Novel Insights into the Functional Elaboration of Polyketide Backbones

M.S. Vesna Simunovic and Prof. Dr. Rolf Müller

2007. Copyright John Wiley & Sons. Reproduced with permission.

DOI. 10.1002/cbic.200700153

Abstract

Two acyl carrier proteins (ACPs) TaB and TaE, and two 3-hydroxy-3-methylglutaryl synthases (HMGSs) TaC and TaF, have been proposed to constitute two functional ACP-HMGS pairs (TaB/TaC and TaE/TaF) responsible for incorporation of acetate and propionate units into the myxovirescin A scaffold, leading to the formation of β -methyl and β -ethyl groups, respectively. Three more proteins, TaX and TaY, which are members of the superfamily of enoyl-CoA hydratases (ECH), and a variant ketosynthase (KS) TaK, were proposed to be shared between two ACP-HMGS pairs, to give the complete set of enzymes required to perform the β -alkylations. The β -methyl branch is presumably further hydroxylated (by TaH) and methylated to produce the methylmethoxy group observed in myxovirescin A. To substantiate this hypothesis, a series of gene deletion mutants were created and the effects of these mutations on myxovirescin production examined.

As predicted, ΔtaB and ΔtaE ACP mutants revealed similar phenotypes to their associated HMGS mutants ΔtaC and ΔtaF , respectively, providing direct evidence for the role of TaE/TaF in the formation of the β -ethyl branch and implying a role of TaB/TaC in the formation of the β -methyl group. Production of myxovirescin A was dramatically reduced in a ΔtaK mutant and abolished in both ΔtaX and ΔtaY mutant backgrounds. Analysis of a ΔtaH mutant confirmed the role of the cytochrome P450 TaH in hydroxylation of the β -methyl group. Taken together, these experiments support a model in which discrete ACPs TaB and TaE are compatible only with their associated HMGSs TaC and TaF, respectively, and function in a substrate specific manner. Both TaB and TaC are essential for myxovirescin production and the TaB/TaC pair can rescue antibiotic production in the absence of either TaE or TaF. Finally, the reduced level of myxovirescin production in the ΔtaE mutant relative to the ΔtaF strain suggests an additional function of the TaE ACP.

Introduction

Polyketides and nonribosomal peptides are structurally diverse classes of secondary metabolites assembled from carboxylic-CoA esters and amino acids, respectively.^[1] They are biosynthesized by specialized protein megacomplexes which are organized into functional units called modules, each of which accomplishes a specific round of chain extension. These multienzyme systems are known respectively as polyketide synthases (PKS) and nonribosomal peptide synthetases (NRPS). Typically, each module minimally incorporates three domains: an acyltransferase (AT) which selects specific extension units, a ketosynthase (KS) which catalyses carbon-bond formation, and an acyl carrier protein (ACP), to which the growing chain is tethered in thioester linkage. Following condensation, the β -ketoacyl-S-ACP intermediate may be further reduced by one of the optional domains (keto reductase (KR), dehydratase (DH) and enoyl reductase (ER)), before it is transferred from the ACP to the KS of the next module for another round of chain extension. Thus, the biosynthesis follows a linear assembly program directed by the particular combination of catalytic domains present within each module, and the number and order of modules within the PKS. The thioesterase (TE) located within the last module terminates the assembly process by facilitating the release of the fully extended product by hydrolysis or lactonization.

In addition to the genes encoding type I PKSs, the biosynthetic gene clusters responsible for myxovirescin, bacillaene, mupirocin, and several other compounds also include a set of discrete genes named "HMG-cassettes".^[2-5] Each HMG-cassette comprises a set of five genes encoding for a 3-hydroxy-3-methylglutaryl-CoA synthase (HMGS), an ACP, a variant KS (in which the active site Cys is mutated to Ser) and two homologous of enoyl-CoA hydratases (ECH)^[5] (Figure 1 a). Furthermore, the PKS responsible for these compounds

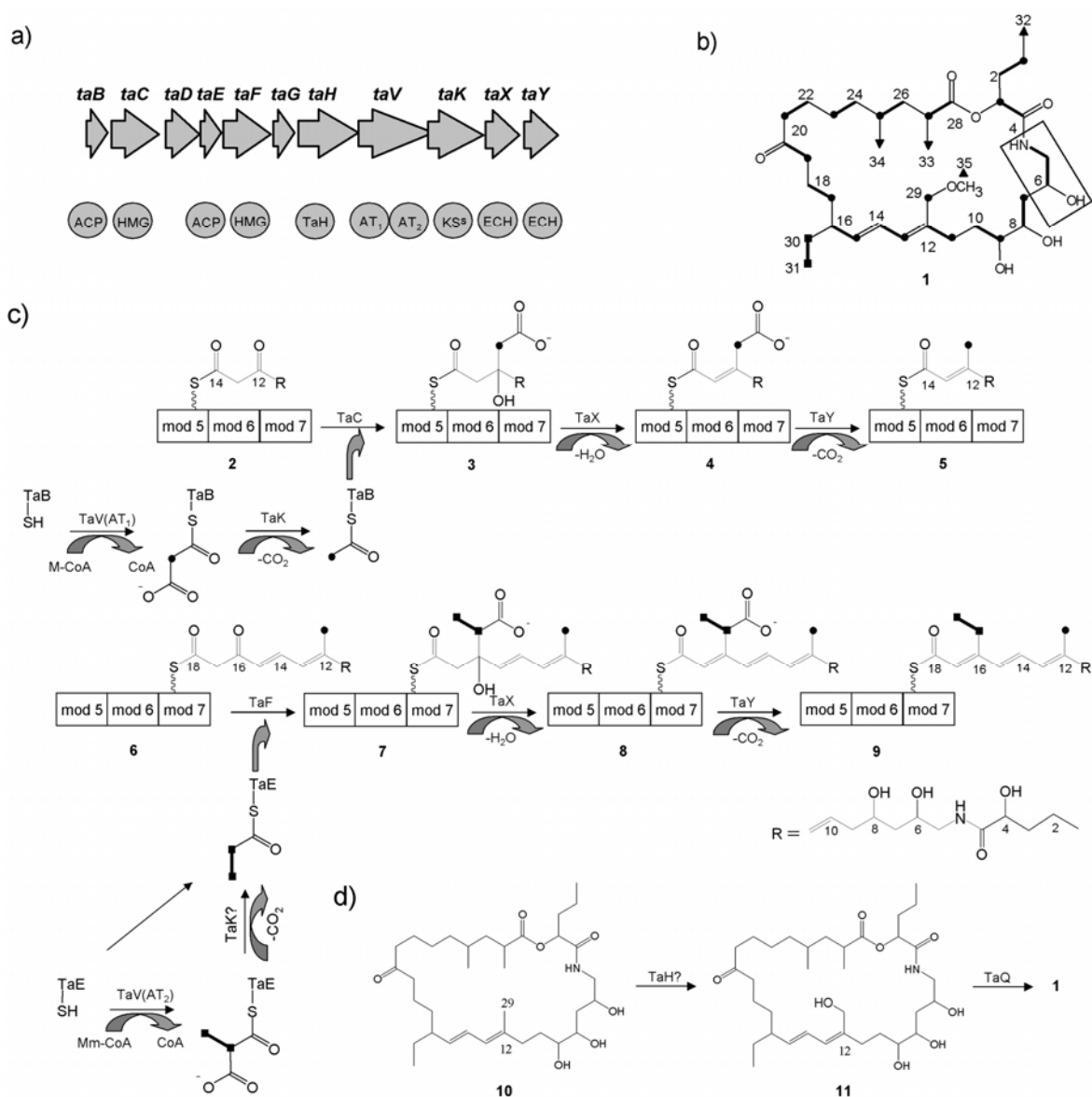


Figure 1. a) 10.9 kb fragment of the myxovirescin A biosynthetic gene cluster encoding for monofunctional enzymes. TaB and TaE are putative ACPs, TaC and TaF homologues of HMG-CoA synthases, TaK is a variant β -ketoacyl-ACP synthase (KS^S), TaX and TaY are homologues of enoyl-CoA hydratases (ECH), and TaH is a putative cytochrome P450.

b) Structure of myxovirescin A (**1**) indicating the biosynthetic origin of its building units.^[6] Boxed carbons originate from glycine, black circles indicate C2 of acetate, triangles indicate methyl groups derived from methionine, and connected squares show the ethyl group originating from carbons 2 and 3 of succinate. c) A working model of myxovirescin A assembly depicts two rounds of modification reactions leading to the formation of C12 β -methyl and C16 β -ethyl side groups in myxovirescin scaffold. Two ATs encoded by TaV load malonyl-CoA (M-CoA) and methylmalonyl-CoA (Mm-CoA), respectively, onto their cognate ACPs (TaB and TaE), that become substrates of the decarboxylase TaK. Alternatively, propionyl-CoA may be directly loaded on TaE to give propionyl-S-TaE. Condensation of intermediate **2** with acetyl-S-TaB and intermediate **6** with propionyl-S-ACP catalyzed by the HMGs TaC and TaF, respectively, creates intermediates **3** and **7**. Removal of the carboxyl groups from intermediates **3** and **7** is a two step process involving dehydration by TaX

(resulting in intermediates **4** and **8**), followed by their sequential decarboxylation to yield **5** and **9**. The carbon labelling pattern is described in b). d) Following the formation of intermediate **9**, five more rounds of polyketide extension encoded by TaO and TaP PKSs and hydroxylation at C9 take place to yield **10**. Hydroxylation of **10** at C29 yields **11** which becomes the subsequent target of *O*-methyltransferase TaQ, giving myxovirescin A (**1**).

often belong to the so-called "*trans* AT" family of type I synthases, which lack integral AT domains, and hence compensate for these activities with "*trans*"-acting ATs.

The gene products of the HMG-cassettes have been proposed to constitute a separate pathway dedicated to the formation of the β -methyl branches in these secondary metabolites. Studies of HMG cassette enzymes from the bacillaene (PksX) pathway *in vitro* have demonstrated their likely roles in the biosynthesis *in vivo*: the discrete AT charges the ACP with the appropriate substrate (typically malonyl-CoA or methylmalonyl-CoA), the variant KS catalyzes decarboxylation, while the HMGS acts to couple the resulting acetate or propionate unit to the polyketide backbone (Figure 1 c). Finally, the two ECH homologues modify the resulting intermediate further by removing water and carboxylic group.

In comparison with similar metabolites which display characteristic β -methyl branches, myxovirescin A has a unique β -ethyl branch originating from the C2,C3 of succinate, via methylmalonate (Figure 1 b).^[6] Formation of both β -branches has been speculated to take place via this newly characterized pathway and to require the two pairs of free standing ACPs and HMGS activities (TaB/TaC and TaE/TaF), respectively (Figure 1 a). The two HMG-CoA-like synthases TaC and TaF have been proposed to carry out nucleophilic additions of acetyl-*S*-TaB and propionyl-*S*-TaE onto the C12 and C16 β -keto positions of the β -ketoacyl-*S*-ACP polyketide intermediates **2** and **6**, respectively.^[3; 7] As the other three enzymes, the variant KS (TaK^S) and the two enoyl-CoA hydratases homologues (TaX and TaY), are encoded only once in the gene cluster, they have been proposed to be

involved in both rounds of modification reactions (Figure 1 c). Following the formation of the C29 methyl carbon connected to C12 and the ethyl group attached to C16, antibiotic biosynthesis is suggested to switch back to the classical polyketide biochemistry to generate the myxovirescin lactone ring (**10**). Hydroxylation of the C29 carbon and its subsequent methylation would then yield the methylmethoxy group present in myxovirescin A (**1**) (Figure 1 d).

In our previous study, we presented genetic evidence that both HMGSs are required for biosynthesis of myxovirescin A. Deletion of *taC* caused the loss of **1**, proving that TaC is indispensable for myxovirescin production. However, TaF was not absolutely required, as its inactivation led to the production of a novel myxovirescin analogue.^[7] This new metabolite contained a methyl in place of the ethyl group at C16, providing direct evidence for the role of TaF in the formation of the ethyl group. Furthermore, production of this novel myxovirescin was not dependent on the primary metabolic HMGS *mvaS*, the only other HMGS homologue identified in the *M. xanthus* DK1622 genome.^[7] Hence, the presence of a novel β -methyl branch in the new myxovirescin analogue (myxovirescin Δ F) has been rationalized by the double action of TaC, which appears to be capable of complementing the function of TaF.^[7]

To test the remainder of the proposed biosynthetic model, a series of in-frame mutants was created and extracts of the resulting strains analyzed by high performance liquid chromatography/mass spectrometry (HPLC-MS) for the production of **1**, its analogues, or possible precursors.

Results

ΔtaB* and *ΔtaE* mutants produce similar phenotypes to those observed for their respective HMGSs mutants *ΔtaC* and *ΔtaF

As suggested by the gene organization in the cluster and low level of sequence homology between the two discrete ACPs TaB and TaE (33% identity, 51% similarity), TaB and TaE were predicted to interact with their associated HMGS TaC and TaF by forming two functional complexes (TaB/TaC and TaE/TaF) (Figure 1 a). Hence, each functional ACP/HMGS pair was hypothesized to perform one round of substrate-specific β-alkylation on the C12 and C16 β-keto positions of intermediates **2** and **6** (Figure 1, b-c). However, prior to associating with their presumed HMGS, each ACP would have to be acylated with a specific substrate (TaB with malonate and TaE with methylmalonate), by one of the two ATs present in the cluster, and further decarboxylated by a common decarboxylase TaK (Figure 1 c). If the two ACPs and HMGS indeed formed two distinct functional pairs, removal of each ACP from the megacomplex should have yielded the same phenotype observed for deletions of their presumed HMGSs.^[7]

To test these assumptions, both *taB* and *taE* were deleted from the DK1622 genome to yield *M. xanthus* strains VS1038 (*ΔtaB*) and VS1039 (*ΔtaE*). HPLC-MS analysis of their mutant extracts revealed the loss of production of **1** in both strains (data not shown).

Moreover, the *ΔtaE* mutant displayed production of the modified myxovirescin analogue that was previously isolated from the *ΔtaF* HMGS mutant background.^[7] This myxovirescin analogue contains a novel C16 β-methyl branch, and was designated as myxovirescin ΔF (**12**) (Figure 2 a). However, since the levels of **12** in *ΔtaE* mutant were reproducibly lower than in the *ΔtaF* background, quantitative HPLC-MS analysis was performed to establish its exact

concentration. Figure 2 a shows that in comparison with the ΔtaF strain, the production of **12** in the ΔtaE background was 10-fold lower, indicating an additional role of TaE.

TaB and TaK are required for the formation of β -methyl branches

Because the ΔtaF strain specifically produces analogue **12**, which contains two acetate derived β -methyl groups (one of which is subsequently modified into a β -methylene), this background was chosen to confirm that TaB/TaC, along with TaK, act in the pathway leading to the formation of **12**. Accordingly, both *taB* and *taK* were deleted from the ΔtaF and the effects of the double mutations on the production of **12** were analyzed. As expected, HPLC-MS analysis of the resulting VS1041 ($\Delta taBF$) and VS1042 ($\Delta taKF$) double mutant extracts indicated the loss of production of **12** (Table 2).

Table 1. Plasmids generated in this study.

Plasmid	Plasmid description
pVS44	627 bp fragment obtained by amplification with TaX1 and TaX2 primer pair cloned in pTOPO
pVS45	617 bp fragment obtained by amplification with TaX3 and TaX4 primer pair cloned in pTOPO
pVS46	578 bp fragment obtained by amplification with TaY1 and TaY2 primer pair cloned in pTOPO
pVS47	550 bp fragment obtained by amplification with TaY3 and TaY4 primer pair cloned in pTOPO
pVS59	Inserts from pVS46 and pVS47 cloned in <i>XbaI</i> and <i>SpeI</i> sites of pSWU41
pVS60	Inserts from pVS44 and pVS45 cloned in <i>XbaI</i> and <i>SpeI</i> sites of pSWU41
pVS66b	2560 bp fragment amplified with H1/H2 primer pair containing <i>taH</i> plus ca. 600 bp on either side of the gene; cloned in pTOPO vector
pVS68	2560 bp fragment amplified with H1/ H2 primers and cloned in <i>XbaI</i> and <i>SpeI</i> sites of pSWU41
pVS71	Derivative of pVS68 obtained by amplification with H3/H4 primer pair; the construct lacks 1422 bp of <i>taH</i>
pVS72	2276 bp fragment containing <i>taK</i> plus ca. 600 bp on both sides of the gene amplified with K1/K2 primer pair and cloned in pTOPO vector
pVS73	1484 bp fragment containing <i>taB</i> and ca. 600 bp on both sides of the gene amplified with B2/B3 primer pair and cloned in pTOPO vector
pVS77	1425 bp fragment containing <i>taE</i> and ca. 600 bp on both sides of the gene amplified with E2/E3 primer pair and cloned in pTOPO vector
pVS78	Derivative of pVS72 lacking 1179 bp of <i>taK</i> (ΔtaK). Obtained by amplification of pVS72 with K3/K4 primer pair.
pVS79	Derivative of pVS73 lacking 240 bp of <i>taB</i> (ΔtaB). Obtained by amplification of pVS73 with B1/B4 primer pair.
pVS80	Derivative of pVS77 lacking 201 bp of <i>taE</i> (ΔtaE). Obtained by amplification of pVS77 with E1/E4 primer pair.
pVS81	1097 bp fragment from pVS78 subcloned in <i>BamHI/XbaI</i> sites of pSWU41
pVS82	1244 fragment from pVS79 subcloned in <i>BamHI/XbaI</i> sites of pSWU41
pVS83	1224 bp fragment from pVS80 subcloned in <i>BamHI/XbaI</i> sites of pSWU41

TaK, a variant ketosynthase, is not absolutely required for myxovirescin A production

taK, like many other discretely encoded KS domains found in the HMGS-containing natural product gene clusters, can be distinguished from standard KSs because of its Cys to Ser substitution in the active site (KS^S). Biochemical analysis of fatty acid KSs from *E. coli* with the identical mutation have shown the enzymes to be severely deficient in catalyzing

Table 2. List of *M. xanthus* strains used in this study.

Strain	Genotype	Myxovirescin Analogue	Reference
DK1622	<i>M. xanthus</i> wild type	A (1)	^[8]
VS1019	pVS59 x DK1622	-	This study
VS1020	pVS60 x DK1622	-	This study
VS1028	pVS71 x DK1622	-	This study
VS1032	pVS83 x DK1622	-	This study
VS1033	pVS82 x DK1622	-	This study
VS1034	pVS82 x VS1012	-	This study
VS1035	pVS81 x DK1622	-	This study
VS1036	pVS81 x VS1012	-	This study
VS1023	ΔtaY	-	This study
VS1026	ΔtaX	-	This study
VS1038	ΔtaB	-	This study
VS1039	ΔtaE	ΔF (12)	This study
VS1012	ΔtaF	12	^[7]
VS1040	ΔtaK	1	This study
VS1041	$\Delta taBF$	-	This study
VS1042	$\Delta taKF$	-	This study
VS1030	ΔtaH	ΔH (10)	This study

condensation, while retaining their decarboxylative functions.^[9; 10] Recently, PksF of *B. subtilis*, which shows 54% identity and 71% similarity with TaK, has been shown to participate in the pathway dedicated to β -methylation, by catalyzing decarboxylation of malonyl-*S*-ACP to acetyl-*S*-ACP^[5] (compare Figure 1 c). Since there is only a single copy of such mutant KS^S present in the whole DK1622 genome, and two predicted decarboxylation reactions, TaK has been postulated to act twice during biosynthesis to cleave carboxyl groups from both malonyl and methylmalonyl-*S*-ACP substrates (Figure 1 c). Therefore, removing *taK* from the system would be expected to abolish myxovirescin biosynthesis. In order to verify the involvement of TaK in myxovirescin biosynthesis, *taK* was deleted from the genome and the effect of this mutation on **1** was analyzed. However, contrary to our

expectations, production of **1** was still observed in VS1040 (ΔtaK), although at 120-fold reduced levels relative to the wild type (Figure 2 b).

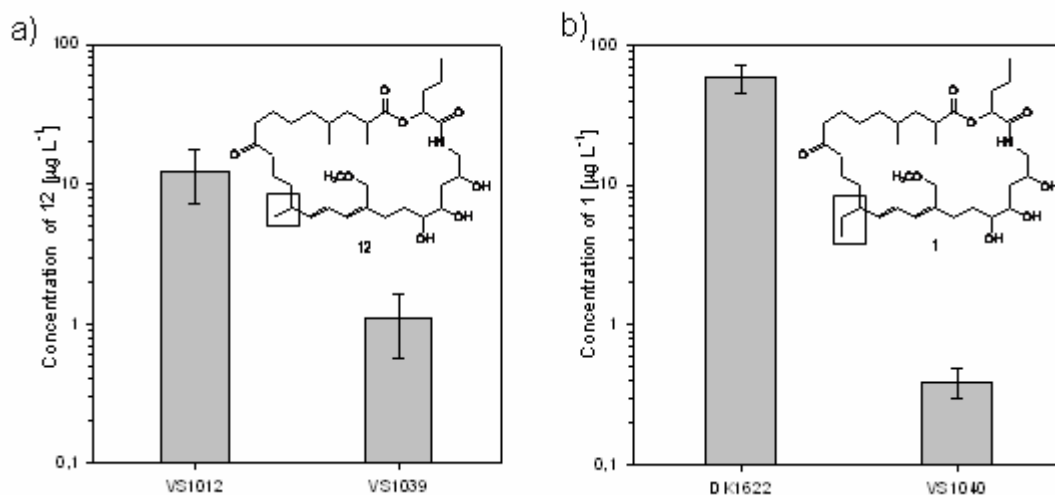


Figure 2. Quantitative HPLC-MS analysis of the VS1012 (ΔtaF) and VS1039 (ΔtaE) a) and DK1622 and VS1040 (ΔtaK) b). The error bars represent the standard deviation obtained from five independent experiments. **1** and **12** were quantified using Bruker quantification software by integrating three major $[M+H]^+$ peaks (578.5, 560.5 and 542.5) of **12** and 592.5, 574.5 and 556.5 peaks of **1**.

TaX and TaY, two members of ECH superfamily, are required for myxovirescin A production

Both TaX and TaY show similarity with members of enoyl-CoA hydratase superfamily. In particular, TaX is more similar to PksH of bacillaene and CurE from the curacin systems, which both catalyze dehydrations (Figure 3 a), whereas TaY is more closely related to the decarboxylases PksI and CurF (Figure 3 b).^[5; 11] Based on the sequence homologies with these biochemically characterized enzymes, TaX was proposed to dehydrate intermediates **3** and **7**, respectively, to yield **4** and **8**. Further removal of carboxyl groups from **4** and **8** by TaY should yield intermediates **5** and **9**, respectively (Figure 1 c). Unfortunately, aside from the observed loss of **1**, HPLC-MS analysis of VS1026 (ΔtaX) and VS1023 (ΔtaY) mutant extracts did not reveal the production of new analogues of **1** with additional hydroxyl

and carboxyl groups attached to carbons C12/C29 and C16/C31, or hydrolytic release of possible intermediates **3**, **4**, **7** or **8** (Figure 1, b-c).

TaH, a cytochrome P450, hydroxylates the β -methyl group of myxovirescin A

As indicated in Figure 1 d, following the assembly of the myxovirescin skeleton, formation of mature myxovirescin A requires three more modification reactions. We have previously shown that the last step in the formation of the methylmethoxy group is catalyzed by the SAM-dependent methyltransferase TaQ (Figure 1 b).^[3] The two remaining reactions are

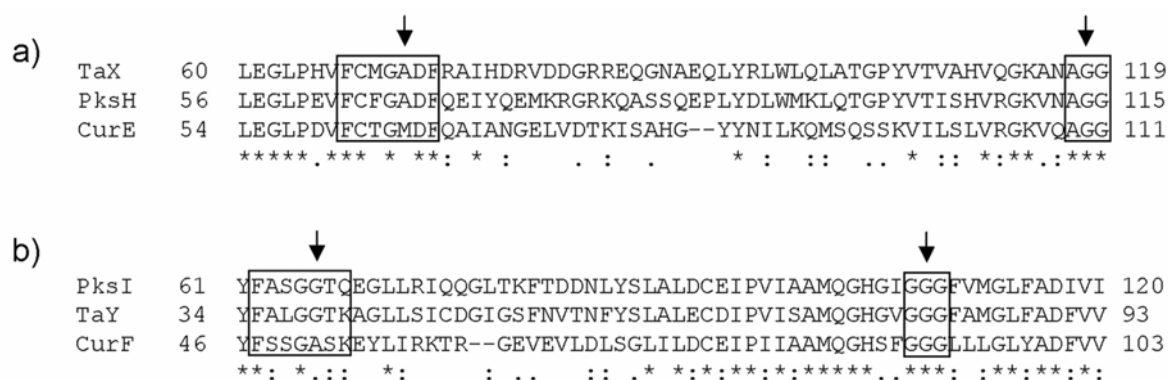


Figure 3. ClustalW alignments of members of TaX and TaY with members of the ECH superfamily from bacillaene (PksX) and curacin (Cur) systems. PksH (CAB13587) and CurE (AAT70100) have been demonstrated to function as dehydratases, while PksI (CAB13588) and CurF (AAT70101) as decarboxylases.^[5; 11] The accession numbers are indicated in parenthesis. Arrows indicate amino acids which stabilize the thioester carbonyl by hydrogen bonding via their peptidic NH groups.

hydroxylations which are expected to target carbons C9 and C29. The three candidates for these two reactions are TaH, annotated as a cytochrome P450 hydroxylase (E value = 3×10^{-51}), and two putative oxygenases TaN and TaJ.^[3]

To determine the molecular target of TaH, *taH* was deleted in frame from the DK1622 chromosome, resulting in strain VS1030. Comparative analysis of mass chromatograms of extracts of wild type DK1622 (Figure 4 a, left panel) and VS1030 (Figure 4 a, right panel)

(m/z 590–625) revealed an approximately 1 minute delay in the retention time of myxoviorescins in strain VS1030 relative to the wild type. The UV absorption maxima at 239 nm showed the same trend (Figure 4 b). In particular, strain VS1030 did not produce **1** ($[M+H]^+ = 624$), but a novel myxovioreascin analogue of $[M+H]^+ = 594$. A tandem MS fragmentation of $[M+H]^+ = 594$ confirmed that this new compound, named myxovioreascin ΔH , does not fragment to give a $[M+H-32]^+$ ion, which is characteristic of the fragmentation of **1** (Figure 4 c, bottom panel). Yet, all the subsequent fragmentations followed a pattern identical to the one observed with the reference compound (compare Figure 4 c). Furthermore, the high resolution mass spectrum (HRMS) of myxovioreascin ΔH $[M+H]^+ = 594.4358$ is in good agreement with the molecular formula $C_{34}H_{60}O_7N^+$ (calculated m/z $[M+H]^+ = 594.4364$, $\Delta m/z = -1.08$ ppm, see Supplementary materials), consistent with the loss of a methoxy group relative to **1**.

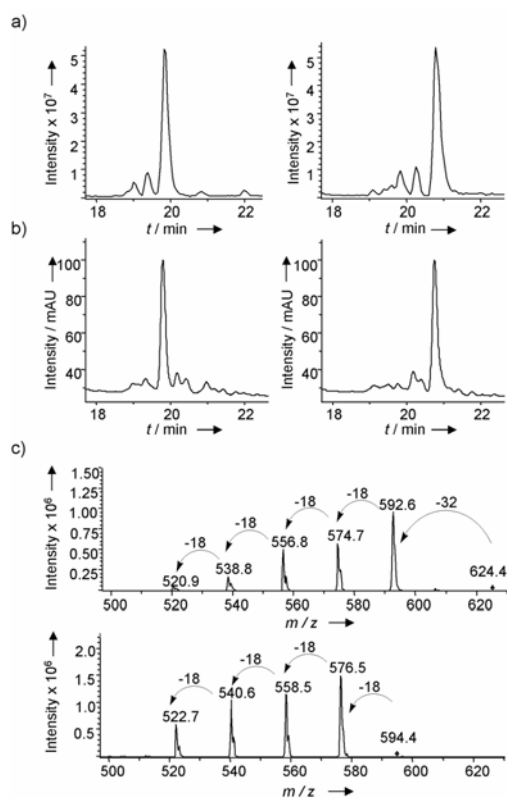


Figure 4. Analysis of the cytochrome P450 mutant strain VS1030 (ΔtaH). a) Mass ion chromatograms in the 590-625 range from the *M. xanthus* DK1622 (left) and VS1030 (ΔtaH) strain (right). b) UV₂₃₉ nm absorption measured in the DK1622 (left) and VS1030 (right). c) Tandem MS fragmentation patterns of myxovirescin A ($[M+H]^+ = 624$) (top) and the novel myxovirescin ΔH ($[M+H]^+ = 594$) (bottom).

To confirm whether the largest fragment ion resulting from the fragmentation of **1** is indeed a product of the elimination of the C29 methoxy group (neutral loss, $\Delta m/z = 32$ units), **1** was subjected to MS-MS fragmentation and the HRMS of the largest molecular ion ($[592]^+$) was determined. The calculated HRMS of 592.4208 was in agreement with the experimentally determined mass, and corresponds to the molecular formula $C_{34}H_{58}O_7N^+$, reflecting the loss of methanol (CH_3OH) relative to **1** (Supplementary material). As there is only one methoxy group present in **1**, myxovirescin ΔH was assigned structure **10** (Figure 1 d). Interestingly, the production of **10** in VS1030 was equal to the levels of **1** measured in the reference strain (Figure 4 b).

Discussion

Our model for myxovirescin A (**1**) assembly proposes that the two ACP/HMGS pairs are β -branch-specific, whereas TaK, TaX and TaY are shared between the two pathways (Figure 1 c). Indeed, in our previous study we have shown that removal of TaC halts myxovirescin biosynthesis whereas the loss of TaF leads to the production of a new myxovirescin with two methyl groups at the C12 and C16 positions (the methyl group at C12 being further elaborated into methylmethoxy functionality). In this study we have demonstrated that deletions of their proposed accompanying ACPs, TaB and TaE, yield similar phenotypes (Table 2 and Figure 2 a). These results provide direct evidence that each ACP has a cognate HMGS with which it forms a functional pair (e.g. TaB with TaC and TaE with TaF). Thus, the ACPs are not functionally exchangeable during biosynthesis, e.g. TaB does not function in combination with TaF and TaE with TaC. Furthermore, these results

demonstrate the functional roles of the two enzyme pairs: the TaB/TaC pair directs formation of the methyl group, while TaE/TaF directs formation of the ethyl group.

Another important conclusion arising from this genetic study is that the functions of the two ACP/HMGS enzyme pairs are not mutually complementary. Our results suggest that TaB/TaC can rescue myxovirescin production in the absence of either TaE or TaF, most likely by performing two rounds of acetate delivery (TaB) and acetate condensation (TaC) with intermediates **2** and **6** to manufacture myxovirescin ΔF (**12**). However, the reverse complementation cannot occur, as the TaE/TaF enzyme duo cannot substitute for TaB/TaC. Therefore, both TaB and TaC are essential for antibiotic assembly. In addition, the ability of TaB/TaC to complement TaE/TaF implies a level of flexibility of the TaB/TaC pair in docking with module 7 of Ta-1, as well as module 8 in processing the intermediate with the shorter side chain. However, the molecular determinants for these protein-protein interactions are not known at present time.

Given the expectation that deletions of *taB* and *taE* were anticipated to phenotypically mimic deletions of their partner HMGSs, it was surprising to measure a 10-fold drop in the production of **12** in ΔtaE strain relative to ΔtaF background (Figure 2 a). This result demonstrates that the loss of TaE is even more incapacitating to the megasynthetase than the loss of the condensing enzyme TaF, and points to an additional and yet unknown function of TaE in biosynthesis. The observed functional differences between TaB and TaE are also consistent with their low sequence identity. Indeed, given the central role of ACPs in PKS and fatty acid biosynthesis, as well as in the pathway leading to β -methyl group formation, it is plausible that the divergence of the ACPs was required to insure the correct spatial implementation of two different substrates in myxovirescin polyketide scaffold.

Unlike the two ACPs, TaK was proposed to act twice during biosynthesis, by decarboxylating both malonyl-*S*-TaB and methylmalonyl-*S*-TaE intermediates (Figure 1 c). Unexpectedly, production of myxovirescin A continued in the ΔtaK background, albeit at a 120-fold reduced level. However, the production of **12** was completely abolished in $\Delta taKF$ background. The genome search for possible homologues of TaK did not identify another monofunctional KS exhibiting a similar mutation. Taken together, these results indicate the role of TaK in the formation of the β -methyl branch and suggest that either a different enzyme decarboxylates methylmalonyl-*S*-TaE, or that the corresponding "*trans* AT" loads propionyl-CoA directly onto TaE ACP. Alternatively, the residual amount of myxovirescin A observed in the ΔtaK background could be generated through availability of the low amount of spontaneously decarboxylated malonyl-*S*-ACP and methylmalonyl-*S*-ACP.

Finally, analysis of the cytochrome P450 mutant has provided the last clue towards understanding the biosynthesis of the methylmethoxy group (Figures. 1 d and 4). Formation of **10** in the strain VS1030 fully confirms our hypothesis regarding the two-step conversion of the methyl into the methylmethoxy group. In contrast to the severe impact of other mutations on myxovirescin production (Table 2),^[3; 7] production of **10** in ΔtaH was equal to the production of **1** in DK1622 (Figure 4 b). Based on this result we conclude that the conversion of **10** to **1** takes place following formation of the lactone ring.

An emerging body of evidence combining both in vitro and in vivo observations on the bacillaene and myxovirescin systems demonstrates the evolutionary divergence of primary and secondary metabolic (SM) HMGSs. These differences include the demonstrated use of ACP- instead of CoA-activated substrates.^[5] Furthermore, SM HMGSs show wide promiscuity toward different substrates. For example, certain HMGS are likely to accept

propionyl-*S*-ACP in addition to acetyl-*S*-ACP as the first substrates, and perform nucleophilic additions on β -ketoacyl-*S*-ACP intermediates of different chain lengths. For example, PksG is catalytically active with acetoacetyl-*S*-ACP even though its natural substrate is predicted to be fifteen carbons long.^[5; 12] Similarly, our results suggest that TaF acts on a substrate with C18 chain length.^[7] As the structure of a SM HMGS has not yet been solved, it is to hope that the future high-resolution structural information on members of this newly recognized family of condensing enzymes will be able to provide deeper insights into their flexibility toward heterogeneous substrates.

In contrast to the HMG-like synthases, which have preserved the overall reaction mechanism, members of the ECH superfamily are well-known for their mechanistic diversity and catalyze various reactions ranging from dehalogenation, (de)hydration, decarboxylation, formation/cleavage of carbon-carbon bonds, hydrolysis of thioesters etc.^[13] Despite the overall differences in their reaction mechanisms, ECH family members share a partial reaction mechanism which enables stabilization of enoyl-CoA anion intermediates within an oxyanion hole (residues outlined in two boxes, Figure 3). However, consistent with different overall reactions they catalyze, the active site residues within the superfamily vary.

Two homologues of this superfamily have been found to be conserved across several biosynthetic gene clusters.^[2; 5; 14; 15] In vitro characterizations of two pairs of ECHs from the bacillaene and curacin systems, and the very recent characterization of TaX and TaY (Calderone C. et al., personal communication) have demonstrated their functions as dehydratases and decarboxylases, respectively.^[5; 11] At this point we cannot differentiate whether the observed loss of myxovirescin production in ΔtaX and ΔtaY backgrounds is a

result of the rejection of the proposed intermediates **3**, **4**, **7** or **8** by the assembly line, by the requirement of the two enzymes for megasynthetase turnover, or both.

Conclusions

The mutagenic analysis of eight discrete genes encoded in the myxovirescin gene cluster constitutes the first comprehensive *in vivo* study toward elucidation of the biosynthetic pathway leading to the formation and tailoring of β -branches in one secondary metabolite. In addition to the elucidation of functional roles of certain genes, our results present evidence for the plasticity of myxovirescin megasynthase. However, several aspects of the biosynthesis remain to be elucidated, including the nature of protein-protein interactions between β -modifying enzymes and the PKS multienzyme. Nonetheless, the relative ease of manipulating discretely encoded activities in contrast to the giant polyketide synthases, coupled with the observed broad substrate specificity of HMGS and ECH homologues, suggests that HMG toolboxes and their accessory enzymes may be successfully exploited in future attempts to generate new, ' β -modified' bioactive compounds.

Experimental Section

Creation of deletion mutants: The general cloning strategy used for the construction of vectors intended for creation of in-frame deletions of ΔtaB , ΔtaE , ΔtaH and ΔtaK is exemplified here with the deletion of *taK*. To delete *taK*, the chromosomal region including *taK* and approximately 600 bp upstream and downstream from it was amplified using K1 and K2 primers (see Supplementary material) and Phusion polymerase (New England Biolabs). The resulting 2276 bp PCR product carrying *Bam*HI and *Xba*I overhangs was gel purified (Macherey und Nagel), modified with A overhangs, and cloned in pCR2.1[®]-TOPO vector

yielding plasmid pVS72. Plasmid pVS72 was amplified in the second PCR reaction using primers K3 and K4, designed to be in-frame with *taK*, with Phusion polymerase. Following amplification, the PCR reaction was treated with *DpnI* enzyme to eliminate the template DNA. The 5 kb PCR product was gel purified, treated with T4 kinase and T4 ligase, and transformed into *E. coli* DH10B. The new plasmid, pVS76, lacking the *taK* gene but containing the 600 bp upstream and downstream of the gene was submitted for sequencing. Finally, the approximately 1200 bp insert was subcloned from pVS76 into *Bam*HI and *Xba*I sites of vector pSWU41 to create plasmid pVS79, which was used for electroporation in *M. xanthus* DK1622. The cloning strategy used to generate plasmids for ΔtaX and ΔtaY mutations as well as the creation of in-frame deletion mutants was carried out as described in.^[3] To create $\Delta taEF$ and $\Delta taKF$ double mutants, plasmids pVS81 and pVS79, respectively, were electroporated, and later excised, from the chromosome of VS1012 (ΔtaF background). Sequences of all primers are provided in Supplementary materials and the list of generated plasmids is given in Table 1.

Growth conditions: Myxovirescin production was assayed in MD-1 medium that consisted of casitone (0.3%), $\text{CaCl}_2 \cdot 2 \text{H}_2\text{O}$ (0.07%), and $\text{MgSO}_4 \cdot 7 \text{H}_2\text{O}$ (0.2%); vitamin B12 ($5 \times 10^{-4} \mu\text{g L}^{-1}$) was added after cooling and analyzed for myxovirescin production as reported previously.^[3]

HPLC-MS analysis and quantification of 1 and myxovirescin ΔF : HPLC-MS analysis and quantitative HPLC-MS analysis was carried out as described.^[3] Myxovirescin ΔF was quantified by integrating three major peaks at *m/z* 576.5, 558.5 and 540.6 peaks.

High resolution mass spectral analysis (HRMS): Determination of HRMS of myxovirescin Δ H and its fragment ions was carried out using ESI-FT/Orbitrap mass spectrometry.

Measurements were performed using an UPLC-coupled LTQ Orbitrap instrument (Thermo Finnigan, Bremen/Germany) in positive ionization mode with a resolution setting of $R = 60000$. External calibration in the m/z range 195–2000 was done using "LTQ Calibration solution" containing caffeine, MRFA (Met-Arg-Phe-Ala tetrapeptide) and the "Ultramark 1621" reference mixture. Calculation of the putative molecular formula from the accurate mass spectra of target compounds was performed using the XCalibur 2.0 software suite.

Acknowledgments

The authors would like to thank Dr. K. J. Weissman for helpful comments in preparation of this manuscript and D. Krug for help with quantitative HPLC-MS and for performing the Orbi-Trap measurements. This study was funded by the Deutsche Forschungsgemeinschaft (DFG) and the Bundesministerium für Bildung und Forschung (BMBF).

References

- [1] M. A. Fischbach, C. T. Walsh, *Chem.Rev.* 2006, **106**, 3468-3496.
- [2] A. K. El-Sayed, J. Hothersall, S. M. Cooper, E. Stephens, T. J. Simpson, C. M. Thomas, *Chem.Biol.* 2003, **10**, 419-430.
- [3] V. Simunovic, J. Zapp, S. Rachid, D. Krug, P. Meiser, R. Müller, *ChemBioChem* 2006, **7**, 1206-1220.
- [4] R. A. Butcher, F. C. Schroeder, M. A. Fischbach, P. D. Straight, R. Kolter, C. T. Walsh, J. Clardy, *P.Natl.Acad.Sci.USA* 2007, **104**, 1506-1509.
- [5] C. T. Calderone, W. E. Kowtoniuk, N. L. Kelleher, C. T. Walsh, P. C. Dorrestein, *P.Natl.Acad.Sci.USA* 2006, **103**, 8977-8982.
- [6] W. Trowitzsch-Kienast, K. Schober, V. Wray, K. Gerth, H. Reichenbach, G. Höfle, *Liebigs Ann.Chem.* 1989, 345-355.
- [7] V. Simunovic, R. Müller, *ChemBioChem* 2007, **8**, 497-500.
- [8] H. Chen, I. M. Keseler, L. J. Shimkets, *J.Bacteriol.* 1990, **172**, 4206-4213.
- [9] C. Davies, R. J. Heath, S. W. White, C. O. Rock, *Structure Fold Des.* 2000, **8**, 185-195.
- [10] K. A. McGuire, M. Siggaard-Andersen, M. G. Banger, J. G. Olsen, P. von Wettstein-Knowles, *Biochemistry-US* 2001, **40**, 9836-9845.
- [11] L. Gu, J. Jia, H. Liu, K. Hakansson, W. H. Gerwick, D. H. Sherman, *J.Am.Chem.Soc.* 2006, **128**, 9014-9015.
- [12] R. A. Butcher, F. C. Schroeder, M. A. Fischbach, P. D. Straight, R. Kolter, C. T. Walsh, J. Clardy, *P.Natl.Acad.Sci.USA* 2007, **104**, 1506-1509.
- [13] H. M. Holden, M. M. Benning, T. Haller, J. A. Gerlt, *Acc.Chem.Res.* 2001, **34**, 145-157.
- [14] J. Piel, G. P. Wen, M. Platzer, D. Q. Hui, *ChemBioChem* 2004, **5**, 93-98.
- [15] D. J. Edwards, B. L. Marquez, L. M. Nogle, K. McPhail, D. E. Goeger, M. A. Roberts, W. H. Gerwick, *Chem.Biol.* 2004, **11**, 817-833.

Supporting material

for

Mutational Analysis of the Myxovirescin Biosynthetic Gene Cluster Reveals
Novel Insights into the Functional Elaboration of Polyketide Backbones

V. Simunovic and R. Müller

2007. Copyright John Wiley & Sons.

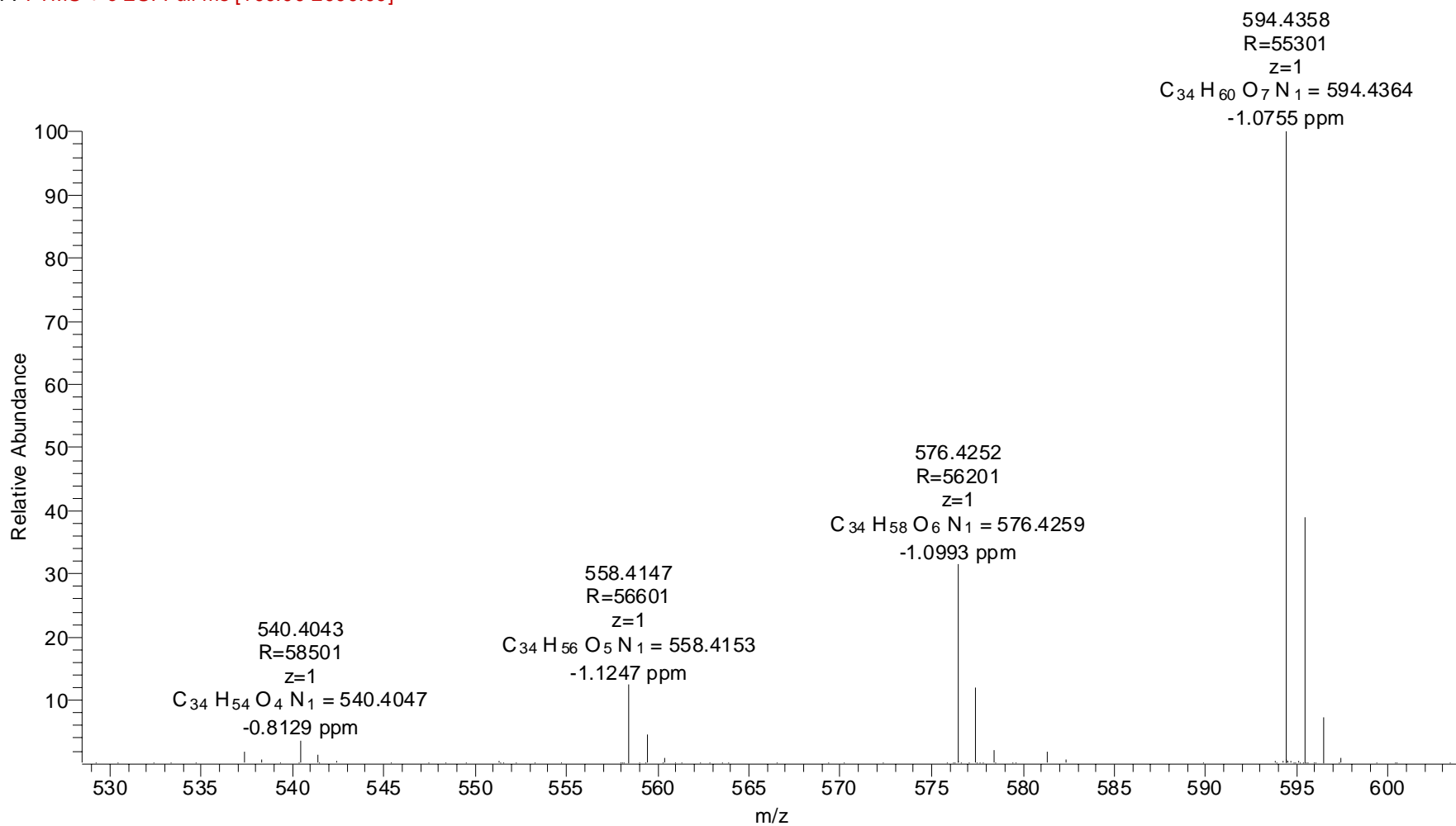
Table 1. List of primers used in the study.

Primer name	Primer sequence (5'→3')
B1	GGTCCCTGAAGCCTTGCTGCG
B2	CGGGATCCGTTGGTGTGCCAGTTATTGCCA*
B3	GCTCTAGACCATCACCTCGTAGCCGTAGT
B4	GCGAGGCTGTGAGGCGAAGC
E1	TTCGTCTGTCATCGGCTCACC
E2	CGGGATCCCATGAAGAGCTGTACGAGCAG
E3	GCTCTAGATCGTAGCTGTAGTTGCCGAAC
E4	CTGGTGGCGTTCCTGGCC
K1	CGGGATCCGCCGTGGAACAGGTCCTTCG
K2	GCTCTAGAGAGGAACGGCATCACGCAG
K3	CGAGACAACCAGCTCCTGCAC
K4	GACCCGATTGATTCATCGTTC
E5f	ATGTTGCGGATGTCGGCG
E6f	TGCATCGCCAGGTAGTCG
E7r	GTCGAAGGCGTACAACCTC
B5f	CCAGCTTCTCCAGCGTGAG
B6f	TTCACCATGCCGCCAAACG
B7r	GCTTGACACGCTGCCTCAT
K5f	TGGACTTCGTGGTGTGAC
K6f	GCAACAGCTTCTCGCTATC
K7r	GAGACGGGACTGCGGCTGGT
TaX1	GCTCTAGAAGGCGTGGGGCAAGACTTCCTT
TaX2	CGGGATCCGCCATCCATCGCTACGTGG
TaX3	CGGGATCCACAGGTCTGCGCCTCGAAG
TaX4	GGACTAGTATCTTTGGAGAGGCGTGCGG
taX5	ACGCAGCAGTTCGCCATCCA
taX6	CACATAACCGTGTGCGTGGT
taX7	CGCACTACCTGACGCTGATG
TaY1	GCTCTAGAATCAGCGGCGTGATGATGGC
TaY2	CGGGATCCAAACCTCGGCTGTGCTCGTGA
TaY3	CGGGATCCACCTTGCCGAACACGGTGATGA
TaY4	GGACTAGTATCGTGCTGGCAAAGGCGGA
taY5	GGACAACACCATCAGCCGCA
taY6	GCAGTCACCGAAGAGCAGCT
taY7	GGTGATTTCGCCATGCAGG
H1	GGACTAGTCCACCTCCAATTCCGACGAA
H2	GCTCTAGATAGTTGATGGCTGCAACC
H3	CAGGAACAACATCATCAACTG
H4	TTCGCCTACTACGAGATGAAG
H5 rev	GAAAGAGAACCTTCGCTGTCT
H6 for	AGTTCCTGCTGAATCCGTCC
H7 del	GAATCACCTCCAGCATGATC

*Underlined nucleotides indicate restriction sites

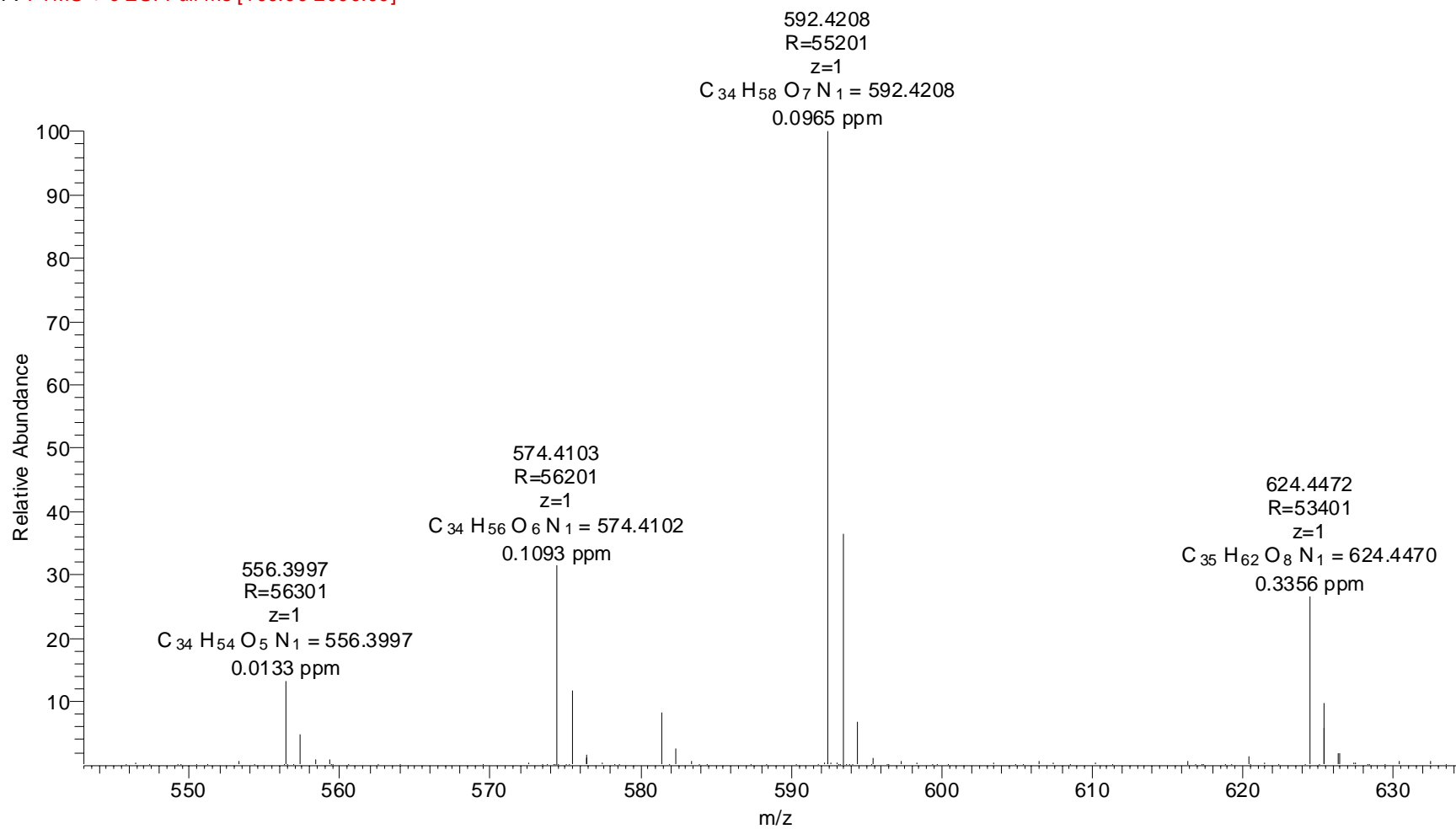
Orbitrap measurements for myxovirescin Δ H, in source fragmentation

VS_dH_001 #539 RT: 8.38 AV: 1 NL: 2.37E7
F: FTMS + c ESI Full ms [100.00-2000.00]



Orbitrap measurements for myxovirescin A, in source fragmentation

VS_myva_001 #515 RT: 8.01 AV: 1 NL: 1.19E7
F: FTMS + c ESI Full ms [100.00-2000.00]



Chapter 5

Regulation of myxovirescin production in *M. xanthus* DK1622

Introduction

Early attempts to optimize myxovirescin production indicated the importance of reduced carbon conditions in the production medium. In *M. xanthus* TA, concentrations of peptone larger than 1% caused complete inhibition of antibiotic production, whereas alanine, serine and glycine stimulated its formation.^[79] Accordingly, the subsequent fermentation processes were carried out in 0.5% or 0.3% casitone medium. The importance of the quantity and rate of peptone addition, as well as aeration, for myxovirescin production has also been documented for a related myxococcus strain, *M. virescens*.^[80] Growth of *M. virescens* was also inhibited by increased intracellular concentrations of ammonium and accumulation of aspartic and glutamic acids in the culture supernatants during fermentation. Hence, continuous extraction of ammonium boosted myxovirescin production by up to 13-fold.^[18]

Aside from these early physiological studies, there are no published experiments addressing the molecular mechanisms of regulation of secondary metabolism in *M. xanthus*. Therefore, we were encouraged to identify a gene locus approximately 11 kb in size located upstream from the myxovirescin biosynthetic cluster, which suggested a possible regulatory function (**Figure 1**).

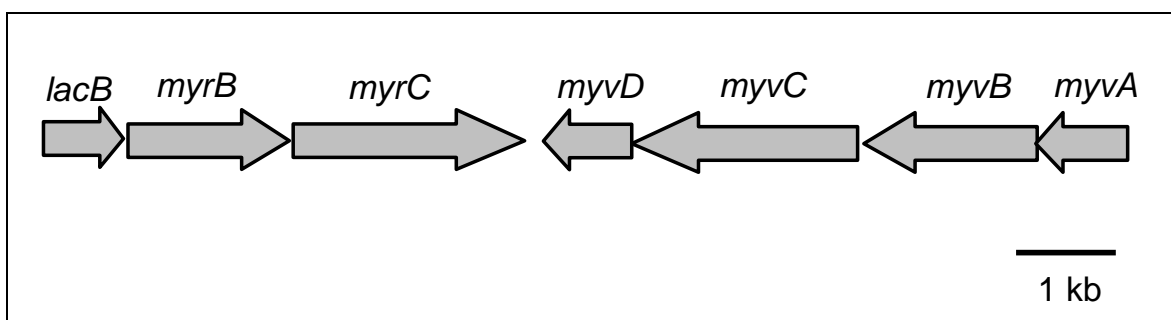


Figure 1. 10.9 kb of myxovirescin regulatory region. Seven genes are organized into two putative operons with predicted functions listed in Table 1. The myxovirescin biosynthetic gene cluster starts upstream from *lacB* in the reverse direction.

Organization and in silico annotation of the 10.9 kb locus upstream from the myxovirescin biosynthetic gene cluster

As outlined in **Figure 1**, the 10.9 kb region appears to be organized into two operons (*myr* and *myv*) transcribed in opposite directions. The *myr* operon consists of three genes. The *lacB* shows similarity ($E = 2 \times 10^{-6}$) with the B superfamily of Zn-dependent lactamases (<http://pfam.janelia.org/>) (**Table 1**). In addition to hydrolysis of the beta lactam rings, members of this family also catalyze other reactions such as thioesterifications and hydrolysis. The second gene, *myrB*, encodes a σ^{54} -dependent activator protein, also known as enhancer binding protein (EBP). MyrB has multimodular structure consisting of a central AAA domain specialized in binding and hydrolysis of ATP and C-terminal helix-turn-helix motif for binding DNA. The N-terminus of MyrB plays a sensory role and consists of the small-molecule-binding GAF domain (**Figure 2**). The EBP class of transcriptional activators bind to the enhancer boxes upstream or downstream from the promoter, and initiate transcription via σ^{54} contact-dependent hydrolysis of ATP (**Figure 3**). This process requires EBP-dependent

Table 1. List of genes comprising two myxovirescin regulatory operons, their proteins and identified conserved domains.

ORF/ protein	Size (bp) Amino acids (aa)	Closest homologue in the PubMed database (% identity/similarity)	Putative function	Protein domains identified by Pfam search engine (amino acid coordinates)
<i>lacB</i> / LacB	795/265	TaR-3 from <i>S. aurantiaca</i> DW4/3-1 (78/86)	Thioesterase, hydrolase of unknown function	Lactamase B (2-203)
<i>myrB</i> / MyrB	1590/530	TaR-2 from <i>S. aurantiaca</i> DW4/3-1 (81/88)	σ^{54} -dependent enhancer binding protein (EBP)	GAF (43-180) AAA (207429) HTH (483-523)
<i>myrC</i> / MyrC	2358/786	-	Unknown	-
<i>myvD</i> / MyvD	879/293	<i>S. aurantiaca</i> DW4/3-1 (50/67)	Unknown	-
<i>myvC</i> / <i>MyvC</i> (<i>pkn10</i>)	2244/748	Pkn10 of <i>S. aurantiaca</i> DW4/3-1 (62/73)	Serine/tyrosine/ threonine kinase (STK)	STK (168-412)
<i>myvB</i> / MyvB	1734/578	Adenylate cyclase of <i>S.</i> <i>aurantiaca</i> DW4/3-1 (78/87)	Signal transduction/ transcriptional regulation	FHA (61-124) GAF (204- 338) AC (377-564)
<i>myvA</i> / MyvA	912/304	STIAU_4297 of <i>S. aurantiaca</i> DW4/3-1 (59/76)	Unknown	-

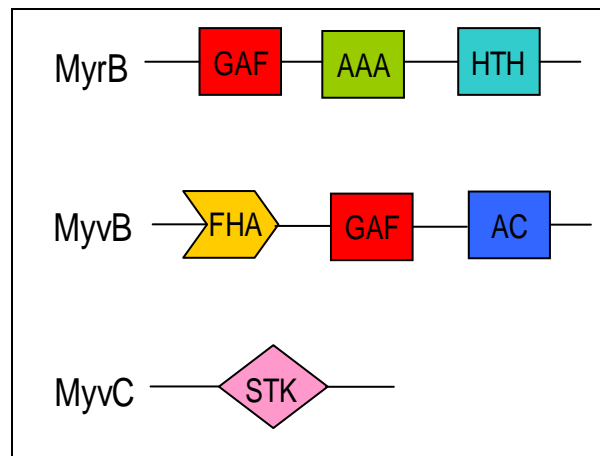


Figure 2. The modular organization of MyrB, MyvB and MyvC indicates a complex regulatory network involving a variety of domains. GAF domains bind small molecules, adenylate cyclases (AC) synthesize cyclic adenylyl monophosphates (cAMP) from ATP. FHA domains function as phosphothreonine/phosphotyrosine binding epitopes, and hence may transduce a signal to serine/threonine kinase MyvC or vice versa.

bending (looping) of DNA. The conformational switch from the closed to an open RNA-polymerase- σ^{54} complex is driven by energy released from ATP hydrolysis.^[81] σ^{54} binds to the relatively conserved -12/-24 region upstream from the +1 transcriptional start site. One such putative σ^{54} binding region was identified 242 bp upstream from Ta-1PKS:

TTGGCTCGCGTCTGGCT, where the letters in bold indicate the conserved nucleotides at -12 and -24 positions from the presumed transcriptional start site (Materials and methods).

MyrB exhibits the same domain organization (GAF-AAA-HTH) as the transcriptional activator NifA from *Azotobacter vinelandii*.^[82] NifA is involved in the activation of all but one operon carrying out nitrogen fixation. MyrB is also similar to FhlA of *E. coli*, the transcriptional regulator of the formate regulon.^[83] However, unlike MyrB and NifA, FhlA contains two amino terminal GAF domains. Interestingly, MyrC, MyvA and MyvD do not show similarity to any other protein in the database. However, MyvB is composed of three conserved protein domains: the adenylate cyclase (AC) domain, which presumably cyclizes ATP into cAMP, the GAF domain, and the FHA domain. FHA domains have been shown to interact with phosphothreonine/phosphotyrosine residues.^[63] Hence, MyvB may be a part

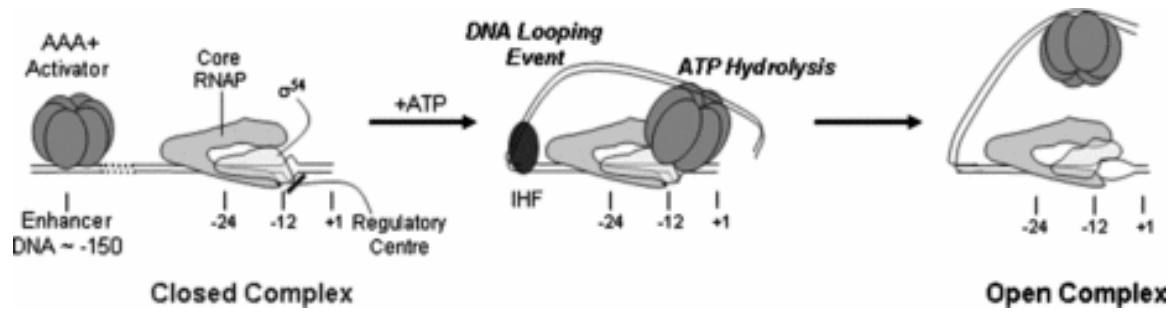


Figure 3. A three-step mechanism for EBP-dependent activation of transcription from σ^{54} -specific promoters (Figure reproduced from).^[81]

of a signal transduction cascade involving putative serine/threonine kinase MyvC. Curiously, *myvB* and *myvC* are most likely transcriptionally coupled.

The presence of the AC domain and two GAF domains suggests a possible role of cAMP in the regulation of EBPs. However, analysis of the two GAF domains did not reveal the conservation of five residues (NKFDE motif) which were shown to be essential for binding of cGMPs to a mammalian phosphodiesterase (PDEs) containing tandem GAF domains.^[84] These residues were also found to be conserved in cAMP-binding *Anabaena* adenylate cyclase.^[85]

Results

To examine the involvement of some of the genes in myxovirescin production, we decided to knockout *myrC* and *myvD*, as the resulting mutations could not cause polar effects on the downstream genes (**Figure 1**). A third mutant containing a disruption in the gene *myvD*, was obtained from the Prof. Inouye's laboratory. Upon construction of the two merodiploid mutants (**Table 1**), the three mutants were grown alongside the DK1622 (wild type) strain, and the resulting cell extracts were examined for myxovirescin production using HPLC (**Table 2**). Our results indicate that all three mutations exhibit negative effects on myxovirescin production: the *myrC* mutant yields 28 % reduced production relative to the DK1622, whereas *myvC* and *myvD* mutants produce only 6.5 % and 12.5 % of the wild type antibiotic levels.

Table 2. *M. xanthus* strains, their genotypes and the level of myxovirescin production.

<i>M. xanthus</i> strain	Genotype	% of wild type production*
DK1622	Wild type	100
<i>myrC</i> (VS1013)	pVS64 x DK1622	72
<i>myvD</i> (VS1014)	pVS66 x DK1622	12.5
<i>myvC</i>	ppkn10 x DK1622	6.5

*Percentages indicate the average of two independent experiments.

Experimental Section

Creation of *myrC* (VS1013) and *myrD* (VS1014) mutants: To knock out *myrC*, a 500 bp amplificate was generated using DK1622 genomic DNA and tar_up 5'-ACTTCAACTAGCTGGGCGAC-3'/ tar_down 5'-CTGGTAGTCGTCGGTGAGGG-3' primer pair. The resulting PCR fragment was cloned in pTOPO vector resulting in construct pVS64 (**Table 2**). To disrupt *myrD*, a 594 bp amplificate was obtained using 29_up 5'-CTCTGTTGAGGTTCCGACTTCTGGC-3'/ 29_down 5'-ACGCGGGCGAAAAGGACACC-3' primer pair and cloned in pTOPO to give construct pVS66. Nucleotides indicated in bold show changes from the original sequence needed to create STOP codons in both genes. Following electroporation of constructs pVS64 and pVS66 in *M. xanthus* DK1622, mutant strains VS1013 and VS1014 respectively were verified by PCR reaction as reported^[39] (Table 2). The *myvC* (*pkn10*) mutant was obtained from Inouye's laboratory and was generated by disrupting the central, conserved serine/threonine kinases domain. Growth of *M. xanthus* for myxovirescin production was performed as previously reported.^[39; 86]

Identification of putative σ^{54} binding sites was carried out using manual analysis of promoter regions and <http://molbiol-tools.ca/mtoolwww-cgi/promscan.cgi> web site.

Discussion

In silico and genetic analysis of two myxovirescin sensory and regulatory operons suggests a complex regulatory scheme involving the σ^{54} -dependent, NifA-like enhancer binding protein MyrB, the serine/threonine kinase (STK) MyvC and several other unknown proteins. The presence of two GAF domains (one of which is a part of MyrB EBP), known to bind small effector molecules, suggests that the regulation of myxovirescin production may be subject to allosteric control by as yet unknown effectors. For example, 2-oxoglutarate binds to the GAF domain of NifA,^[82] and formate to the GAF domain of FhlA.^[83] In addition, GAF domains of cyanobacteria and eukaryotes bind cAMP and cGMP.^[84; 85] Given the observed negative effect of high concentrations of ammonia on cell growth, and the upregulation of myxovirescin production observed under reduced carbon and nitrogen conditions, it seems likely that the key signals of carbon and nitrogen metabolism may be some of the effectors.

The presence of an adenylate cyclase domain in combination with GAF domains in MyvB and MyrB suggests a possible role for cAMP in the regulation of myxovirescin production. Interestingly, inspection of the two GAF domains for the presence of the conserved signature motif that is involved in binding cyclic cAMP in eukaryotes and cyanobacteria,^[84; 85] failed to identify classical recognition sites. Unlike in *E. coli* where the role of cAMP as a global regulator has been well established, nothing is known about its role in gene expression in *M. xanthus*.

Three gene knockouts provide evidence for the role of MyrC, MyvC, and MyvD in regulation and (or) sensory transduction circuits leading to myxovirescin production. Two of these genes, *myrC* and *myvD* do not resemble any other genes in the database. However, despite their "uniqueness," we have shown the involvement of both MyrC and MyvD in the regulation of antibiotic production. Moreover, the additive effects of *myvC* and *myvD* knockouts on myxovirescin production suggest that MyvC and MyvD are a part of the same

signal transduction cascade. In summary, the concerted action of the proteins with known function (such as STK and EBPs) with proteins of unknown function suggests that myxovirescin production may be directed by novel regulatory mechanism(s).

Chapter 6

Discussion

General remarks on the myxovirescin biosynthetic factory

In silico analysis of the myxovirescin biosynthetic gene cluster from *M. xanthus* DK1622 indicated several deviations from the classical rules of polyketide assembly, as exemplified in the introductory chapter. For example, there appear to be two sets of catalytic domains which can function to provide the proposed starter unit 2-hydroxyvaleryl-*S*-ACP.^[39] Indeed, we were able to show that myxovirescin production persists upon elimination of either the ACP-KS-KR-ACP domains of TaI or ACP-KS-ACP domains of TaL PKS, albeit with the greatly reduced titers, demonstrating their functional redundancy. As expected, inactivation of both TaI and TaL eliminated myxovirescin production entirely. This set of experiments provides genetic evidence that initiation of myxovirescin production may commence on either one of the two PKSs. Therefore, the myxovirescin megasynthase is one of the rare PKS/NRPS systems known to date which has evolved a dual pathway dedicated to starter unit biosynthesis.

Sequence analysis suggests that the myxovirescin modules lack the three enoyl reductase domains required to saturate the C10-C11, C16-C17 and C22-C23 double bonds.^[39] In addition, one ER is inserted between the ACP and TE domains of the last module, an irregular modular organization without precedent to date. Another unusual feature is encountered in module 11, which is missing the full reductive loop required to reduce the C24 carbonyl. Furthermore, module 11 is physically "split" between the PKS TaO, which contains the KS domain, and the PKS TaP, which contains a methyltransferase (MT) and ACP domains. Whereas such domain separation requires specific protein-protein interactions between the C-terminus of TaO and the N-terminus of TaP, this separation might provide special access for the required reductive domains.

Evidently, many aspects of myxovirescin biosynthetic system do not fit the classical prototype of a type I system (such as the erythromycin PKS, DEBS). Therefore, the question

arises as to how these "irregular," multi-hybrid (PKS/NRPS/HMGS) systems operate? Before we can answer this question, a more clear understanding of the structural and mechanistic details of the canonical systems is needed. Even though the crystal structure of a canonical PKS has not yet been solved, the crystal structure of the KS-AT didomain of module 5 of DEBS^[87] and the ketoreductase (KR) domain have been reported.^[88] In addition, there has been significant progress recently in the understanding of the structural aspects of similar, multimodular systems responsible for fatty acid biosynthesis. In the past year structures of fatty acid synthases from both, mammals and fungi have been solved.^[89; 90] In addition, new insights in the workings of both acyl and peptidyl carrier proteins have been reported.^[91; 92] Among the important observations coming from the animal FAS structure are that the electron density corresponding to the acyl carrier protein and thioesterase was missing from the electron density map.^[89; 90] This finding suggests that the acyl carrier protein and thioesterase are highly mobile within the megacomplex. Moreover, calculated distances between different catalytic domains ranged between 32–87 Å,^[87; 89; 90] signifying that the 20 Å long Ppant arm is not sufficient to reach within the active site pockets of other domains, but is rather used to "inject" substrates deep into the active site cavities. These insights challenge the previous model of a "static" ACP and suggest that ACPs have to undergo significant interdomain rearrangements in order to supply all catalytic domains with their needed substrates. In addition to the presumed mobility of the acyl carrier proteins in PKS and FAS systems, several NMR solution structures of both acyl and peptidyl carrier domains have revealed their conformational flexibility.^[93-95] Furthermore, a PCP from the tyrocidine synthetase was shown to adopt distinct conformational states in order to interact with particular partner domains.^[95]

In summary, knowledge obtained from structural studies of fatty acid synthases, KS-AT didomain and KR domain of a PKS suggest that at least some elements of the structures

might be similar, and has led to a proposal that the modular architectures between fatty acid and polyketide synthases will be essentially the same.^[87; 88] These new insights are relevant to understanding of the myxovirescin multihybrid PKS/NRPS/HMGS synthase.

Conservation of the Pathway Leading to Formation of β -alkyl groups in Secondary Metabolites

The increasing number of secondary metabolic biosynthetic gene clusters in the public databases over the last few years has provided evidence that PK/NRP gene clusters can include "nonstandard" sets of genes. Annotation of seven such gene clusters has revealed a shared set of discrete genes collectively known as a "HMG-cassette", consisting of an ACP, a variant KS, a HMG-like synthase and one or two homologues of the enoyl-CoA hydratase (ECH) superfamily (**Figure 1**). HMG-cassettes have been correlated with the presence of C2 carbon acetate labels, and in some cases, with the carbons derived from methylmalonate (myxovirescin, leinamycin) at the so called β -positions in their related natural products (**Figure 2**). This link has led to a proposal regarding the common biochemical roles of their respective gene products in the biosynthesis of these β -functionalities.

HMG boxes are present in the chromosomes of phylogenetically diverse bacterial genera such as *Bacillus*, *Streptomyces*, *Pseudomonas*, *Cyanobacteria* and *Myxococci*. Recent genome sequencing continues to expand the number of genera that incorporate these gene sets, demonstrating their presence in *Burkholderia mallei*,^[96] *B. pseudomallei*,^[97] and *Candidatus Endobugula sertula*.^[98] Such a wide distribution of this gene group across diverse

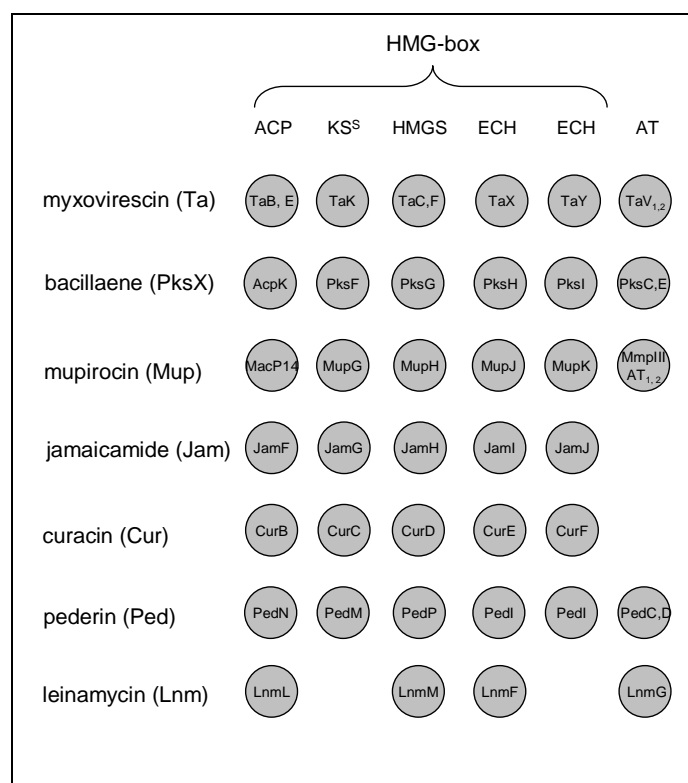


Figure 1. Homologues of the gene products of the "HMG-cassette" have been identified in seven gene clusters responsible for secondary metabolite production. Another characteristic feature of these clusters is that they belong to the family of "AT-less" systems.

bacterial phyla suggests that the genes were acquired from a common ancestor long ago, and retained during the subsequent divergence of the strains.

Systems which incorporate HMG cassettes often also belong to the family of so-called "AT-less" PKSs, in which the AT function is provided "*in trans*." However, this is not always the case, as the two cyanobacterial systems which incorporate HMG cassettes (jamaicamide and curacin) contain AT domains integrated into the modules (**Figure 1**). This observation raises the possibility that the acquisition and transmission of HMG-cassettes and genes encoding the "*trans* ATs" were independent of each other.

Discrete acyltransferases

In contrast to the paradigm established by the DEBS PKSs, DNA sequencing has revealed increasing numbers of type I PKS biosynthetic systems which lack the *cis* or intramodular acyltransferase (AT) domains. In these systems, the integral AT activities

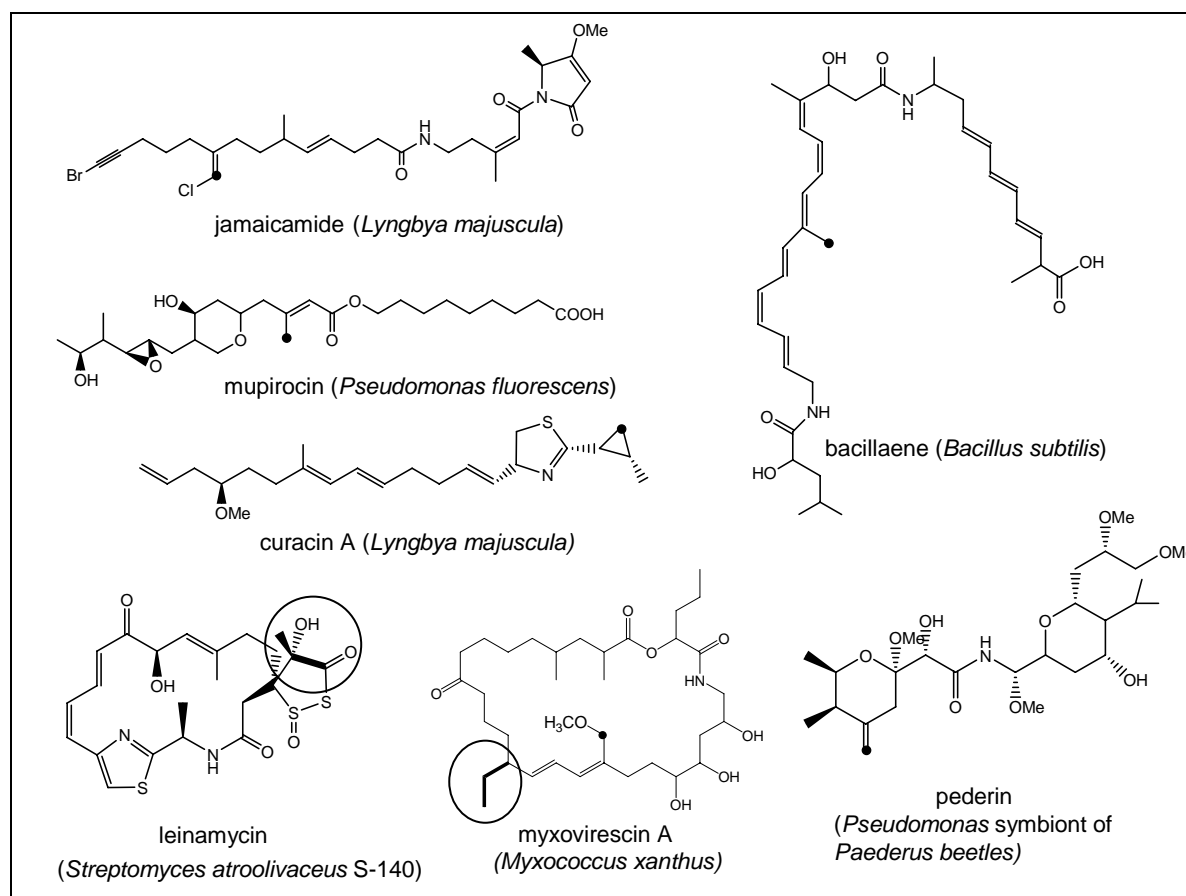


Figure 2. Incorporation of the C-2 acetate carbons (indicated with a black circle) and in some cases C-2-C-3 carbons of methylmalonate (outlined with the circle) into this selection of secondary metabolites, has been correlated with the presence of HMG-cassettes in their respective gene clusters.

are presumably compensated for by "*trans* ATs." In addition to the examples of pathways incorporating both HMG-cassettes and "*trans* ATs" (**Figure 1**), "*trans* ATs" are present on their own in the clusters responsible for biosynthesis of many other natural products, including lankacidin,^[99] mycosubtilin,^[100] chivosazol,^[101] disorazol^[102] and several others. Interestingly, *in silico* analysis of "*trans* AT" domains reveals conserved signature sequences which correlate with specificity for malonyl-CoA.^[103]

Even though "trans ATs" have been detected in many clusters, our knowledge of this class of ATs is very limited. Up to date, only two such ATs have been characterized biochemically. LnmG, a discrete AT of the leinamycin hybrid PKS-NRPS has been shown in vitro to load malonyl-CoA onto five recombinant ACP domains from the system, and to a tridomain derived from module 4 (DH-ACP-KR) of LnmJ (**Figure 3**), but not onto the discrete PCP of leinamycin cluster.^[104] Similarly, a recent investigation of FenF, the "trans AT" of the mycosubtilin system, demonstrated its strong preference for malonyl-CoA, and only marginal tolerance towards acetyl- and methylmalonyl-CoA. Moreover, FenF could not distinguish between ACPs derived from the mycosubtilin and PksX systems.^[100]

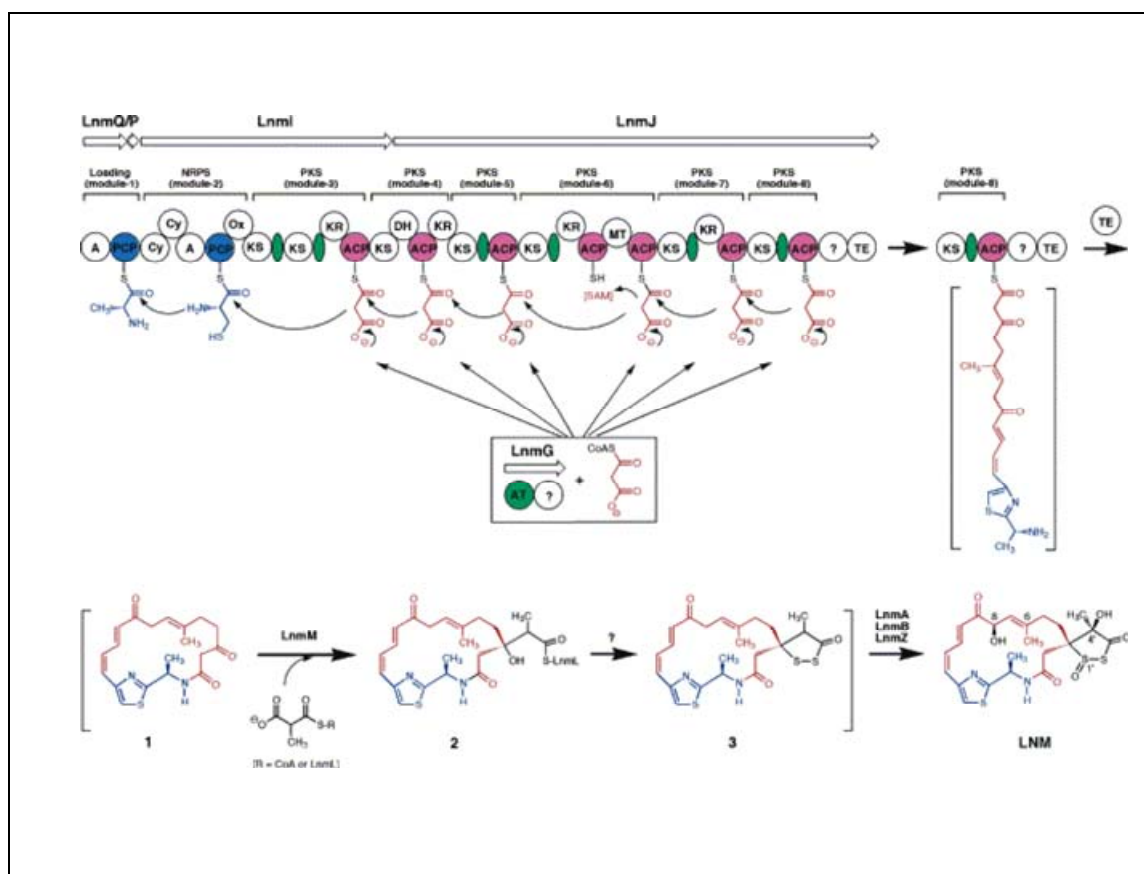


Figure 3. Postulated assembly of leinamycin. Loading of malonyl-CoAs onto the six modules of LnmI and LnmJ by the "trans AT" LnmG has been demonstrated in vitro (Figure taken from).^[105]

Thus, FenF shows a tight specificity in substrate selection, but is more promiscuous towards the acyl carrier proteins it charges. Broad tolerance of "trans ATs" towards acyl carrier

proteins could be anticipated considering the number of ACPs within these clusters they have to serve.

In myxovirescin gene cluster, the two discrete ATs (AT₁ and AT₂) are found encoded within one open reading frame *taV*. We hypothesized that AT₁ loads malonate extender units "in trans" to the AT-less PKS modules of Ta-1, TaO and TaP, as well as onto the discrete ACP TaB. AT₂ was speculated to load methylmalonyl-CoA/propionyl-CoA onto the discrete ACP TaE, thereby supplying the building block specific for the ethyl branch formation. A mechanism for loading both malonate and methylmalonate units onto the PKS is also required in leinamycin assembly. The leinamycin pathway encodes an "incomplete" HMG-cassette consisting of discrete ACP LnmL, a HMGS homologue LnmM, and the ECH LnmF.^[104] LnmL and LnmM have been proposed to incorporate methylmalonyl-CoA into the dithiolane moiety of leinamycin (**Figure 3**). However, due to the absence of the decarboxylase KS^S in the leinamycin cluster, the "trans AT" LnmG may directly load propionyl-CoA onto LnmL, instead of the proposed methylmalonyl-CoA. This idea remains speculative, as the specificity of LnmG for propionate has not yet been assessed. What it suggests, however, is that "trans ATs" in these systems may exhibit a certain degree of substrate promiscuity. Thus, one possible scenario to explain why the decarboxylase TaK is not required for myxovirescin production is by direct loading of the propionyl-CoA onto the TaE ACP by TaV.

Role of discrete ACPs in the pathway dedicated to β -branch formation

Investigation of the functional roles of HMG-cassette proteins (AcpK and PksFGHI enzymes) from the bacillaene (PksX) system in vitro (**Figure 4**), has demonstrated the importance of the discrete ACP AcpK in this pathway. Prior to delivering a substrate to

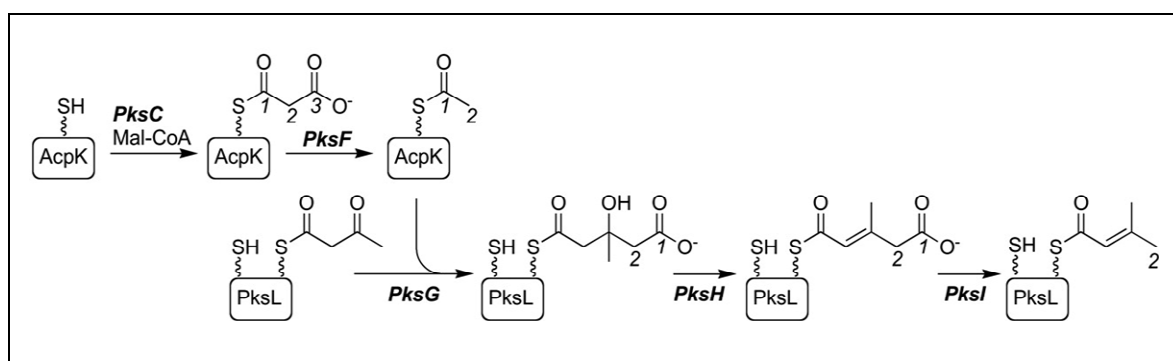


Figure 4. Assignment of functions of six enzymes from the PksX system have demonstrated their likely roles *in vivo* in the formation of β -methyl branches observed in some secondary metabolites (Figure reproduced from).^[106]

the HMGS PksG, AcpK interacts with the "trans AT" PksC and the KS^S decarboxylase PksF. Therefore, AcpK participates in multiple protein-protein interactions with other enzymes in the pathway.

The presence of two β -alkyl groups in myxovirescin A is consistent with the presence of two pairs of genes coding for ACPs and HMGSs in its associated assembly line (**Figures 1 and 2**). Hence, each discrete ACP, TaB and TaE, has been proposed to deliver the specific substrate (acetate or propionate) to their associated, HMGS TaC and TaF, respectively. Following substrate delivery, each HMGS would then couple one of the substrates onto the growing polyketide backbone. Based on this proposal, it was expected that each discrete ACP would form a functional pair with only one HMGS, to ensure that the final product has two different β -methyl groups.

Indeed, phenotypic characterization of in frame mutants of *taB*, *taC*, *taE* and *taF* has confirmed this hypothesis,^[73; 86] delineating distinct roles for the TaB/TaC and TaE/TaF ACP-HMGS pairs. Our results indicate *i*) the requirement of TaB for the formation of β -methyl group and *ii*) the requirement of TaE in the biosynthesis of β -ethyl group, as well as an additional role of this ACP in megasynthetase turnover. Given that the pathway to β -methyl

formation is ACP-dependent, it is possible that the divergence of the two ACPs has provided the structural basis for the functional separation of the two ACP-HMGS enzyme pairs.

Secondary metabolic HMG-like synthases and the divergence of superfamily of carbon-carbon condensing enzymes

Until recently, the only known HMGS were those involved in the mevalonate pathway of primary metabolism (PM), known to produce 3-methyl-3-methylglutaryl-CoA (HMG-CoA) by coupling acetyl-CoA with the 4-carbon compound acetoacetyl-CoA. However, the discovery of HMGS homologues in secondary metabolic (SM) gene clusters, where they appear to install β -alkyl branches in the growing intermediates, implied recognition of significantly longer substrates. Specifically, our model for myxovirescin biosynthesis predicted that TaC and TaF HMGS should catalyze condensations onto β -ketoacyl-*S*-ACP substrates containing C14 and C18 carbon chains, respectively. In addition, our model also required that one HMGS homologue would introduce propionate, a substrate not recognized by primary metabolic HMGS. Hence, even though it was shown in vitro that the HMGS PksG could catalyze the classical HMG-reaction on ACP-coupled substrates (**Figure 4**), genetic evidence demonstrating the function of HMGS in the biosynthesis of any secondary metabolite was still lacking. In particular, it was desirable to demonstrate directly that SM HMGS can accept much longer and more complex substrates than acetoacetyl-*S*-ACP.

Indeed, we have shown that upon inactivation of TaF HMGS from the myxovirescin cluster, the mutant strain (ΔtaF) produced new myxovirescin with a shorter (methyl) side group at C16 (**Figure 5**). Furthermore, production of the same compound was observed upon removal of the ACP TaE, confirming our hypothesis that TaF uses a substrate tethered to a specific ACP to construct the β -ethyl group. Simultaneously, this experiment provided

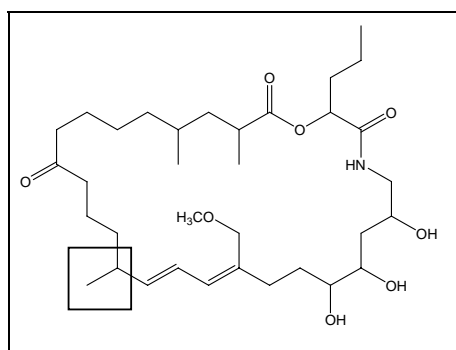


Figure 5. Production of the new myxovirescin analogue myxovirescin ΔF , which displays a methyl (in square) instead of an ethyl side group, was observed with both the ΔtaE and ΔtaF mutants. These results confirm our hypothesis that TaF HMGS directs formation of the β -ethyl group in an ACP (TaE)-dependent manner.^[73; 86]

the first evidence that, as postulated, SM HMGS couple substrates longer than acetate.

Furthermore, production level of this novel metabolite (myxovirescin ΔF) was not altered upon disruption of the primary HMGS *mvaS* in the ΔtaF background (ΔtaF , *mvaS* double mutant).^[73] This experiment showed that despite their overall sequence similarity, no cross-talk between the primary and secondary HMGS in *M. xanthus* occurs.

Taken together, genetic and biochemical characterization of three HMGS-like synthases (PksG, TaC and TaF) of secondary metabolism demonstrate three significant differences in respect to the HMGS of primary metabolism, in that SM HMGS can: *i*) operate on ACP tethered, instead of CoA activated substrates; *ii*) accept propionyl-*S*-ACP, in addition to acetyl-*S*-ACP as nucleophiles; *iii*) condense their substrates (acetyl-*S*-ACP or propionyl-*S*-ACP) onto β -ketoacyl-*S*-ACP intermediates of varying chain lengths. Therefore, although the overall catalytic mechanism of both PM and SM HMGS appears to be conserved, SM HMGS apparently display much greater tolerance towards the type and lengths of their substrates.

Based on these results, SM HMGS should have an active site tunnel longer than the 16 Å reported for the *S. aureus* MvaS,^[107] in order to accommodate the long chain substrates. However, as there are no crystal structures of any SM HMGS yet available, a simple sequence alignment was used to identify any potential differences between primary and secondary

Discussion

HMGSs in terms of their amino acid sequences. This analysis (**Figure 6**) reveals that secondary HMGSs contain two insertions relative to primary metabolic HMGSs. One insertion, about 10 amino acids in length, is located about 40 amino acids after the active

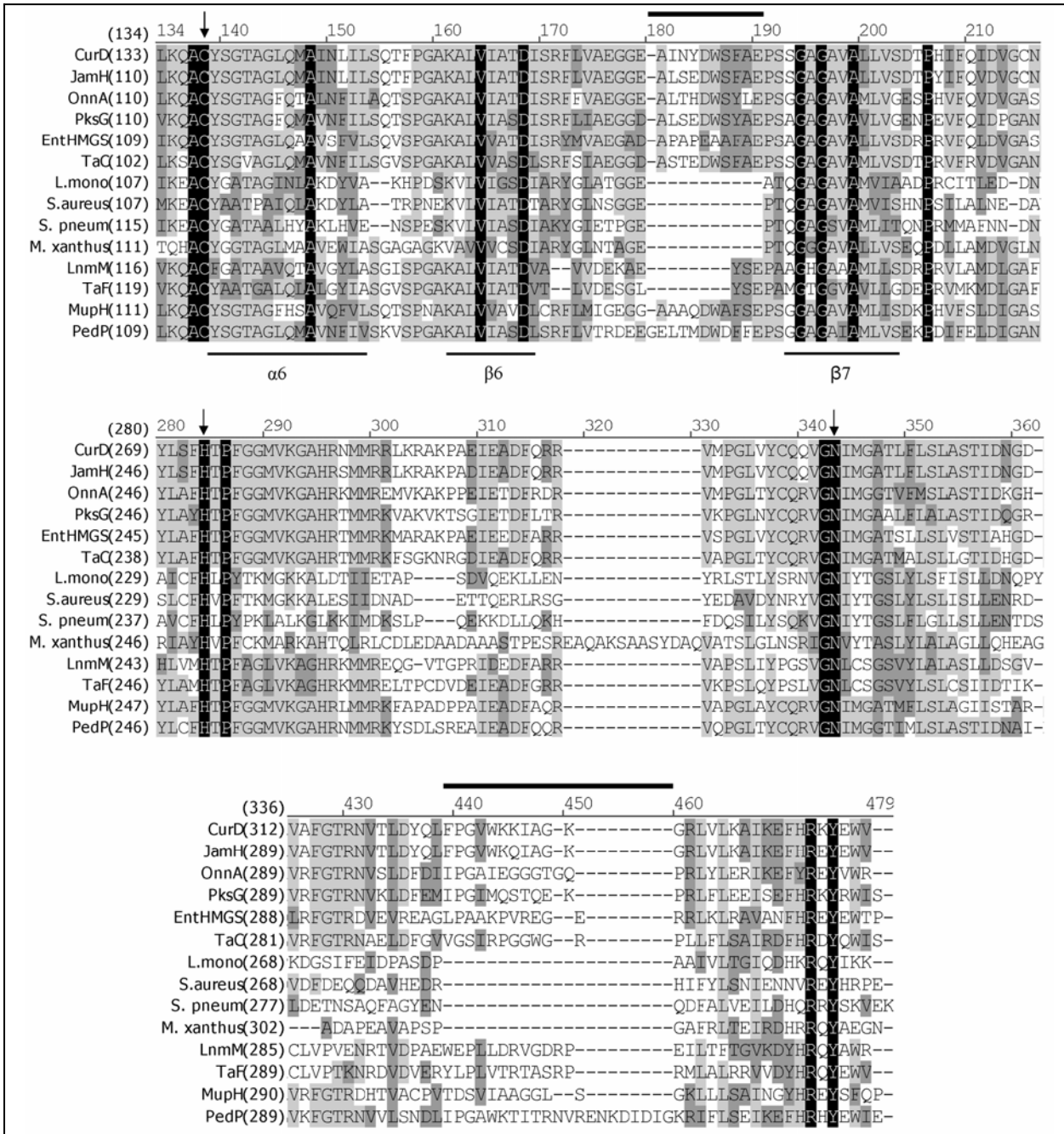


Figure 6. Amino acid alignment of primary metabolic (PM) and secondary metabolic (SM) HMGS indicates two insertions, each approximately 10 amino acids long (indicated with the solid bars). Designation of the tertiary structure was done by comparison to the *S. aureus* HMGS, whose crystal structure has been determined (see **Figure 7**). Arrows indicate completely conserved active site residues. Solid bars indicate positions of amino acid insertions specific to SM HMGS. Regions shaded in black indicate identical residues; those highlighted in light grey indicate conserved residues, while those shown in dark grey are

similar. The accession numbers of the PM HMGS are as follows: *S. aureus* (CAG 41605), *M. xanthus* (YP_632442), *S. pneumoniae* (YP_816991), and *L. monocytogenes* (ZP_00232976). The accession numbers of the secondary HMGS are: JamH (AAS 98779), CurD (AAT 70099), MupH (AAM 12922), PksG (CAB 13586), OnnA (AAV97869), and PedP (AAW 33975). EntHMGS is an HMGS homologue from the etnangien gene cluster (Perlova, O. & Müller, R., unpublished results).

site Cys, precisely between β sheets 6 and 7 of the *S. aureus* HMGS. However, this insertion is significantly smaller (4 amino acids) in both the TaF and LnmM HMGSs, the only two HMGS proposed to be specific for propionyl-S-ACP instead of acetate. The second insertion is located at the extreme C-terminus and is typically 10 amino acids in length, though the insertion in PedP is significantly longer.

Although the functional significance of these insertions remains only hypothetical, it is perhaps significant that the locations of these insertions coincide with those observed for other members of the condensing enzyme superfamily (**Figure 7**).^[107] For example, the hallmark of the thiolase family of condensing enzymes (relative to chalcone synthases, HMGS, and FabH) is a characteristic insertion of approximately 100 residues between β -sheets 6 and 7, whereas the PM HMGS exhibit a C-terminal insertion of about 67 amino acids, relative to other members of the superfamily (**Figure 7**).^[107] Thus, the alignment in **Figure 6** indicates that the SM HMGS incorporate two insertions relative to PM HMGS. Nonetheless, the significance of the observed sequence differences between primary and secondary HMGS will need to be evaluated through specific structural and biochemical studies.

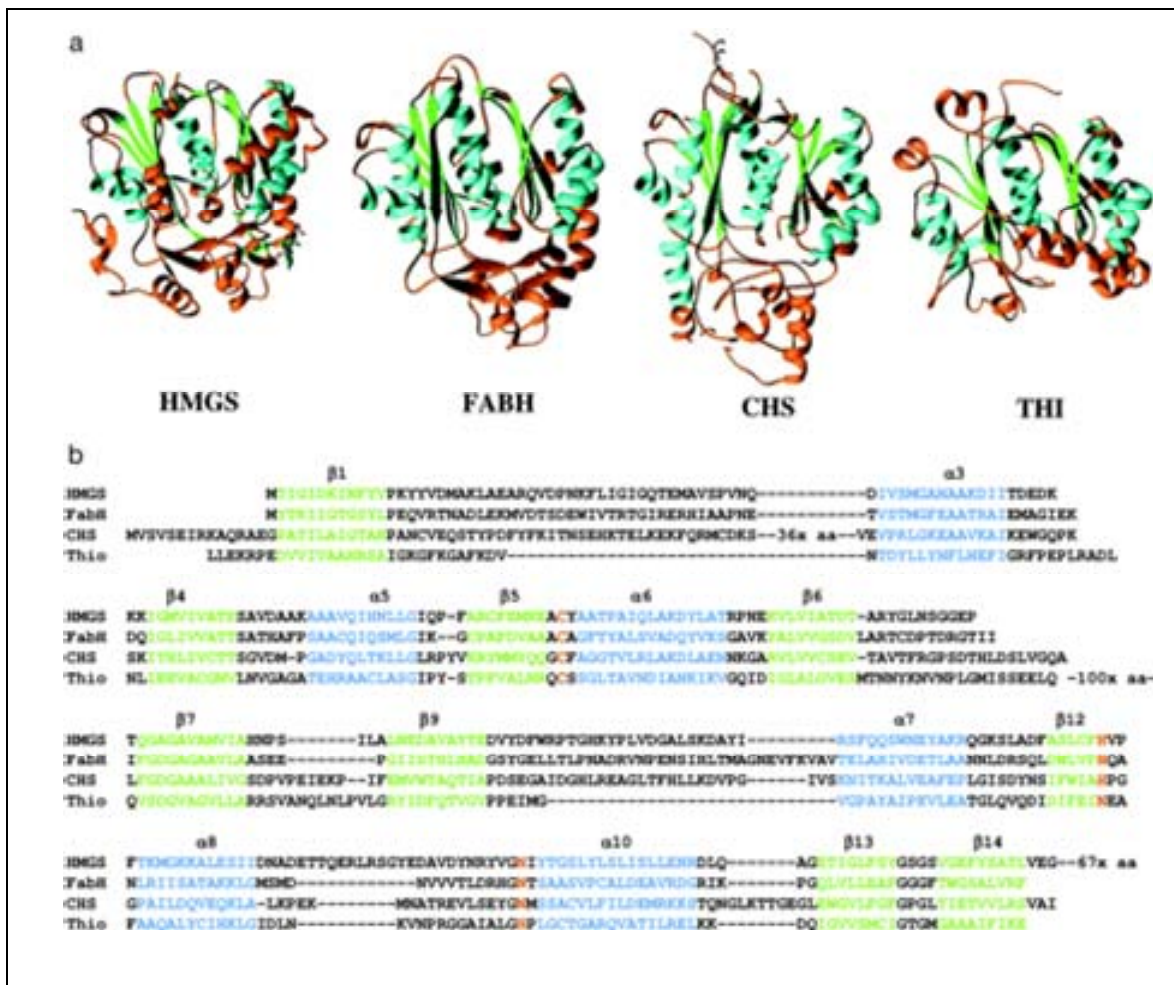


Figure 7. a) Tertiary structure comparison of four acyl-condensing enzymes. The enzymes shown are *S. aureus* HMG-CoA synthase (*HMGS*), *E. coli* FabH, *M. sativa* chalcone synthase (*CHS*), and *S. cerevisiae* thiolase (*THI*) (Protein Data Bank accession numbers 1TVZ, 1D9B (35), 1B15 (32), and 1PXT (9)). b) Structure-based sequence alignment. Conserved Cys, His, and Asn residues are shown in red. The core structure is cyan and green; cyan indicates helices, and green indicates β -strands (Figure adopted from).^[107]

Homologues of Enoyl-CoA Hydratase (Crotonase) Superfamily

With the exception of the leinamycin pathway, all HMG cassettes contain two homologues from the ECH or crotonase superfamily (**Figure 1**).^[106; 108-110] In vitro characterization of two pairs of crotonases from the bacillaene and curacin systems have demonstrated their functions as dehydratases and decarboxylases.^[106; 111] This finding is not surprising, as members of the ECH superfamily catalyze diverse reactions including dehalogenation, (de)hydration, decarboxylation, formation/cleavage of carbon-carbon bonds,

observed loss of myxovirescin A production upon deletion of either *taX* or *taY* may be due to the structural disruption of the complex, failure to accept the unmodified intermediates **2**, **3**, **5**, or **6** by the next KS, or both reasons. These observations should be taken into consideration during future biocombinatorial efforts to re-engineer this pathway.

Plasticity of the myxovirescin HMG toolbox and perspectives toward biocombinatorial engineering

Mutagenesis of the seven genes comprising the two HMG-cassettes in the myxovirescin megasynthetase constitutes the first comprehensive in vivo study towards understanding the formation of the antibiotic's two β -branches. In addition, this study represents the first attempt towards manipulating the biosynthesis by directed modification of the HMG pathway. One of the conclusions derived from this work is that discrete ACPs and HMGSs which work in tandem are substrate-specific and not mutually exchangeable. We have demonstrated that removal of either TaB or TaC halts myxovirescin production. On the other hand, removal of either TaE or TaF is tolerated by the system, causing a switch in the programming algorithm and leading to the production of a new myxovirescin analogue. In light of our genetic experiments, the observed flexibility of the myxovirescin megasynthase is most likely due to the repeated action of TaB-TaK-TaC enzyme trio in introducing two acetates at both positions C12 and C16. The observed complementation also strongly supports the ability of the TaB/ TaC pair to functionally interact with module 7 of the Ta-1 PKS.

Despite these important new insights, it is clear that a more thorough understanding of protein-protein interactions within myxovirescin megasynthetase is needed. Future studies should be directed toward unravelling the nature of docking between the discrete enzymes in the pathway (HMGS, their cognate ACPs, the "*trans* ATs") and the PKS modules. Furthermore, detailed biochemical characterization of the substrate selectivity of the "*trans*

ATs" will be needed. Elucidating these features of the biosynthesis in detail should significantly enable future development and application of the HMG-toolbox and the "trans ATs" in the production of novel biologically active metabolites.

As an approach in combinatorial biosynthesis, it is significantly easier to manipulate enzymes encoded by discrete genes, than those which are part of the multifunctional polypeptides. For example, to engineer domain swaps with the PKS proteins, it is necessary to define precise domain boundaries and linker regions, an issue which continues to be challenging.^[87; 89; 90; 113] Also, due to their small size, the corresponding genes can be easily cloned either individually, or as sets of genes, using conventional restriction enzyme approaches. Furthermore, expression of medium-sized enzymes (50–60 kDa) versus megadalton PKSs has a higher probability of yielding properly folded and functionally competent enzymes.

One prospect for introducing β -alkyl groups at different positions in additional natural products is through heterologous expression of the HMG-cassettes as part of the existing assembly lines which possess at least one minimal module (KS-AT-ACP or KS-ACP). In principle, this strategy may be successful, given the demonstrated broad substrate flexibility of HMGS and ECH enzymes.

The auxilliary enzymes of myxovirescin biosynthesis

There are four candidates for the three predicted auxiliary reactions leading to myxovirescin A. These include a cytochrome P450 hydroxylase TaH, oxygenases TaJ and TaN, and a methyltransferase TaQ. In this study we have been able to show that two of these enzymes, TaH and TaQ, are responsible for transformation of the C29 β -methyl group into the methylmethoxy functionality. By eliminating the cytochrome P450 TaH from the myxovirescin megacomplex, we have been able to characterize a new myxovirescin analogue with a unique β -methyl group at C12 (**Figure 9**). Elucidation of this structure supports our

biosynthetic model and provides essential genetic and biochemical evidence that the incorporation of acetate (and its decarboxylation) take place prior to the addition of the methoxy group in myxovirescin A. Furthermore, by analysis of the novel, desmethyl analogue of myxovirescin A, myxovirescin Q_A, we could prove that the SAM-dependent methyltransferase completes the modification of this functional group by converting the C29-hydroxyl into the C29-methoxy functionality. Because removal of TaQ and TaH had little or no effect on the yields of the respective desmethyl and desmethylmethoxy analogues of myxovirescin A, these enzymes most likely comprise the myxovirescin auxiliary toolbox which acts following assembly of the lactam. At this time it is not clear which one of the remaining two oxygenases (TaJ and TaN) hydroxylate carbons C3 and C9.

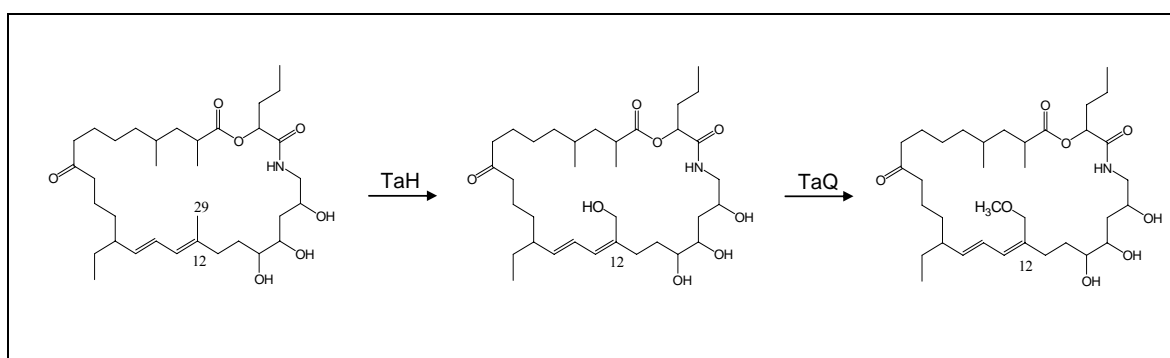


Figure 9. Formation of the methylmethoxy group attached at C29 is a two-step process, catalyzed by the cytochrome P450 TaH and the SAM-dependent methyltransferase TaQ.^[39; 86]

Regulation of myxovirescin production

In silico analysis of two myxovirescin sensory and regulatory operons (**Figure 10**) suggests that regulation of its production will be subject to σ^{54} -dependent, NifA-like enhancer binding protein MyrB, the serine/threonine kinase (STK) MyvC and several other proteins. Three gene knockouts provide evidence for the role of serine/threonine kinase MyrC, and two other proteins (MyvC, and MyvD) of unknown function, in the regulation of myxovirescin

production. Genetic organization of *myvC* and *myvD*, coupled with the additive effects of their respective knockouts on myxovirescin production (yielding 6.5 and 12.5% of wild type

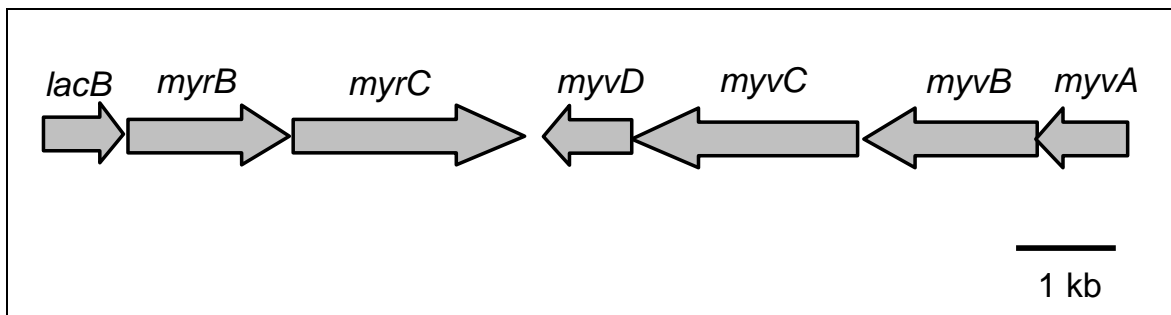


Figure 10. Knockouts of *myrC* and *myvD*, encoding for proteins of unknown function, and *myvC*, encoding for a serine/threonine kinase, produce lower amounts of myxovirescin A relative to the wild type strain.

myxovirescin production respectively), suggest that MyvC and MyvD may be part of the same signal transduction cascade.

Even though we do not yet have a phenotype of a *myrB* (EBP) knockout, an independent line of experiments currently under way in our laboratory gave evidence for the role of additional EBPs, encoded elsewhere in the chromosome, in the regulation of myxovirescin production (Kegler C. & Müller R., unpublished results). Three additional EBPs have been shown to bind to the 750 bp intergenic region located between myxovirescin biosynthetic gene cluster and *myr* operon. Curiously, all three EBP knockout phenotypes were characterized with a 70–90% drop in myxovirescin A production, whereas their double knockouts lead to an even greater reduction of the antibiotic titre. Taken together, these data demonstrate that multiple gene products activate and (or) stimulate myxovirescin production, revealing their role in the positive regulatory/signal transduction circuitry.

In addition to the role of the σ^{54} in the regulation of myxovirescin production, of particular interest will be unravelling of the roles of two GAF domains, elucidation of function of the adenylate cyclase (AC) domain, as well as the confirmation of protein-protein

interactions between FHA domain of MyvB and STK MyvC. Given the observed negative effect of high concentrations of ammonia on cell growth, and the upregulation of myxovirescin production observed under reduced carbon and nitrogen conditions, it is tempting to speculate that the key signals of the carbon and nitrogen metabolism may be some of the effectors.

In this work *Myxococcus xanthus* DK1622 was shown to be a producer of two myxovirescin antibiotics: myxovirescin A, the main antibiotic form, and myxovirescin C, its C20-deoxy analogue. From the publicly available genome of *M. xanthus* DK1622, 83 kb of the myxovirescin biosynthetic gene cluster were identified. In addition, an approximately 11 kb region upstream from the gene cluster, has been presumed to be involved in the regulation of myxovirescin production.

Annotation of the myxovirescin gene cluster lead to the biosynthetic model proposing *in trans* loading of malonyl-CoA building blocks onto the "AT-less" multimodular PKSs, as well as the possibility of either one of the two PKSs (TaI or TaL) performing the biosynthesis of the 2-hydroxyvaleryl-S-ACP starter unit. Biosynthesis of the unusual β -methyl and β -ethyl groups was proposed to be executed by seven enzymes comprised of acyl carrier proteins (ACPs), 3-hydroxy-3-methylglutaryl-CoA-like synthases (HMGS), variant ketosynthase (KS) and homologues of the enoyl-CoA hydratase superfamily. Two acyl carrier proteins (ACPs) TaB and TaE, and two 3-hydroxy-3-methylglutaryl synthases (HMGSs) TaC and TaF, were proposed to constitute two functional ACP-HMGS pairs (TaB/TaC and TaE/TaF) responsible for incorporation of acetate and propionate units into the myxovirescin A scaffold, eventually leading to the formation of β -methyl and β -ethyl groups, respectively. Three more proteins, TaX and TaY, which are members of the superfamily of enoyl-CoA hydratases (ECH), and a variant ketosynthase (KS) TaK, were proposed to be shared between two ACP-HMGS pairs, to give the complete set of enzymes required for β -alkylations. The β -methyl branch was presumed to be further hydroxylated (by TaH) and methylated (by TaQ) to produce the methylmethoxy group observed in myxovirescin A.

To test the biosynthetic model of myxovirescin biosynthesis, a palette of fourteen in-frame deletion mutants in the myxovirescin gene cluster were created and their effects on the production of myxovirescin antibiotics evaluated by HPLC-MS analysis of the resulting

mutant extracts. Novel myxovirescin analogues arising from certain mutant backgrounds were subjected to the detailed chemical structure elucidation using the high resolution mass spectrometry (HRMS) and the nuclear magnetic resonance (NMR) studies or the combination of tandem mass spectrometry (MS-MS) and HRMS analyses.

Results of our experiments have revealed the indispensability of "*trans* AT" TaV for myxovirescin production. Furthermore, myxovirescin production continued in both ΔtaI and ΔtaL mutants, but was abolished in the $\Delta taIL$ double mutant, suggesting that the production of the proposed 2-hydroxyvaleryl-S-ACP can commence on either one of the two PKSs. As predicted, ΔtaB and ΔtaE ACP mutants revealed similar phenotypes to their associated HMGS mutants ΔtaC and ΔtaF , respectively. Based on the structural elucidation of the novel myxovirescin analogue produced in both ΔtaF and ΔtaE mutants, direct evidence for the role of TaE/TaF in the formation of the β -ethyl branch, and implied roles of TaB/TaC in the formation of the β -methyl group, could be deduced. Unexpectedly, production of myxovirescin A continued in a ΔtaK mutant but was abolished in $\Delta taKF$ double mutant, indicating the need of TaK in the formation of the β -methyl group and questioning its role in the formation of the β -ethyl group. However, both TaX and TaY were shown to be required for myxovirescin biosynthesis. Analysis of two novel myxovirescin analogues arising from ΔtaH and taQ mutant backgrounds have confirmed the role of the cytochrome P450 TaH in hydroxylation of the β -methyl group and TaQ methyltransferase in its subsequent methylation. Additional disruption of genes positioned upstream from the biosynthetic gene cluster has demonstrated that the serine/threonine kinase MyvC, and two other proteins of unknown functions, have a positive effect on myxovirescin production.

In der vorliegenden Arbeit konnte gezeigt werden, dass das Bakterium *Myxococcus xanthus* DK1622 zwei verschiedene Derivate des Antibiotikum Myxovirescin bildet: Sowohl Myxovirescin A als Hauptkomponente, als auch Myxovirescin C, einem C20-Deoxy-Analog. Anhand der veröffentlichten Genomsequenz von *Myxococcus xanthus* DK1622 konnte das entsprechende Biosynthesegencluster innerhalb eines 83 kb großen Bereiches identifiziert werden. Des Weiteren konnten in einem Sequenzausschnitt von ungefähr 11 kb stromaufwärts des Genclusters zusätzliche Gene identifiziert werden, deren Genprodukte an der Regulation der Naturstoffbildung beteiligt sind.

Die Annotation des Genclusters und der korrespondierenden Genprodukte führten zur Aufstellung eines hypothetischen Biosynthesewegs. In diesem Modell wird die "AT-lose, " multimodular Myxovirescin-PKS "in trans" mit den entsprechenden Malonyl-CoA Bausteinen beladen. Die Starterereinheit 2-Hydroxyvaleryl-S-ACP wird entweder von der PKS TaI oder TaL synthetisiert. An der Biosynthese der ungewöhnlichen β -Methyl- und β -Ethylgruppe sind demnach sieben Enzyme des Genclusters beteiligt. Die beiden ACPs TaB und TaE bilden zusammen mit den 3-Hydroxy-3-Methylglutaryl-CoA ähnliche Synthasen (HMGS) TaC und TaF funktionsfähige ACP-HMGS Paare (TaB/TaC und TaE/TaF), welche für den Einbau von Acetat beziehungsweise Propionat in das wachsende Myxovirescin-Grundgerüst verantwortlich sind. Im weiteren Verlauf der Biosynthese werden diese beiden Einheiten zur β -Methyl- und β -Ethylgruppe modifiziert. Drei weitere Enzyme, TaX und TaY, die zur Klasse der Enoyl-CoA Hydratasen (ECH) gehören, als auch die Ketosynthase (KS) TaK sind an der β -Alkylierung beteiligt. Die β -Methylgruppe wird anschließend hydroxyliert (TaH) und methyliert (TaQ), um schließlich die Methylmethoxygruppe im Myxovirescin A zu bilden.

Um den postulierten Biosyntheseweg zu beweisen wurden vierzehn „in-frame“ Deletionsmutanten innerhalb des Genclusters erzeugt und die Auswirkungen auf die

Myxovirescin Produktion mittels HPLC/MS Analyse der jeweiligen Kulturextrakte überprüft. Auf diesem Weg neu gebildete Myxovirescin-Derivate wurden mittels hochauflösender Massenspektrometrie (HRMS) und Kernresonanzspektroskopie (NMR) oder in Kombination mit der Tandemmassenspektrometrie (MS/MS) aufgeklärt.

Die Mutageneseexperimente zeigten eindeutig die Unentbehrlichkeit der *trans* AT TaV für die Biosynthese des Myxovirescins. In den Kulturextrakten der beiden Deletionsmutanten ΔtaI und ΔtaL konnte nur eine geringe Menge an Myxovirescin A nachgewiesen werden, wohingegen in der Doppelmutante $\Delta taIL$ kein Myxovirescin gebildet wird. Diesem Zusammenhang folgend könnte die Startereinheit 2-Hydroxyvaleryl-S-ACP von beiden PKSs unabhängig voneinander synthetisiert werden. In den Deletionsmutanten ΔtaB und ΔtaC beziehungsweise ΔtaE und ΔtaF konnte ein ähnlicher Myxovirescin-Phänotyp nachgewiesen werden. Die Strukturaufklärung der neuen Myxovirescin Derivate aus den Deletionsmutanten ΔtaE und ΔtaF zeigt, dass TaE und TaF direkt an der Bildung der β -Ethylgruppe beteiligt sind. Weiterhin impliziert sie die Beteiligung des TaB/TaC Paares an der Synthese der β -Methylgruppe. Entgegen der postulierten Biosynthese konnte in Kulturextrakten der Mutante ΔtaK Myxovirescin nachgewiesen werden, das in der Doppelmutante $\Delta taKF$ nicht mehr produziert wurde. Diese Ergebnisse deuten darauf hin, dass TaK an der Synthese der β -Methylgruppe beteiligt ist, aber nicht an der Bildung der β -Ethylgruppe.

Zusätzliche Inaktivierungsexperimente von stromaufwärts liegenden Genen des Biosynthesegenclusters zeigen eindeutig eine Beteiligung an der Regulation der Myxovirescin-Produktion. Dabei handelt es sich um eine Serin/Threonin Kinase (MyvC) und zwei weitere Proteine mit unbekannter Funktion.

References

- [1] J. Drews, *Science* 2000, **287**, 1960-1964.
- [2] T. E. Starzl, *The Puzzle People; Memoirs of a Transplant Surgeon*, University of Pittsburgh Press, 1992.
- [3] C. Walsh, G. Wright, *Chem.Rev.* 2005, **105**, 391-394.
- [4] K. Becker, Y. Hu, N. Biller-Andorno, *Int.J.Med.Microbiol.* 2006, **296**, 179-185.
- [5] R. Johnson, E. M. Streicher, G. E. Louw, R. M. Warren, P. D. van Helden, T. C. Victor, *Curr.Issues Mol.Biol.* 2006, **8**, 97-111.
- [6] D. J. Newman, G. M. Cragg, *J.Nat.Prod.* 2004, **67**, 1216-1238.
- [7] J. Clardy, C. Walsh, *Nature* 2004, **432**, 829-837.
- [8] I. Paterson, E. A. Anderson, *Science* 2005, **310**, 451-453.
- [9] C. Zhang, B. R. Griffith, Q. Fu, C. Albermann, X. Fu, I. K. Lee, L. Li, J. S. Thorson, *Science* 2006, **313**, 1291-1294.
- [10] S. C. Wenzel, R. Müller, *Curr.Opin.Biotechnol.* 2005, **16**, 594-606.
- [11] H. B. Bode, R. Müller, *Angew.Chem.Int.Ed.* 2005, **44**, 6828-6846.
- [12] J. L. Fortman, D. H. Sherman, *ChemBioChem* 2005, **6**, 960-978.
- [13] J. Piel, D. Hui, G. Wen, D. Butzke, M. Platzner, N. Fusetani, S. Matsunaga, *P.Natl.Acad.Sci.USA* 2004, **101**, 16222-16227.
- [14] J. Piel, I. Hofer, D. Hui, *J.Bacteriol.* 2004, **186**, 1280-1286.
- [15] R. D. Charan, G. Schlingmann, J. Janso, V. Bernan, X. Feng, G. T. Carter, *J.Nat.Prod.* 2004, **67**, 1431-1433.
- [16] T. Iizuka, Y. Jojima, R. Fudou, S. Yamanaka, *FEMS Microbiol.Lett.* 1998, **169**, 317-322.
- [17] H. Reichenbach, *J.Ind.Microbiol.Biotechnol.* 2001, **27**, 149-156.
- [18] K. Gerth, S. Pradella, O. Perlova, S. Beyer, R. Müller, *J.Biotechnol.* 2003, **106**, 233-253.
- [19] B. S. Goldman, W. C. Nierman, D. Kaiser, S. C. Slater, A. S. Durkin, J. Eisen, C. M. Ronning, W. B. Barbazuk, M. Blanchard, C. Field, C. Halling, G. Hinkle, O. Iartchuk, H. S. Kim, C. Mackenzie, R. Madupu, N. Miller, A. Shvartsbeyn, S. A. Sullivan, M. Vaudin, R. Wiegand, H. B. Kaplan, *P.Natl.Acad.Sci.USA* 2006, **103**, 15200-15205.
- [20] S. Jennewein, R. Croteau, *Appl.Microbiol.Biotechnol.* 2001, **57**, 13-19.

References

- [21] J. M. Larkin, S. B. Kaye, *Expert.Opin.Investig.Drugs* 2006, **15**, 691-702.
- [22] G. Kaur, M. Hollingshead, S. Holbeck, V. Schauer-Vukasinovic, R. F. Camalier, A. Domling, S. Agarwal, *Biochem.J.* 2006, **396**, 235-242.
- [23] L. Pridzun, F. Sasse, H. Reichenbach, in *Antifungal agents* (Eds.: G. K. Dixon, C. L.G., D. W. Hollomon), BIOS Scientific Publishers Ltd, Oxford, UK 1995, pp. 99-109.
- [24] Y. A. Elnakady, F. Sasse, H. Lünsdorf, H. Reichenbach, *Biochem.Pharmacol.* 2004, **67**, 927-935.
- [25] M. W. Khalil, F. Sasse, H. Lunsdorf, Y. A. Elnakady, H. Reichenbach, *ChemBioChem* 2006, **7**, 678-683.
- [26] S. Goodin, M. P. Kane, E. H. Rubin, *J.Clin.Oncol.* 2004, **22**, 2015-2025.
- [27] T. M. Gronewold, F. Sasse, H. Lunsdorf, H. Reichenbach, *Cell Tissue Res.* 1999, **295**, 121-129.
- [28] Gronewold, Thomas, Dissertation thesis, Techn. Universität Carolo-Wilhelmina, **1996**.
- [29] F. Sasse, B. Kunze, T. M. Gronewold, H. Reichenbach, *J.Natl.Cancer Inst.* 1998, **90**, 1559-1563.
- [30] W. Kohl, A. Gloe, H. Reichenbach, *Journal of General Microbiology* 1983, **129**, 1629-1635.
- [31] C. W. Bird, J. M. Lynch, F. J. Pirt, W. W. Reid, C. J. W. Brooks, *Nature* 1971, **230**, 473-474.
- [32] A. Pearson, M. Budin, J. J. Brocks, *P.Natl.Acad.Sci.USA* 2003, 15352-15357.
- [33] H. B. Bode, B. Zeggel, B. Silakowski, S. C. Wenzel, H. Reichenbach, R. Müller, *Mol.Microbiol.* 2003, **47**, 471-481.
- [34] H. B. Bode, S. C. Wenzel, H. Irschik, G. Höfle, R. Müller, *Angew.Chem.Int.Ed.* 2004, **43**, 4163-4167.
- [35] A. Sandmann, J. Dickschat, H. Jenke-Kodama, B. Kunze, E. Dittmann, R. Müller, *Angew.Chem.Int.Ed.* 2006, **46**, 2712-6.
- [36] A. M. Hill, B. L. Thompson, J. P. Harris, R. Segret, *Chem.Commun.* 2003, 1358-1359.
- [37] S. C. Wenzel, R. M. Williamson, C. Grunanger, J. Xu, K. Gerth, R. A. Martinez, S. J. Moss, B. J. Carroll, S. Grond, C. J. Unkefer, R. Müller, H. G. Floss, *J.Am.Chem.Soc.* 2006, **128**, 14325-14336.
- [38] B. Julien, Z. Q. Tian, R. Reid, C. D. Reeves, *Chem.Biol.* 2006, **13**, 1277-1286.

References

- [39] V. Simunovic, J. Zapp, S. Rachid, D. Krug, P. Meiser, R. Müller, *ChemBioChem* 2006, **7**, 1206-1220.
- [40] W. Trowitzsch-Kienast, K. Schober, V. Wray, K. Gerth, H. Reichenbach, G. Höfle, *Liebigs Ann.Chem.* 1989, 345-355.
- [41] R. Jansen, B. Kunze, H. Reichenbach, G. Höfle, *Liebigs Ann.* 1996, 285-290.
- [42] J. C. Braekman, D. Daloz, B. Moussiaux, *J.Nat.Prod.* 1987, **50**, 994-995.
- [43] T. M. Zabriskie, J. A. Klocke, C. M. Ireland, A. H. Marcus, T. F. Molinski, D. J. Faulkner, C. Xu, J. Clardy, *J.Am.Chem.Soc.* 1986, **108**, 3123-3124.
- [44] H. Irschik, W. Trowitzsch-Kienast, K. Gerth, G. Höfle, H. Reichenbach, *J.Antibiot.* 1988, **41**, 993-998.
- [45] S. Rachid, D. Krug, I. Kochems, B. Kunze, M. Scharfe, H. Blöcker, M. Zabriski, R. Müller, *Chem.Biol.* 2006, **14**, 667-681.
- [46] M. Dworkin, M. J. Ward, D. R. Zusman, D. Kaiser, L. J. Shimkets, D. White, H. U. Schairer, in *Prokaryotic Development* (Eds.: Y. V. Brun, L. Shimkets), ASM Press, Washington, DC **2000**, pp. 219-294.
- [47] R. Jansen, B. Kunze, H. Reichenbach, G. Höfle, *Eur.J.Org.Chem.* 2000, **6**, 913-919.
- [48] F. Sasse, H. Steinmetz, G. Höfle, H. Reichenbach, *J.Antibiot.* 1993, **46**, 741-748.
- [49] J. E. Gonzalez-Pastor, E. C. Hobbs, R. Losick, *Science* 2003.
- [50] S. Rachid, K. Gerth, I. Kochems, R. Müller, *Mol.Microbiol.* 2007, **63**, 1783-1796.
- [51] P. Meiser, H. B. Bode, R. Müller, *P.Natl.Acad.Sci.USA* 2006, **103**, 19128-19133.
- [52] Z. Feng, J. Qi, T. Tsuge, Y. Oba, Y. Sakagami, M. Ojika, *Biosci.Biotechnol.Biochem.* 2006, **70**, 699-705.
- [53] R. Jansen, G. Reifenstahl, K. Gerth, H. Reichenbach, G. Höfle, *Liebigs Ann.Chem.* 1983, **7**, 1081-1095.
- [54] R. Jansen, G. Reifenstahl, K. Gerth, H. Reichenberg, G. Höfle, *Liebigs Ann.Chem.* 1983, 1081-1095.
- [55] S. C. Wenzel, B. Kunze, G. Höfle, B. Silakowski, M. Scharfe, H. Blöcker, R. Müller, *ChemBioChem* 2005, **6**, 375-385.
- [56] N. Gaitatzis, B. Kunze, R. Müller, *P.Natl.Acad.Sci.USA* 2001, **98**, 11136-11141.
- [57] Y. Paitan, E. Orr, E. Z. Ron, E. Rosenberg, *FEMS Microbiol.Lett.* 2001, **203**, 191-197.
- [58] Y. Paitan, G. Alon, E. Orr, E. Z. Ron, E. Rosenberg, *J.Mol.Biol.* 1999, **286**, 465-474.

References

- [59] C. Schley, M. O. Altmeyer, R. Swart, R. Müller, H. CG, *J. Proteome Res.* 2006, **5**, 2760-2768.
- [60] M. Buck, M. T. Gallegos, D. J. Studholme, Y. Guo, J. D. Gralla, *J. Bacteriol.* 2000, **182**, 4129-4136.
- [61] P. Bordes, S. R. Wigneshweraraj, M. Chaney, A. E. Dago, E. Morett, M. Buck, *Mol. Microbiol.* 2004, **54**, 489-506.
- [62] I. M. Keseler, D. Kaiser, *P. Natl. Acad. Sci. USA* 1997, **94**, 1979-1984.
- [63] D. Durocher, S. P. Jackson, *FEBS Lett.* 2002, **513**, 58-66.
- [64] E. Rosenberg, S. Fytlovitch, S. Carmeli, Y. Kashman, *J. Antibiot.* 1982, **35**, 788-793.
- [65] M. Varon, N. Fuchs, M. Monosov, S. Tolchinsky, E. Rosenberg, *Antimicrob. Agents Chemother.* 1992, **36**, 2316-2321.
- [66] S. Tolchinsky, N. Fuchs, M. Varon, E. Rosenberg, *Antimicrob. Agents Chemother.* 1992, **36**, 2322-2327.
- [67] D. Zafriri, E. Rosenberg, D. Mirelman, *Antimicrob. Agents Chemother.* 1981, **19**, 349-351.
- [68] I. Eli, H. Judes, M. Varon, A. Manor, E. Rosenberg, *Refuat Hashinayim* 1988, **6**, 14-15.
- [69] A. Manor, I. Eli, M. Varon, H. Judes, E. Rosenberg, *J. Clin. Periodontol.* 1989, **16**, 621-624.
- [70] A. Manor, M. Varon, E. Rosenberg, *J. Dent. Res.* 1985, **64**, 1371-1373.
- [71] K. Kashefi, P. L. Hartzell, *Mol. Microbiol.* 1995, **15**, 483-494.
- [72] B. Julien, A. D. Kaiser, A. Garza, *P. Natl. Acad. Sci. USA* 2000, **97**, 9098-9103.
- [73] V. Simunovic, R. Müller, *ChemBioChem* 2007, **8**, 497-500.
- [74] Y. S. Ho, L. M. Burden, J. H. Hurley, *EMBO J.* 2000, **19**, 5288-5299.
- [75] M. A. Fischbach, C. T. Walsh, *Science* 2006, **314**, 603-605.
- [76] R. H. Lambalot, A. M. Gehring, R. S. Flugel, P. Zuber, M. LaCelle, M. A. Marahiel, R. Reid, C. Khosla, C. T. Walsh, *Chem. Biol.* 1996, **3**, 923-936.
- [77] D. Schwarzer, R. Finking, M. A. Marahiel, *Nat. Prod. Rep.* 2003, **20**, 275-287.
- [78] J. Staunton, K. J. Weissman, *Nat. Prod. Rep.* 2001, **18**, 380-416.
- [79] S. Fytlovitch, P. D. Nathan, D. Zafriri, E. Rosenberg, *J. Antibiot.* 1983, **36**, 1525-1530.

References

- [80] J. N. Nigam, J. Lehmann, K. Gerth, H. Piehl, R. Schultze, W. Trowitzsch, *Appl.Microbiol.Biotechnol.* 1984, **19**, 157-160.
- [81] M. Buck, D. Bose, P. Burrows, W. Cannon, N. Joly, T. Pape, M. Rappas, J. Schumacher, S. Wigneshweraraj, X. Zhang, *Biochem.Soc.Trans.* 2006, **34**, 1067-1071.
- [82] I. Martinez-Argudo, R. Little, R. Dixon, *Proc.Natl.Acad.Sci.U.S.A* 2004, **101**, 16316-16321.
- [83] D. A. Skibinski, P. Golby, Y. S. Chang, F. Sargent, R. Hoffman, R. Harper, J. R. Guest, M. M. Attwood, B. C. Berks, S. C. Andrews, *J.Bacteriol.* 2002, **184**, 6642-6653.
- [84] S. E. Martinez, S. Bruder, A. Schultz, N. Zheng, J. E. Schultz, J. A. Beavo, J. U. Linder, *P.Natl.Acad.Sci.USA* 2005, **102**, 3082-3087.
- [85] A. Y. Wu, X. B. Tang, S. E. Martinez, K. Ikeda, J. A. Beavo, *J.Biol.Chem.* 2004, **279**, 37928-37938.
- [86] V. Simunovic, R. Müller, *ChemBioChem* 2007, in press.
- [87] Y. Tang, C. Y. Kim, I. I. Mathews, D. E. Cane, C. Khosla, *P.Natl.Acad.Sci.USA* 2006, **103**, 11124-11129.
- [88] A. T. Keatinge-Clay, R. M. Stroud, *Structure* 2006, **14**, 737-748.
- [89] S. Jenni, M. Leibundgut, T. Maier, N. Ban, *Science* 2006, **311**, 1263-1267.
- [90] T. Maier, S. Jenni, N. Ban, *Science* 2006, **311**, 1258-1262.
- [91] J. R. Lai, A. Koglin, C. T. Walsh, *Biochemistry-US* 2006, **45**, 14869-14879.
- [92] K. J. Weissman, H. Hong, B. Popovic, F. Meersman, *Chem.Biol.* 2006, **13**, 625-636.
- [93] Y. Kim, J. H. Prestegard, *Biochemistry-US* 1989, **28**, 8792-8797.
- [94] H. C. Wong, G. Liu, Y. M. Zhang, C. O. Rock, J. Zheng, *J.Biol.Chem.* 2002, **277**, 15874-15880.
- [95] A. Koglin, M. R. Mofid, F. Lohr, B. Schafer, V. V. Rogov, M. M. Blum, T. Mittag, M. A. Marahiel, F. Bernhard, V. Dotsch, *Science* 2006, **312**, 273-276.
- [96] W. C. Nierman, D. DeShazer, H. S. Kim, H. Tettelin, K. E. Nelson, T. Feldblyum, R. L. Ulrich, C. M. Ronning, L. M. Brinkac, S. C. Daugherty, T. D. Davidsen, R. T. DeBoy, G. Dimitrov, R. J. Dodson, A. S. Durkin, M. L. Gwinn, D. H. Haft, H. Khouri, J. F. Kolonay, R. Madupu, Y. Mohammoud, W. C. Nelson, D. Radune, C. M. Romero, S. Sarria, J. Selengut, C. Shamblyn, S. A. Sullivan, O. White, Y. Yu, N. Zafar, L. Zhou, C. M. Fraser, *P.Natl.Acad.Sci.USA* 2004, **101**, 14246-14251.
- [97] M. T. Holden, R. W. Titball, S. J. Peacock, A. M. Cerdeno-Tarraga, T. Atkins, L. C. Crossman, T. Pitt, C. Churcher, K. Mungall, S. D. Bentley, M. Sebahia, N. R.

References

- Thomson, N. Bason, I. R. Beacham, K. Brooks, K. A. Brown, N. F. Brown, G. L. Challis, I. Cherevach, T. Chillingworth, A. Cronin, B. Crossett, P. Davis, D. DeShazer, T. Feltwell, A. Fraser, Z. Hance, H. Hauser, S. Holroyd, K. Jagels, K. E. Keith, M. Maddison, S. Moule, C. Price, M. A. Quail, E. Rabinowitsch, K. Rutherford, M. Sanders, M. Simmonds, S. Songsivilai, K. Stevens, S. Tumapa, M. Vesaratchavest, S. Whitehead, C. Yeats, B. G. Barrell, P. C. Oyston, J. Parkhill, *P.Natl.Acad.Sci.USA* 2004, **101**, 14240-14245.
- [98] S. Sudek, N. B. Lopanik, L. E. Waggoner, M. Hildebrand, C. Anderson, H. B. Liu, A. Patel, D. H. Sherman, M. G. Haygood, *J.Nat.Prod.* 2007, **70**, 67-74.
- [99] S. Mochizuki, K. Hiratsu, M. Suwa, T. Ishii, F. Sugino, K. Yamada, H. Kinashi, *Mol.Microbiol.* 2003, **48**, 1501-1510.
- [100] Z. D. Aron, P. D. Fortin, C. T. Calderone, C. T. Walsh, *ChemBioChem* 2007.
- [101] O. Perlova, K. Gerth, A. Hans, O. Kaiser, R. Müller, *J.Biotechnol.* 2006, **121**, 174-191.
- [102] M. Kopp, H. Irschik, S. Pradella, R. Müller, *ChemBioChem* 2005, **6**, 1277-1286.
- [103] C. D. Reeves, S. Murli, G. W. Ashley, M. Piagentini, C. R. Hutchinson, R. McDaniel, *Biochemistry-US* 2001, **40**, 15464-15470.
- [104] G. L. Tang, Y. Q. Cheng, B. Shen, *Chem.Biol.* 2004, **11**, 33-45.
- [105] Y. Q. Cheng, G. L. Tang, B. Shen, *P.Natl.Acad.Sci.USA* 2003, **100**, 3149-3154.
- [106] C. T. Calderone, W. E. Kowtoniuk, N. L. Kelleher, C. T. Walsh, P. C. Dorrestein, *P.Natl.Acad.Sci.USA* 2006, **103**, 8977-8982.
- [107] N. Campobasso, M. Patel, I. E. Wilding, H. Kallender, M. Rosenberg, M. N. Gwynn, *J.Biol.Chem.* 2004, **279**, 44883-44888.
- [108] A. K. El-Sayed, J. Hothersall, S. M. Cooper, E. Stephens, T. J. Simpson, C. M. Thomas, *Chem.Biol.* 2003, **10**, 419-430.
- [109] J. Piel, G. P. Wen, M. Platzer, D. Q. Hui, *ChemBioChem* 2004, **5**, 93-98.
- [110] D. J. Edwards, B. L. Marquez, L. M. Nogle, K. McPhail, D. E. Goeger, M. A. Roberts, W. H. Gerwick, *Chem.Biol.* 2004, **11**, 817-833.
- [111] L. Gu, J. Jia, H. Liu, K. Hakansson, W. H. Gerwick, D. H. Sherman, *J.Am.Chem.Soc.* 2006, **128**, 9014-9015.
- [112] H. M. Holden, M. M. Benning, T. Haller, J. A. Gerlt, *Acc.Chem.Res.* 2001, **34**, 145-157.
- [113] C. D. Richter, D. A. Stanmore, R. N. Miguel, M. C. Moncrieffe, L. Tran, S. Brewerton, F. Meersman, R. W. Broadhurst, K. J. Weissman, *FEBS J.* 2007, **274**, 2196-2209.

PERSONAL

Date of Birth: 03. 01. 1974.

Place of Birth: Sarajevo, Bosnia & Herzegovina

Nationality: Croatian

EDUCATION

PhD Studies

Universität des Saarlandes, Germany
Under direction of Prof. Dr. Rolf Müller

June 2004-April 2007

PhD Studies

Gesellschaft für Biotechnologische Forschung, Germany
Under direction of Dr. Rolf Müller

Febr 2003-Mai 2004

Master of Science (M. S.) Degree

Dec 2002

Master Studies

University of Georgia, U.S.A.
Department of Microbiology
Under direction of Prof. Dr. Larry Shimkets

Aug 1999-Dec 2002

Research Assistant

University of Georgia, U.S.A.
Department of Microbiology

Sept 1998-June 1999

Bachelor of Science (B. S.) Degree in Chemistry

Mai 1998

Bachelor's Studies

Mercer University, U.S.A.

Jan 1996-Mai 1998

Bachelor's Studies

University of Zagreb, Croatia

Oct 1994-June 1995

High School Education

Mathematics Gymnasium, Bosnia & Herzegovina

Sept 1988-Mai 1992